The Suspension of Dust and Volcanic Ash in Iceland

Mary Kristen Butwin

Faculty of Earth Sciences
University of Iceland
2019

The Suspension of Dust and Volcanic Ash in Iceland

Mary Kristen Butwin

Dissertation submitted in partial fulfillment of a
Philosophiae Doctor degree in Geophysics

PhD Committee
Throstur Thorsteinsson
Sibylle von Löwis of Menar
Melissa A. Pfeffer

Opponents
Frances Beckett
Anna María Ágústsdóttir

Faculty of Earth Sciences
School of Engineering and Natural Sciences
University of Iceland
Reykjavik, 27 August 2019

The Suspension of Dust and Volcanic Ash in Iceland
The Suspension of Dust and Volcanic Ash in Iceland
Dissertation submitted in partial fulfillment of a *Philosophiae Doctor* degree in Geophysics

Faculty of Earth Sciences
School of Engineering and Natural Sciences
University of Iceland
Sturlugata 7
101, Reykjavik
Iceland

Telephone: 525 4000

Bibliographic information:
Mary Kristen Butwin, 2019, The Suspension of Dust and Volcanic Ash in Iceland, PhD dissertation, Faculty of Earth Sciences, University of Iceland, 121 pp.

Author ORCID: 0000-0002-3369-4470
ISBN: 978-9935-9300-7-1

Printing: Háskólaprent
Reykjavik, Iceland, August 2019

Abstract

Dust is an important component of the earth-atmosphere system, affecting amongst other things air quality, vegetation, infrastructure, animal and human health. Iceland produces a large amount of dust, with dust storms reported frequently especially along the South Coast and in the Highlands. Nearly 20% of the country is classified as a desert with a highly erodible surface coupled with frequent windy conditions from synoptic and mesoscale weather systems which favors dust storms to occur. In addition, new material is constantly being created through glacial, fluvial, and aeolian erosion processes, as well as input of volcanic ash from volcanic eruptions. Due to the volcanic nature of Iceland, most of the material that can be suspended regularly in the atmosphere is of volcanic origin, changing critical properties of the dust relative to other major dust source regions outside of Iceland. Fresh ash, a young component of Icelandic dust, can have different properties than more aged dust particles. The different properties of fresh and aged Icelandic dust, and dust from outside of Iceland changes the parameters used for the measuring, modeling, and forecasting of dust. Fresh volcanic ash can be distinguished from aged dust particles in the lab by observing particle shapes and surface textures. Observations of dust transport, for example by satellite imagery and by weather observers, can help identify if a dust storm originated from a source area rich in young ash or more aged dust. In situ particle counting instrumentation in conjunction with meteorological measurements as well as numerical models can be used to determine when a large dust event has occurred.

Synergistic use of these techniques is used to show that fresh ash provided by volcanic eruptions have a smaller impact on the number of dust events than previously assumed. Only volcanic eruptions with a Volcanic Explosive Index of 3 or greater, occurring outside of the winter season, increase the number of dust events in Iceland above the background numbers. This increase in dust events lasts typically on the scale of months, not years as previously thought. Fresh volcanic ash can be resuspended months after an eruption, but this typically occurs during dust events when more aged material is also being suspended, and therefore is not increasing the number of dust events. The conditions for dust events are very dependent on wind speed and topographical features, as a small shift in direction can dramatically change the amount of material being suspended. Precipitation and high humidity effect the strength of a dust or resuspension event, but not as much as they do in dusty areas outside of Iceland. Both aged dust and fresh volcanic ash particles have distinctive volcanic morphologies when they are greater than 20 μm in diameter. Aged dust and fresh ash particles smaller than 20 μm have a more crystalline like structure, predominantly made of blocks and plates, similar to dust from other major sources in the world. Additionally, distinguishing the surface material and ash is not possible by physical characteristics alone. The lower density of Icelandic dust compared with dust from other parts of the world allows Icelandic material to be more easily suspended and transported when compared to denser particles. For particles > 20 μm their shape and porosity has a major impact on the extent of their transport.

Útdráttur

Ryk er mikilvægur þáttur í samspili yfirborðs og lofthjúps og hefur meðal annars áhrif á loftgæði, innviði, og heilsu manna og dýra. Ísland leggur mikið til ryks á háum breiddargráðum og er sandfok (öskufok, moldrok eða sandbylur) algengt á Íslandi, þá helst við suðurströndina og á miðhálendinu. Sandfok á sér stað vegna þess að um 20% af yfirborði Íslands er flokkað sem eyðimörk (öræfi) með yfirborð sem veðrast auðveldlega og tíðs hvassviðris vegna lægða og strengja sem myndast vegna landslags. Einnig er nýtt efni sífellt að myndast vegna jökla-, áa-, og vindrofs ferla og ösku frá eldgosum. Vegna þess hve eldvirkt Ísland er, á megnið af efninu sem þyrlast upp í andrúmsloftið uppruna í eldgosum, sem er ástæða þess að sandfok á Ísland er sérstakt. Nýlega aska og eldri ryk agnir á Íslandi og frá örðrum svæðum geta haft mismunandi eiginleika og áhrif á bæði umhverfið og heilsu, því er mikilvægt að geta gert greinamun á milli þessara efna. Þessi munur hefur einnig áhrif á það hvaða eiginleikar eru notaðir mælingar og líkanreikninga. Athuganir á fokatburðum, til dæmis með gervitunglamyndum og frá mönnuðum veðurstöðvum, geta nýst til að segja til um hvort upptakasvæðið er nýleg aska eða eldra ryk. Agnateljarar (Optical Particle Counter) ásamt veðurathugunum, auk líkanreikninga, má nota til að ákvarða hvenær stór atburður hefur átt sér stað.

Með því að nota gögn frá athugunum í felti, veðurupplýsingum og öðrum gögnum fannst að eldgos hafa mun minni áhrif á ryk umhverfið á Íslandi en upphaflega var talið. Aðeins stór eldgos (Volcanic Explosive Index, VEI, 3 eða hærri) sem eiga sér stað utan vetrartímans hafa sjáanleg áhrif á fjölda sandfoks atburða sem eiga sér stað á Íslandi. Hinsvegar vara áhrifin aðeins í mánuði ekki ár. Eigi að síður, getur askan þyrlast upp mánuðum eftir að eldgosi lauk, en yfirleitt gerist það með öðru fokefni og eykur því ekki tíðni fokatburða. Hvenær fok á sér stað veltur á vindhraða og landslagi, þar sem smávægilegur breytingar á vindátt geta valdið mikilli breytingu á magni efnis sem þyrlast upp. Úrkoma og rakastig hafa áhrif á stærð fokatburða, en þó minna en á öðrum svæðum heimsins. Greinileg ummerki um uppruna í eldgosum sjást á ögnum stærri en 20 µm. Agnir smærri en 20 µm eru hinsvegar líkari ögnum frá öðrum upptakasvæðum. Ekki er hægt að greina í sundur ösku og eldra ryk eingöngu á útliti agnanna. Íslenskt ryk hefur lægri eðlismassa en agnir frá öðrum upptakasvæðum heimsins og því er auðveldara að þyrla þeim upp. Lögun og gropa agna stærri en 20 µm hefur mikil áhrif á hversu langt þær berast í lofti.

Dedication

This work is dedicated to Dean Wadsworth Sr.

who always encouraging and proud of my pursuit in education.

Table of Contents

Table of Figures

List of Tables

List of Acronyms

Acronym	Description
AI	Absorption Index
AMS	American Meteorological Society
ARW	Advanced Research WRF
AVO	Alaska Volcano Observatory
AWS	Automatic Weather Station
CALIOP	Cloud-Aerosol Lidar with Orthogonal Polarization
CALIPSO	Cloud-Aerosol Lidar and Infrared Pathfinder Satellite Observation
CCN	Cloud Condensation Nuclei
EEA	European Environment Agency
EOSDIS	Earth Observing System Data and Information System
GVP	Global Volcanism Program
IMO	Icelandic Meteorological Office
ISAVIA	Icelandic Air Traffic Provider
LIDAR	Light Detection and Ranging
MODIS	Moderate Resolution Imaging Spectroradiometer
MWS	Manned Weather Station
NASA	National Aeronautics and Space Administration
N.H.	Northern Highlands
NSIDC	National Snow and Ice Data Center
OPC	Optical Particle Counter
OPS	Optical Particle Sizer
PM	Particulate Matter
RI	Refractive index
S.C.	South Coast
SEM	Scanning Electron Microscope
SYNOP codes	Synoptic Observation codes
UCAR	University Center for Atmospheric Research
USGS	United States Geological Survey
VEI	Volcano Explosive Index
W.H.	Western Highlands
WMO	World Meteorological Organization
WRF/Chem	Weather Research and Forecasting model coupled with Chemistry

List of Variables

Variable	Description
u_*	Frictional Velocity
$\mathbf{A_{ft}}$	Fluid Threshold
$\mathbf{C_d}$	Drag Coefficient
$\mathbf{d_{eq}}$	Equivalent Diameter
e	Elongation
f	Flatness
g	Acceleration of Gravity
I	Intermediate Dimension of Particle
L	Long Dimension of Particle
$\mathbf{m_p}$	Mass of Particle
$\mathbf{m_w}$	Mass of Water
S	Short Dimension of Particle
w	Settling Velocity
μ	Atmospheric Viscosity
ρ_f	Atmospheric Density
ρ_s	Particle Density
$\boldsymbol{\rho_w}$	Water Density
X	Circularity
Φ	Sphericality
Ψ	Shape Factor

Acknowledgements

Firstly, I would like to thank my entire committee – Throstur, Sibylle, and Melissa – whom were willing to take me on for this project. You three were always supportive and encouraging me to explore different paths of research, even if they did not always work out. I will take the lessons I learned from all the success and setbacks with me throughout my career and life. In addition, the three of you helped me link the worlds of meteorology and geology, which sometimes led to a lot of confusion, but it was worth it.

I am also very grateful for the IceDust Association for the countless discussions and thoughts on the work currently being done as well as what would benefit the future of aerosol research in Iceland. Especially to Pavla, who organized all the events and was excited about all the research being done.

To everyone at IMO, especially Benni and Baldur, who assisted me with sampling, set up and maintenance of the OPC's thank you. Although the trips out to the field were not always the most intensive it was good to have you there for the opinions, ideas and expertise. Not to mention it made the drive out more interesting.

To everyone in Askja and IMO, thank you for welcoming me into your groups and being excited and intrigued about my work. I greatly appreciated your thoughts and ideas throughout this PhD. All your differing areas of expertise helped me approach questions from different angles, which was crucial for the interdisciplinary nature of this project. To Bryndís, Rob, Kate, Sarah, Morgan, Will and Maja, thank you so much for answering all my questions on all things rock related. To Alma, thank you for teaching me how use all the equipment in the lab, and reassuring me that I did in fact know what I was doing, and that it was the samples that were causing difficulty. Cameron, thank you for always being willing to talk about all things dust, I admired your work ethic and dedication throughout this project.

For my friends here in Iceland, thank you for everything. Without all of you I would certainly would not be here finishing my PhD. You all mean the world to me.

To Gus, who has been with me for the entire graduate school journey. Despite not fully understanding why we moved all the way from Alaska to Iceland, you did it full-heartedly and made me smile each and every day.

I also need to thank all my family for never letting me doubt myself and supporting me all these years. I especially need to thank Linda and Brent who have done so much for me and my education ever since I was enrolled in school. Finally, thank you Mom and Dad for never questioning my scientific ambitions, even at ten years old you believed that one day I could receive a PhD.

This work was financially supported by the Icelandic Research Fund (RANNÍS, Grant #152587-051). Meteorological data was provided by the Icelandic Meteorological Office. GIS basemaps for Iceland's erosion were provided by B. Björnsson. Data from Optical Particle Counters prior to 2014 was provided by Prof. K. Weber, University of Applied Science, Dusseldorf, Germany and Magðalena Jónsdóttir from Drangshlíðardalur for the support of the measurements. In addition, we acknowledge the use of imagery from the

NASA Worldview application), part of the NASA Earth Observing System Data and Information System (EOSDIS). Additional thanks to Peter Kühn of University in Tübingen, Germany for discussing the best methods for obtaining the size distribution of fine-grained Icelandic material. Particle size distribution was done at EARTHLAB (NRC 226171) at the University of Bergen, Norway. Mastersizer 3000 measurements were done at EARTHLAB (NRC 226171) at the University of Bergen. Data for size distributions and measurements can be found at DOI 10.17605/OSF.IO/9GXTQ.

1 Introduction

Scientific observations of dust in the atmosphere have been made for at least hundreds of years, with laboratory and field studies beginning at the turn of the twentieth century (Pye, 1987). The early studies examined the conditions in which particles become suspended in the atmosphere (Pye, 1987). Since then there have been numerous studies on the suspension of dust and its interaction with the atmosphere. The reason there has been so much research regarding dust is because of its role in the environment. In the atmosphere, dust affects the radiation budget and serves as cloud condensation nuclei (CCN), which can aid or suppress precipitation formation (Sokolik and Toon, 1999; Rosenfeld et al., 2001). Dust is also responsible for the transport of nutrients throughout the environment, which can be very beneficial depending on the source of dust and its deposition location (McTainsh and Strong, 2007). There are also adverse effects from the suspension of dust. With high concentrations of suspended particulate matter (PM), there is a decrease in visibility, abrasion of infrastructure and vegetation, failure of electrical equipment and engines, as well as a hazard to animal and human health (Baddock et al., 2013; Liu et al., 2014; Lekas et al., 2011; Ágústsdóttir, 2015; Zhang et al., 2016). Concentrations high enough to cause these adverse effects typically occur during dust storms and volcanic eruptions. Dust storms are usually pictured to occur in hot arid deserts or in areas suffering from long-term droughts (Wheaton, 1990). However, dust storms are often observed in the high latitude regions such as Iceland, Alaska, Canada, Russia, Antarctica, New Zealand, and Patagonia (Tarr and Martin, 1913; Prospero et al., 2012; Bullard et al., 2016). In these high latitude regions conditions are cooler and may experience high amounts of precipitation, as is the case with Southern Iceland.

In the high latitudes glacial processes mainly form the dust. Glaciers deliver fine sediment in their melt water to proglacial floodplains. The floodplains are regularly resupplied with new sediment, typically have little vegetation and often experience strong katabatic winds (Bullard et al., 2016). With the melting of glaciers and ice caps it is expected that the size of the proglacial floodplains will increase, resulting in more dust formation (Bullard, 2013). In addition to the proglacial floodplains, dust sources in the high latitudes also originate from river valleys. For example, the Copper River in Alaska, USA, has large dust plumes that travel from the mouth of the river out to the Gulf of Alaska. These events typically occur between late October and mid-November when the river height is at its minimum (Crusius et al., 2011). The third main dust source in the high latitudes are volcanic eruptions. Volcanic ash deposits serve as a source of dust in places such as Alaska, USA; Kamchatka, Russia; Patagonia (Argentina/Chile) and the Eastern and Northern volcanic zones of Iceland (Hadley et al., 2004; Thorsteinsson et al., 2012; Langmann, 2013; Simonella et al., 2015; Bullard et al., 2016). Glacial, fluvial and volcanic dust processes often occur near and with each other (Bullard et al., 2016).

In Iceland, the main source areas for dust are the Highlands in central Iceland and the sandur plains of the South Coast. The surface in the Highlands and sandur areas are made up of loose sediment ranging in grain size from silt to gravel (4 - 64,000 μm) (Arnalds et al., 2016). Due to the differing surface type the source areas can be classified based on

severity of surface material loss (Figure 1.1). The source of these sediments are: volcanic ash, erosion of old lava fields, and glacial deposits that are carried by melt water within the floodplain region. In total these areas cover more than 20,000 km^2, or 19%, of the surface of Iceland (Figure 1.1). The material remains loose and easily suspended into the atmosphere due to the lack of vegetation to hold it in place (Figure 1.2) (Arnalds, 2010; Thorsteinsson et al., 2011; Arnalds et al., 2016). The aeolian transport flux of PM in the Sahara is typically about 30 Mg/km^2/yr whereas in Iceland it ranges from 0.5-500 Mg/km^2/yr (Engelstaedter et al., 2006; Gíslason, 2008; Arnalds et al., 2014). Overall, it is estimated that roughly 4 Tg of dust is emitted annually from Iceland (Groot Zwaaftink et al., 2017). The highest flux rates occur for short time intervals during dust storms or during and shortly after ash-producing volcanic eruptions. Despite its small size, Iceland contributes 0.6 - 7.2 % of the global dust budget (Engelstaedter et al., 2006; Gíslason, 2008; Arnalds et al., 2014).

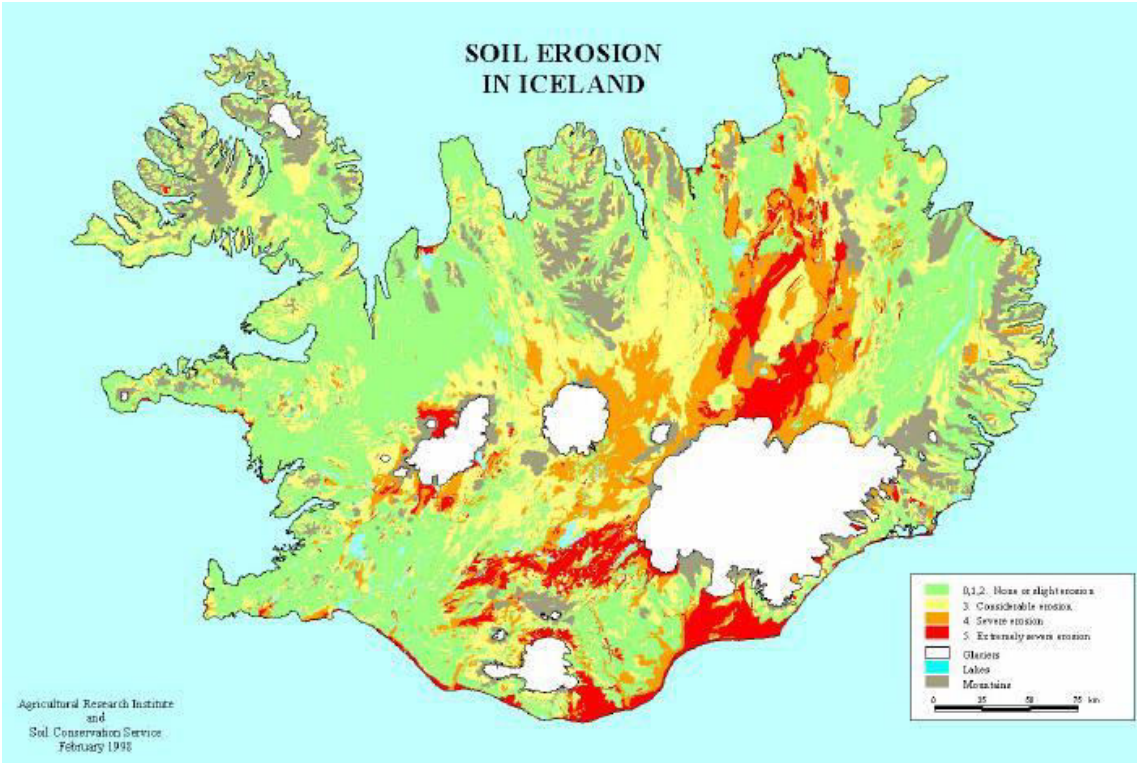

Figure 1.1: Erosion severity map of Iceland provided by the Agricultural Research Institute and Soil Conservation Service (Arnalds et al., 2001b).

The suspension of PM in Iceland is mainly due to frequent high winds over the persistent source areas. The passing of large low-pressure systems over or to the south and east of Iceland creates large pressure gradients resulting in sustained high wind speeds (Einarsson, 1984). In addition to the synoptic scale wind events, mesoscale features can also produce a favorable environment for PM events. The mesoscale winds are often due to thermal circulations forming along mountainsides and land use boundaries, e.g. between cultivated land and sandur areas (Arnalds et al., 2016; Bullard et al., 2016). Optimal conditions for PM to be lofted are high winds coupled with little to no precipitation and a dry, snow free surface (Ashwell, 1986; Arnalds, 2010; Dagsson-Waldhauservoa et al., 2014).

We define a PM event as a time when particulates (which can include fresh volcanic ash and/or aged dust) are observed or measured above the background levels in the atmosphere. Meteorological observers may record observations of PM using the synoptic codes for haze, ash, dust whirls, and dust storms. When all these categories of PM observations are included there is on average 135 days per year in which PM is observed somewhere in Iceland (Dagsson-Waldhauservoa et al., 2014b). Only 25% of these days had PM events that were categorized to be dust storms of differing severity, the remaining 75% of the PM events are due to volcanic eruptions, haze, and widespread suspension not caused by wind at or near the reporting weather station (Dagsson-Waldhauservoa et al., 2014). The average number of PM observations per year was calculated based on weather observer records from 1949-2011, during which time 13 ash-producing volcanic eruptions occurred (Thordarson and Larsen, 2007; Dagsson-Waldhauservoa et al., 2014b; Larsen et al., 2018).

Figure 1.2: Areas that undergo extreme erosion in Iceland. A) Northern Highlands looking NE (65.096°, -16.158°) B) Northern Highlands looking SW (63.918°, -16.757°) C) Western Highlands looking N (64.160°, -19.468°) D) Western Highlands looking N (64.161°, -19.470°) E) South Coast looking N (63.440°, -18.856°) F) South Coast looking SE (63.442°, -18.858°). Photos by Mary K. Butwin.

On average Iceland experiences 20-25 volcanic eruptions per century. Most of these eruptions (91%) are categorized as "explosive" or "mixed", meaning they produce ash that generates a PM event while it is being released and can be resuspended following deposition during future PM events (Thordarson and Larsen, 2007). During an eruption volcanic ash can be deposited throughout Iceland, with the thickest deposits typically being found near the eruption site (Gudmundsson et al., 2012; Arnalds et al., 2013). The amount of ash deposited in a location is a function of distance from the eruption, the height the eruption cloud reaches in the atmosphere and weather conditions during the event (Gudmundsson et al., 2012; Arnalds et al., 2013; Larsen et al., 2018). Areas where ash is deposited that are not persistent source areas (Figure 1.1) become temporary source areas for PM until the fresh ash layer is stabilized by vegetation, blown away, or integrated into the firn on glacial and icecap surfaces (Thorsteinsson et al., 2012; Dagsson-Waldhauservoa et al., 2014a; Liu et al., 2014; Powell, 2018). However, volcanic ash is often deposited on areas that are persistent source areas for PM, already rich in material available for suspension. With volcanic ash present in new and preexisting source areas, the question arises if explosive volcanic eruptions increase the number of PM events in Iceland above the numbers experienced in the absence of recent ash-producing eruptions?

There are multiple hazards associated with PM events, regardless of their ash content. PM events with high concentrations and long duration are the most hazardous (McTainsh et al., 2005). During such events visibility can be reduced to zero, creating a hazard for both vehicular and air traffic (Chepil and Woodruff, 1957; Buritt and Hyers, 1981; Laity, 2003; Miller et al., 2008; Baddock et al., 2013). Infrastructure and agriculture often undergo sandblasting resulting in damages (Chamberlain, 1975; Wilshire et al., 1981; Pye, 1987; Arnalds et al., 2001b; Stefanski and Sivakumar, 2009; Liu et al., 2014). One of the most notable forms of damage from sandblasting is to vehicles, which can be so severe that rental car agencies now inform renters not to drive in dust storms and offer sandblasting insurance policies (Liu et al., 2014). Over time abrasion in automobile and aircraft engines occurs, leading to more frequent replacements, and possibly failure (Lekas et al., 2011). The risk to aircraft is greater than the risk to automobiles as PM entering the pitot tube creates static charges that can lead to incorrect flight speeds (Clements et al., 1963; Carter, 1979; Pye 1987; Lekas et al., 2011; Alexander, 2013).

When PM contains volcanic ash, the hazards are greater than when the PM does not contain ash as ash is more efficient in abrasion, when compared to typical sandy PM (Casadevall et al., 1996; World Meteorological Organization, 2007; Prata and Tupper, 2009; Alexander, 2013). Volcanic ash poses an additional risk to aviation due to the melting temperature of ash being below or at the temperature of airline engines while typical dust melts at a higher temperature (Eliasson et al., 2016). The lower melting temperature of volcanic ash is due to the glass content, and the melting point being lower than that of operational airline engines, where engine temperatures are between 1200-2000°C and the sintering of ash begins between 850-900°C (Perepezko, 2009; Kueppers et al., 2014; Eliasson et al., 2016; Song et al., 2016). The exact temperatures depend on the composition, morphology and particle size of the ash and/or dust (Kueppers et al., 2014). When ash enters the engine it can melt and form a coating of glass. With high concentrations of ash this melting can lead to engine failure (Eliasson et al., 2016). This risk to the engine from PM containing ash remains as long as lower-melting-temperature ash is present on the surface and capable of being suspended into the atmosphere. In Katmai National Park, Alaska, USA, the 17 km^3 ash fields in the Valley of Ten Thousand

Smokes, that were deposited during the 1912 Novarupta eruption, are large enough to preserve ash that remains a hazard to aviation. Aviation warnings for resuspension of the volcanic ash here are still issued by the U.S. National Weather Service (AVO, 2019). Additionally, it is not yet clear at which concentration of volcanic ash creates a hazard for aviation. Clarkson et al., (2016) created new "safe-to-fly" charts following the 2010 eruption of Eyjafjallajökull, and determined there is a range of ash concentration and exposure duration where it is known if it is safe for aviation and another range in which it is not clear if long term damage is done to engines. Due to the known hazard of resuspension of volcanic ash (Clarkson et al., 2016), characterizing the differences between volcanic ash and the suspendable surface material in Iceland is discussed in this thesis in order to assess if the difference changes their relative hazards.

PM, whether in the form of dust or ash, is a risk to human health, especially when the particles are ≤ 10 μm as they can cause aggravated breathing, and irritation to the respiratory tract (Mészáros et al., 2014). Particles smaller than 4 μm can reach the lungs, depending on their shape and compositions, but do not reach the smallest branches of the respiratory track (Beckett; 2000; Fedorovitch, 2019). A subset of the respirable fraction, those particles 2.5 μm or less in diameter ($PM_{2.5}$) is small enough that it can reach alveoli in the respiratory tract causing respiratory irritation (Zhang et al., 2016). When one is exposed to $PM_{2.5}$ repeatedly or in a high enough concentrations, people can experience asthma attacks, respiratory inflammation, heart attacks and even death (Zhang et al., 2016). Those with preexisting conditions, the young, and the elderly are at a higher risk of experiencing these effects (Hong et al., 2010; Leiva et al., 2013; Xing et al., 2016; Zhang et al., 2016). Fresh volcanic ash can be more hazardous to human health than other PM due to morphology and chemical coatings. Volcanic ash can sometimes be in the form of fibers, with the diameter of the fibers, not their length, being the leading factor that determines how far the fiber can travel through the respiratory system (Sturm and Hofmann, 2009). The risk associated with inhalation of high amounts of fibrous material is comparable to that of inhalation of asbestos (Damby et al., 2017). Fresh volcanic ash in Iceland in the respirable fraction is typically not fibrous but blockier in shape (Horwell et al., 2013; Damby et al., 2017). With weathering and hydration, the morphology of ash can change from blocky to more fibrous material (Horwell and Baxter, 2006). Regardless of morphology, fresh volcanic ash is often coated with volatile acids, polycyclic hydrocarbons and trace metals that are toxic to humans. When inhaled these solutions result in respiratory irritation, and are toxic in high concentrations (Horwell et al., 2003; Geptner et al., 2005; Horwell and Baxter, 2006; Kim et al., 2013). The solutions remain on the ash until washed away by precipitation or surface water, which are plentiful in Iceland, so this additional risk would be short-lived in Iceland. Following the eruption of Eyjafjallajökull in 2010 the population living within the area of ash fall reported to have an increase in respiratory complaints during and following the eruption. With fresh volcanic ash causing the greater irritation than resuspended ash, especially for those with preexisting respiratory conditions (Carlsen et al., 2012).

The definition of dust varies by scientific discipline in addition to geographical location (Leathers, 1981). The most general definition for dust in atmospheric sciences is: dry particles suspended in the atmosphere (AMS, 2019). Whereas, volcanic ash refers to all particles that were ejected from a volcano and are ≤ 2000 μm (Cashman and Rust, 2016, USGS, 2019). These definitions would consider newly-formed ash to be "dust" according to the AMS definition from the moment it is ejected into the atmosphere; and would

consider ash to be a component of most Icelandic material available for lofting according to the USGS definition, regardless of how much time has passed from the formation of the ash and how much it has changed as it has aged. In practice, suspendable ash is a subset of Icelandic dust that possesses distinctive morphological and chemical properties that change as the ash ages, until it is indistinguishable from the rest of the suspendable material it resides with. Distinguishing between volcanic ash and the bulk Icelandic dust material is done to determine if they have different properties that influence how they are assessed as an airborne hazard, and how hazardous they may be to infrastructure and health.

Typically, the material that is suspended during dust storms from other regions of the world is composed of quartz, clays and feldspars, which are typically lighter in color and structurally different from the basaltic/mafic dust of Iceland (Sigmarsson and Steinthórsson, 2007; Lawrence and Neff, 2009; Arnalds, 2010; Moroni et al., 2018). Different formation mechanisms will affect the shape and particle densities of PM. Shape and particle density influence how the particles are suspended and transported in the atmosphere, their impacts on weather and climate, and their hazards (Laurent et al., 2008; Wittmann et al., 2017). How the particle is suspended and transported is described by the terms creep, saltation and suspension (Figure 1.3). The transport of particles is mainly a function of wind speed and particle size. When there is not enough force from wind to lift a particle, particles can roll or slide along the surface, this is known as particle creep. When the force of wind creates aerodynamic lift and exceeds the force of gravity and interparticle forces particles will be forced off the ground. If the settling velocity is greater than that of the verticle velocity provided by the wind then particles may experiernce saltation or suspension (Kok et al., 2012). The process of saltation is crucial for the suspension of smaller particles as it often initiates their movement (Kok et al., 2012). For particles on the surface to begin moving in any manner they must overcome the forces of gravity and interparticle forces (Figure 1.4). The amount of force that is needed for movement to begin is dependent on particle diameter, density, shear stress, atmospheric density, and the Reynolds number (Kok et al., 2012).

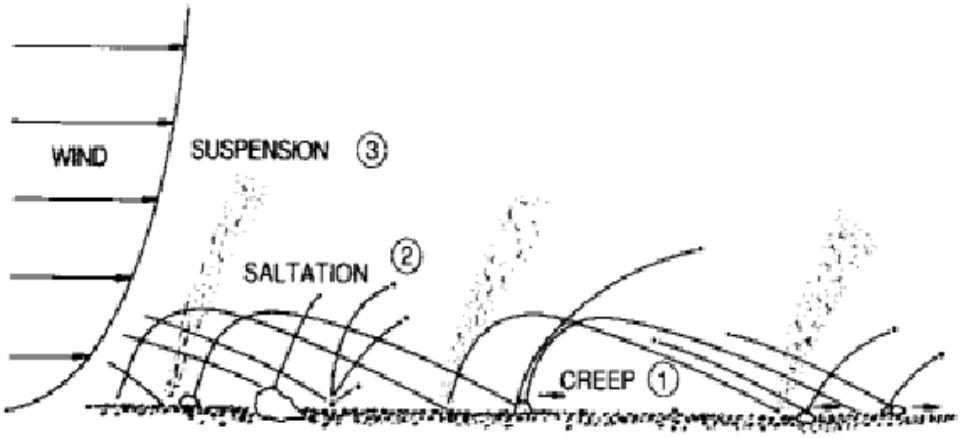

Figure 1.3: Modes of aeolian sediment transport (McTainsh and Leys, 1993).

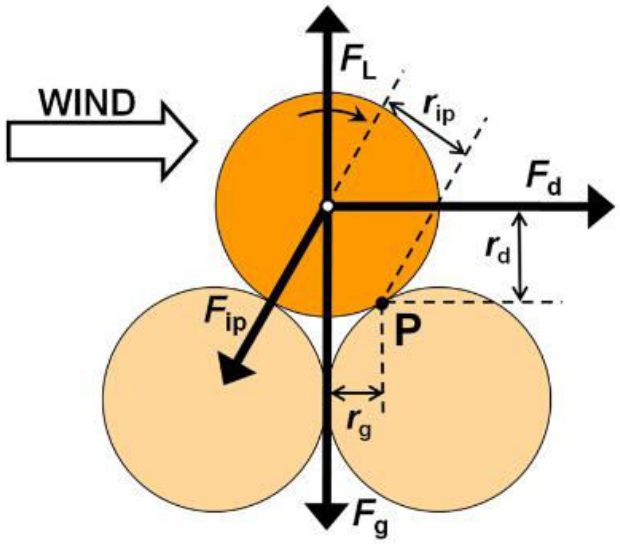

Figure 1.4: Schematic of forces acting on a stationary particle on the surface. Force of aerodynamic drage (F_d), lifting force (F_L), interparticle force (F_{ip}) and gravitiation force (F_g) are shown in bolded arrows and the respective moment applied to the pivot point (P) is shown in thin arrows. (Kok et al., 2012)

Distinguishing if Icelandic dust is different from other major dust sources in the world is important to determine so accurate measurements can be taken, numerical models can be more accurate, and the risk level of Icelandic dust can be determined (Thorarinsdottir and Arnalds, 2012; Dagsson-Waldhauserova et al., 2014a). With greater understanding of the properties of Icelandic dust, the impacts Icelandic dust has on the local and distal environments can be assessed with greater accuracy. This would be extremely beneficial for determining Iceland's impact on the arctic environment, as it is suggested that Icelandic dust is a long-term source of PM in the arctic (Dagsson-Waldhauserova et al., 2013).

1.1 Research Objectives

The goal of this thesis is to better understand Icelandic PM, with focus on the fresh volcanic ash component of Icelandic dust. The research aims to answer the following questions:

1) Does the fresh volcanic ash deposited during explosive volcanic eruptions increase the number of PM events in Iceland? If so, for how long after the eruption and on how large of a spatial scale?

    a. Knowing the impact of eruptions aids in assessing the hazard associated with PM events in Iceland. The long term study of eruption impact on PM events is the first step in determining how long volcanic ash remains on the surface and is suspendable in Iceland.

    b. To address this question, meteorological data and observations were used.

2) What are the optimal conditions for the resuspension of volcanic ash following its deposition? Are these conditions different than those needed for suspension of the bulk dust material in Iceland?

    a. Determining the optimal conditions for the resuspension of volcanic ash and the suspension of dust would improve the forecasts for large PM events. Warnings or advisories could then be issued with greater specificity. With better information, scientists and the public would be more aware of the hazards associated with such areas and events.

    b. Analysis was done using weather data, observations, as well PM concentrations that were measured using Optical Particle Counters.

3) Can one distinguish between fresh volcanic ash and bulk dust material in Iceland? If so, what are the distinguishing qualities?

    a. Being able to determine the difference between the volcanic ash and bulk dust would aid in hazard assessment of PM events occurring after explosive volcanic eruptions. This includes the hazards associated with aviation and health.

    b. In order to determine if there is a difference between the bulk material and volcanic ash, surface samples and fresh volcanic ash were analyzed.

4) Can one distinguish between Icelandic dust and dust from other regions of the world? If so, what are the distinguishing qualities?

    a. Assuming that the properties of Icelandic dust is the same as dust from other dust source areas in the world could lead to errors in environmental impact as well as transport distance. Knowing and using Iceland specific properties for dust would improve forecasts as well as scientific studies involving PM from Iceland.

    b. Surface samples from dust source areas in Iceland were compared to dust from non-volcanic areas using the characteristics found in literature.

5) Are there differences in the properties of fresh Icelandic volcanic ash, Icelandic dust, and dust from other regions of the world that changes their hazards?

    a. The hazards associated with fresh volcanic ash is known to differ from that of dust, especially in terms of health. However, Icelandic dust is also volcanic in origin and could potentially have some of the same health hazards as fresh volcanic ash. Knowing the differences will lead to better hazard assessment which would be beneficial for those working and/or living near volcanic ash deposits and/or long term dust source areas in Iceland.

    b. Based on the results from research questions three and four, an assessment on the different hazard levels of each of the materials was made.

1.2 Papers and Presentations Made During PhD Studies

This doctoral thesis builds on three first author papers to answer the research objectives listed above. The first paper is published in the peer-reviewed journal, *Journal of Aerosol Sciences*. The second paper is in preparation and will be submitted to the *Bulletin of the American Meteorological Society* in 2019. The third paper has been submitted to the *Journal of Sedimentology* in July of 2019. The details of the papers are as follows:

I. **Butwin, M. K**., von Löwis, S., Pfeffer, M. A., & Thorsteinsson, T. (2019). The effects of volcanic eruptions on the frequency of particulate matter suspension events in Iceland. *Journal of Aerosol Science*, *128*. https://doi.org/10.1016/j.jaerosci.2018.12.004

II. **Butwin, M. K**., von Löwis, S., Pfeffer, M. A., & Thorsteinsson, T. (2019). Influence of the weather conditions for particulate matter suspension following the 2010 Eyjafjallajökull volcanic eruption. *To be submitted to the Bulletin of the American Meteorological Society*

III. **Butwin, M. K**., Pfeffer, M. A., von Löwis, S., Støren, E. W. N., Bali, E., & Thorsteinsson, T. (2019). Properties of dust source material and volcanic ash in Iceland. *Submitted to the Journal of Sedimentology*.

In addition to the first author papers that are discussed in this thesis, I also contributed to the following work:

Melissa A. Pfeffer et al. (2018). Ground-Based Measurements of the 2014–2015 Holuhraun Volcanic Cloud (Iceland). *Geosciences*, *8*(1), 29. https://doi.org/10.3390/geosciences8010029

During my doctoral work, I presented at the following conferences:

- High Latitude Cold Climate Dust Conference, 2017, Reykjavík, Iceland: *Physical Characteristics of Particulate Matter in Iceland* (poster)
- High Latitude Cold Climate Dust Conference, 2017, Reykjavík, Iceland: *The frequency of dust and volcanic ash resuspension events in Iceland using varying observational techniques* (talk)
- American Meteorological Society Annual Meeting, 2018, Austin, TX, USA: *Frequency and characteristics of volcanic ash resuspension and dust events in Iceland* (talk and poster)
- European Geosciences Annual Meeting, 2018, Vienna, Austria: *Frequency and characteristics of volcanic ash resuspension and dust events in Iceland* (poster)
- Nordic Meteorological Meeting, 2018, Reykjavík, Iceland: *Frequency and characteristics of volcanic ash and dust suspension events in Iceland* (talk)
- International Aerosol Conference, 2018, St. Louis, MS, USA: *The size distribution and physical characteristics of surface material in Iceland* (talk)
- Workshop on Effects and Extremes of High Latitude Dust, 2019, Reykjavík, Iceland: *Defining Icelandic dust and volcanic ash* (talk)

2 Methods

The methods discussed here are what was implemented during the PhD studies. Most of the techniques discussed here were included in the manuscripts that are in Chapters 3-5.

2.1 Observations of PM and Weather

2.1.1 Weather Observers

Weather observers at permanent manned weather stations throughout Iceland have made most of the observations of PM events. The weather observers at these stations have been trained in how to make weather observations, classify them, and report them based on the surface synoptic observation codes (SYNOP codes) from the World Meteorological Organization (WMO). For a PM observation to be made, the concentration must be high enough for it to be visible to the naked eye. The observed PM does not have to be directly at the station but within the field of view of the observer. Observations are then categorized based on how they were suspended and severity and recorded with the suitable SYNOP code (Table 2.1). Observations are typically made every three hours between 0600 and 2400 UTC. Observations can be made outside of this timeframe, but this is typically only done during ongoing volcanic eruptions.

Table 2.1 Present weather codes for PM at manned weather stations, as classified by the WMO (2015).

SYNOP Codes			
4	Visibility reduced by smoke, e.g. veldt or forest fires, industrial smoke or volcanic ashes	**30**	Slight or moderate dust storm or sandstorm - has decreased during the preceding hour
5	Haze	**31**	Slight or moderate dust storm or sandstorm - no appreciable change during the preceding hour
6	Widespread dust in suspension in the air, not raised by wind at or near the station at the time of observation	**32**	Slight or moderate dust storm or sandstorm - has begun or has increased during the preceding hour
7	Dust or sand raised by wind at or near the station at the time of observation, but not well-developed dust whirl(s) or sand whirl(s),and no duststorm or sandstorm seen; or, in the case of ships, blowing spray at the station	**33**	Severe dust storm or sandstorm - has decreased during the preceding hour
8	Well-developed dust or sand whirl(s) seen at or near the station during the preceding hour or at the time of observation, but no dust storm or sandstorm	**34**	Severe dust storm or sandstorm - no appreciable change during the preceding hour
9	Dust storm or sandstorm within sight at the time of observation, or at the station during the preceding hour	**35**	Severe dust storm or sandstorm - has begun or has increased during the preceding hour

During the last 50-years there have been 61 manned weather stations in Iceland. Each of which has been operational for a unique length of time (Figure 2.1, Appendix A). Stations are primarily located where people live, often on remote farms, and along the coast. The weather conditions reported at these stations include parameters such as: atmospheric pressure, wind speed and direction, air temperature, dew point, precipitation amount, ground conditions, snow depth, and cloud cover and type as well as past and present weather.

A 50-year time series of PM observation data was used to analyze how fresh ash provided by explosive volcanic eruptions affects the number of PM events locally and throughout all of Iceland.

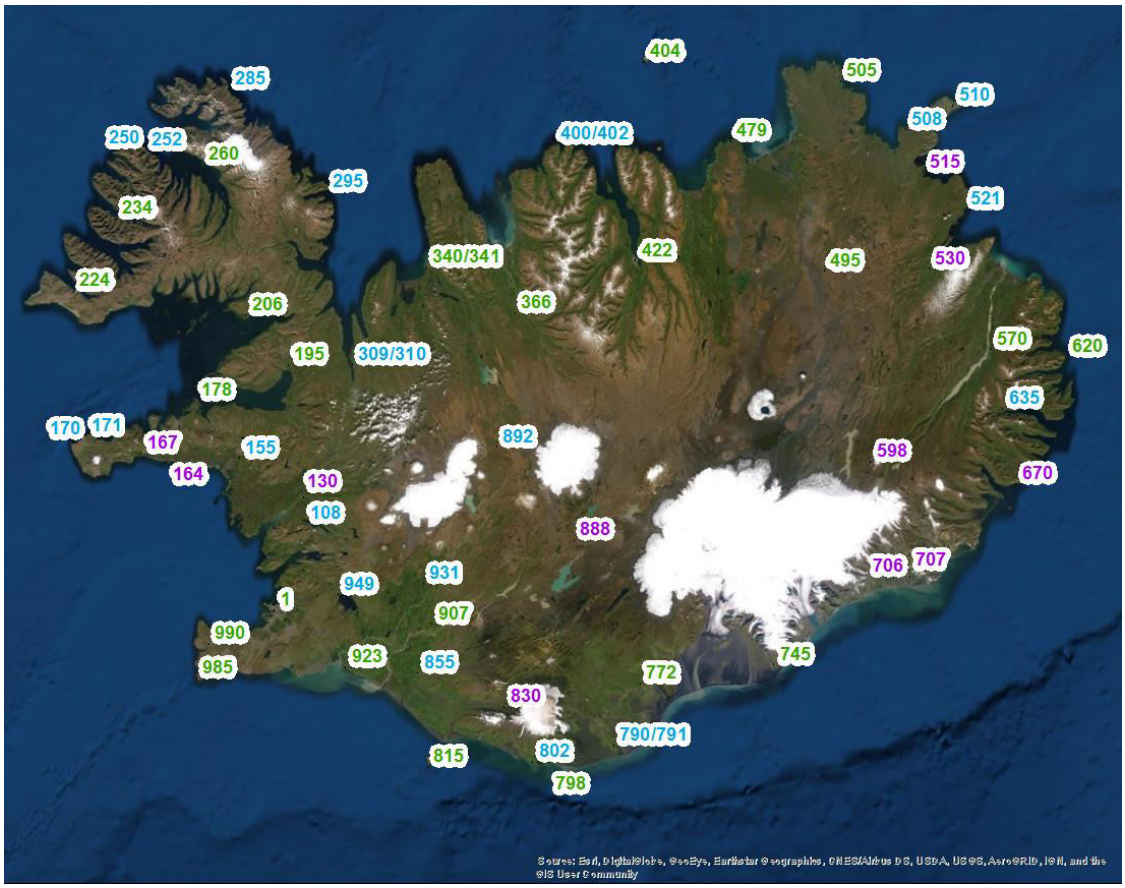

Figure 2.1: Map of 61 manned weather stations that were operational for at least two years during the 50-year period of 1966-2016. The color of the station corresponds to the duration the station was operational. Green: > 50 years, Blue: 20-50 years, Purple: < 20 years.

2.1.2 Automatic Weather Stations

Most weather stations in Iceland are Automatic Weather Stations (AWS). These stations continuously measure weather conditions and transmit the data to the Icelandic Meteorological Office (IMO) every hour. Most of the AWS measure wind speed and direction, air temperature, and relative humidity. Some of the AWS in Iceland also report atmospheric pressure and precipitation amount.

The AWS in Iceland are either owned by IMO, the Icelandic Road Administration, or one of the power companies in Iceland. The Icelandic air traffic provider (ISAVIA) operates Automated Weather Observing Systems (AWOS) at domestic and international airports. The stations owned by IMO are set up according to WMO standards (WMO, 2014). The WMO states that weather stations should be set up in locations that are representative of the area, and not directly next to large buildings, trees, or steep slopes. For proper wind measurements, anemometers should be mounted on a 10 m tower. With the distance between the tower and an obstruction such as buildings, trees, slopes being at least ten times the height of the obstruction (WMO, 2014). Temperature sensors are to be exposed in a radiation screen and between 1.25 and 2 m above the surface. It is important to note that in reality it is not always possible to meet these standards. As a result, it is necessary that each station undergoes a site classification process (Brock and Richardson, 2001).

Automatic weather station data was used to characterize the most likely transport path and most likely origin of PM events, and used to determine if a PM event was likely to be dominated by fresh volcanic ash deposits or dust from persistent source areas. For assessing the most likely transport path and origin wind direction and speed analyzed, as well as precipitation data to determine if PM source area were being suppressed or not. This data was also used to analyze the weather conditions most conducive to PM events.

2.1.3 Satellite Images

Due to the remoteness of Iceland, especially some of the most productive dust source regions, remote sensing is a useful tool for observing PM events. Satellites can potentially record PM events that would otherwise not be seen by weather observers and can also be used to measure the spatial extent of a PM event. Due to Iceland's latitude, polar orbiting satellites provide the most useful images (Zakšek et al., 2013).

The Moderate Resolution Imaging Spectroradiometer (MODIS) is aboard the Terra and Aqua satellites. These two satellites have similar orbital paths and observe the same area over Iceland approximately three hours apart. These two satellites pass over or near Iceland twice a day, providing data four times per day. MODIS measures the atmosphere in 36 spectral bands (Appendix B) (NASA, 2019; NSIDC, 2019). True color images are created using the red, green and blue wavelengths (Bands 1, 4, and 3) (Savtchenko et al., 2004). Combining the data from these bands provides a realistic picture as to what the environment looks like. In addition to the true color images, aerosol optical depth (Bands 20, 30, 31 and 32) can also be determined using MODIS data (Hao and Qu, 2007). Examination of the aerosol optical depth is used to differentiate between suspended material, clouds and the surface using the brightness temperature differences (Hao and Qu, 2007). However, use of the aerosol optical depth can be difficult for PM events which are close to the surface, where temperature differences are too small to detect (Liu et al., 2013).

In addition to MODIS, satellite-based LIDAR (Light Detection and Ranging) is used to acquire atmospheric profiles of clouds and aerosol layers. The Cloud-Aerosol Lidar and Infrared Pathfinder Satellite Observation (CALIPSO) has a Cloud-Aerosol Lidar with Orthogonal Polarization (CALIOP) that collects backscatter and depolarization data. The backscatter and depolarization data are then used to identify where aerosols and clouds are in the atmosphere and differentiate them from each other. The identification of aerosols in

the atmosphere is based on the backscattering power, in the parallel and perpendicular planes, that is sent back to the LIDAR. Irregular shaped particles such as dust and volcanic ash, would have backscattered values in both the parallel and perpendicular directions, whereas spherical particles such as water drops would have neither (Hu et al., 2007; Sassen and Khvorostyanov, 2008).

CALIPSO is part of the "A-train constellation" which is a group of polar orbiting satellites travelling close together. The Aqua satellite, mentioned previously, is also part of the A-train constellation. Using these satellites together gives a more comprehensive picture of what is occurring in the atmosphere.

Due to infrequent clear skies (3-4 days per month) (Einarsson, 1984) and the path of CALIPSO, the data was of little use for the studies discussed in this thesis. However, data should be examined in the future, as is a useful tool for studying individual events.

True color satellite images were used to examine to identify PM plumes and deposits of fresh volcanic ash on surfaces such as the glaciers and icecaps, as well as assessing the snow cover throughout Iceland. The true color images were also used to assess conditions that could influence mesoscale meteorology, such as vegetation state, snow cover extent, and cloud cover. All of which effect the thermal balance which can prohibit or promote PM suspension.

2.2 Surface Material Characterization

2.2.1 Surface Sample Collection

Surface samples from the Highlands and the South Coast were collected during August and September 2016 and September 2017 (Figure 2.2). The samples were taken from the top five centimeters of the surface, from locations that represented the overall area (Figure 1.2). The samples collected were from the large persistent source areas where dust storms are known to originate. In addition, samples of deposited fresh volcanic ash were collected during the Eyjafjallajökull 2010 and Grímsvötn 2011 eruptions. Samples were placed in bags and labeled with location. Back in the lab the samples were dried in an oven at 50°C overnight for all moisture to be removed.

The surface samples were collected for analysis of their properties.

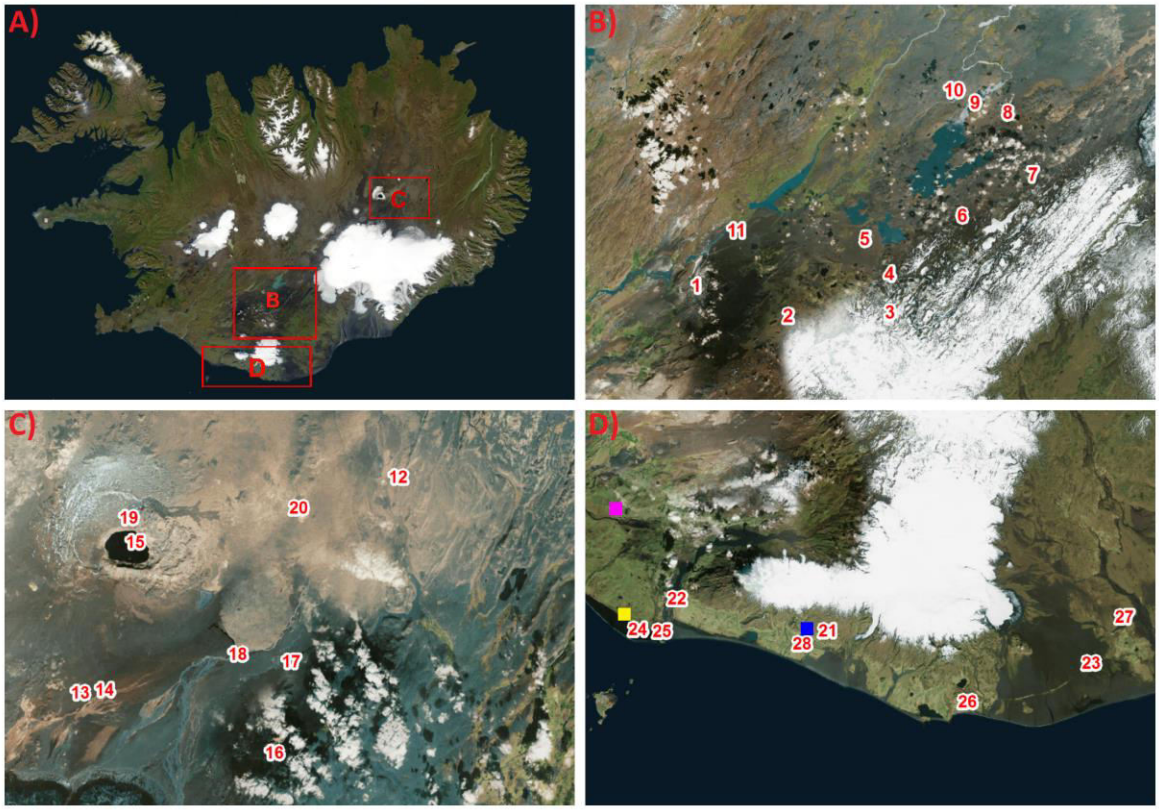

Figure 2.2: A) Surface sample collection locations in B) the Western Highlands, C) the Northern Highlands, and D) the South Coast. Colored squares are OPC locations, with pink operated: September – December 2010, yellow: April – October 2016, blue: December 2010-August 2012. Ash samples are sites 27 (Grímsvötn 2011) and 28 (Eyjafjallajökull 2010).

2.2.2 Sieving

Once samples are dry, their total mass is taken, and then dry sieved at half phi intervals from 0.5 - 4 Φ (710 - 63 µm), and then again at 5.5 Φ (20 µm). Material is placed in the coarsest sieve with the finer meshed sieves below and then placed on the sieve shaker for 10 minutes. The material that was finer than 4 Φ (63 µm) was then hand sieved for particles < 5.5 Φ (20 µm). The mass of the sample that was left in each sieve or pan was then taken for further analysis (sections 2.2.3-2.2.6).

Sieving provides a size distribution of the coarsest suspendable material in each sample area.

2.2.3 Density

The suspension of PM is not only dependent on the weather and surface conditions but also the particle properties. Determining when the forces acting on a particle are greater than the frictional velocity of the surface resulting in particle suspension is a function of particle size as well as density. The relationship between frictional velocity (u_*) and particle density can be seen in Equation 2.1 where A_{ft} is the fluid threshold and a function of

interparticle forces, lifting force and Reynolds number (Kok et al., 2012). Once a particle is suspended the density plays a role in the settling velocity of the particle (*w*) (Equation 2.2) (Green and Lane, 1964; Kok et al., 2012). Particle density is also needed to calculate drag coefficients, which takes into account the particle shape (Equation 2.3) (Corey, 1949; Blott and Pye, 2008; Kok et al., 2012; Kuhn, 2015). Further explanation of these formulas is discussed in 5.2 of this thesis.

$$u_* = A_{ft}\sqrt{\frac{\rho_s - \rho_f}{\rho_f} g d} \tag{2.1}$$

$$w = \sqrt{\frac{4gd(\rho_s - \rho_f)}{3C_d\rho_f}} \tag{2.2}$$

$$C_d = \frac{0.69gd^3\rho_f\left(1.33\rho_s - 1.33\rho_f\right)}{\mu^2\left(\frac{g\Psi^{1.6}d^3\rho_f\left(\rho_s - \rho_f\right)}{\mu^2}\right)^{1.0412}} \tag{2.3}$$

Knowing the particle density is also needed for calculations of particle properties measured by instrumentation, such as with the SediGraph and Mastersizer. For field instruments such as Optical Particle Counters (OPC) particle density is used to covert number concentrations to mass concentrations.

A Gay-Lussac pycnometer is used to measure particle densities. Deionized water is placed in the pycnometer and the mass is taken. The pycnometer is then drained and dried. Next 2-4 g of material is placed in the pycnometer, and then it is once again filled with deionized water and mass is taken. Particle density is then calculated using Equation 2.4, where ρ_s is particle density, ρ_w is water density, m_p is mass of particles, and m_w is the mass of water.

$$\rho_s = \frac{\rho_w(m_p)}{m_p - (m_{p+w} - m_w)} \tag{2.4}$$

Particle density is used to calculate settling velocity and drag coefficient as well as in calculations of the SediGraph, Mastersizer, and OPC instruments. With the use of proper densities, the accuracy of measurments in the lab and field will be improved. As would modeling the suspension and transport of particles in and away from Iceland.

2.2.4 SediGraph

A Micrometrics SediGraph III at the University of Iceland was used to measure the sizes of surface particles < 125 µm. The SediGraph uses a sedimentation method to determine particle size, and X-rays to measure particle mass. Particles are suspended in a liquid of known density and viscosity and Stokes Law is implemented for particle measurements (Gudnason et al., 2017; Micrometrics, 2019). The SediGraph assumes that the particles are spherical and have uniform densities. With these particle assumptions and the known density of the liquid used for suspension and a pump to keep constant flow, particle size is

measured based on how long they take to pass through a glass chamber. The liquid that is used for suspension is a mixture of glycerol and deionized water.

This technique was not successful for the surface material in Iceland. There may be too many magnetic grains in the basaltic surface material, causing little to no measurements to be made of the surface material. The same problem occurred with other basaltic samples (Personal Communication, Peter Kühn). However, it is important to note that basaltic tephra material from Iceland has been successfully analyzed using the SediGraph (Gudnason et al., 2017; Moreland, 2017; Huntingdon-Williams et al., 2018). As of the writing of this thesis the only known difference between the material that was successfully measured using the SediGraph and the material that failed in the SediGraph from this study, is that the successfully measured material was buried and preserved. It is hypothesized that over time erosional processes on the now buried material may have selectively removed magnetic grains. The issues due to measuring the surface material resulted in the SediGraph data being unusable in this thesis.

2.2.5 Mastersizer

A Malvern Mastersizer 3000 using a Hydro Large Volume dispersion unit was used at the EARTHLAB at the University of Bergen, Norway to measure the size distribution of the collected surface samples. The Mastersizer uses laser diffraction to measure particulate size. The measurements are based on the angular scattering of the light and Mie theory. The particle size is then reported as a volume equivalent sphere diameter (Malvern Panalytical, 2019).

The Mastersizer provided a size distribution of the suspendable material (0.01- 3500 µm) in each sample area.

The particle size distribution analyses allowed for the calculation of the percentage of material that can potentially be suspended in the atmosphere or breathed in.

2.2.6 Scanning Electron Microscopy

A Hitachi TM3000 Scanning Electron Microscope (SEM) was used to examine the morphology of individual particles and for further size analysis. The SEM is used to get a topographical image of the sample. Imaging is done using a beam of electrons, where the heating of a metallic filament creates the electrons. The beam of electrons is then focused using a series of electromagnetic lenses and directed towards the sample. When the electrons hit the sample, backscattering occurs as well as secondary electrons being ejected from the sample. The backscattered and secondary electrons are detected by sensors and then convert the information to an image (Figure 2.3) The SEM has a magnification range between 15x and 30000x, which allows for a wide range of particle sizes to be viewed in detail. Images that are used in the thesis were taken at 2000x magnification with a pixel size of 0.07344 µm (13.6 pixels per µm).

For particle analysis, a small portion of material was placed on carbon tape and then gold coated to prevent the overcharging of material that would distort the images produced (Hitachi, 2019). This process also allowed for the material to stay in place within the vacuum of the SEM during analysis. The sample preparation and analysis techniques are

well used and accepted in PM studies (Mangold et al., 2011; Stevenson et al., 2013; Dagsson-Waldhauserova et al., 2015; Dragosics et al., 2016).

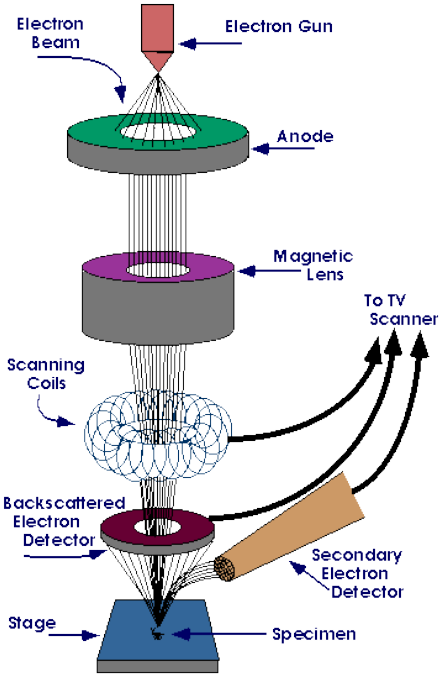

F*igure 2.3: Diagram of how the SEM produces images. Image courtesy of Iowa State University College of Engineering (2019).*

Using the images taken with the SEM particle texture and shape can be examined. The morphology of grains of different sizes and different source locations are logged. With special attention paid to the differences between the material that was collected from permanent source areas of Iceland, and volcanic ash that was collected during an eruption. These morphological properties are also compared to the properties of the dust particles coming from dust source regions outside of Iceland.

Using the imaging software ImageJ, measurements of individual grains can be made using similar techniques as Rasband (2012). Measuring grains using ImageJ allows for shape characteristics such as elongation and flatness to be known. These characteristics are not known with the other sizing instrumentation as the instruments measure the equivalent spherical diameter.

The SEM images were used to analyze particle texture, shape, elongation, and flatness. Examining if the particles texture to determine if they showed signs of formation conditions, weathering, erosion, and physical properties found in volcanic material (e.g. Alastuey et al., 2005; Wang et al., 2011; Buck et al., 2013). Particle shapes were also classified based on how similar to a circle or sphere they are based on measuring the dimensions of particles (Corey, 1949; Blott and Pye, 2008; Kuhn, 2015). Particle shape is then also described in terms of non-circular or spherical particles as described in Bagheri et al., 2015. The shape classifications are based on the elongation and flatness of the particles, which are functions of the length, width, and height of the grains (Bagheri et al., 2015).

2.3 In Situ PM Measurements

The long-term monitoring of PM in Iceland has been restricted to a few stations operated by the Environmental Agency in Reykjavík and Akureyri to monitor PM from urban sources. Other than this, PM monitoring has been done sporadically, and typically around the times of volcanic eruptions. Optical Particle Counters (OPCs) are one of the main instruments that have been used for in situ PM measurements.

2.3.1 Optical Particle Counters

The work discussed in this thesis uses data from two different OPCs. The first being a Grimm EDM 365 OPC, on loan from the University of Applied Science, Dusseldorf, Germany, and the second being a TSI OPS 3300 from the Icelandic Meteorological Office. The Grimm OPC was in use during a period between 2010-2012 and was stationed mainly in the Southern region of Iceland following the Eyjafjallajökull and Grímsvötn eruptions (Figure 2.2). The TSI OPC was deployed in Möðrudalur, Northeast-Iceland, during the Holuhraun/Barðabunga 2014-2015 eruption, as well as at the airport in Bakki, South-Iceland, between April-September 2016 (Figure 2.2).

OPCs record the number particles by counting the number of pulses a beam of light has as particles pass through. Measuring the size of particles is done by measuring the intensity of scattered light from the particle. The intensity of scattered light and particle size is related using Mie light scattering theory where the particles are approximately the same size as the wavelength of the light. To reduce errors produced because of the non spherical shapes, a curved mirror is placed across from the light detector (Figure 2.4).

The Grimm OPC measures particles between 0.25 - 32 µm and places them in 31 size bins. The TSI OPC measures particles between 0.3 - 10 µm and places them in 16 size bins. Both OPCs measure particle number concentrations. To convert to mass concentration, the particle density needs to be either known or assumed. The densities used for this study were calculated using the pycnometer (section 2.2.2). The OPC provided the size distribution of suspended material measured in the atmosphere.

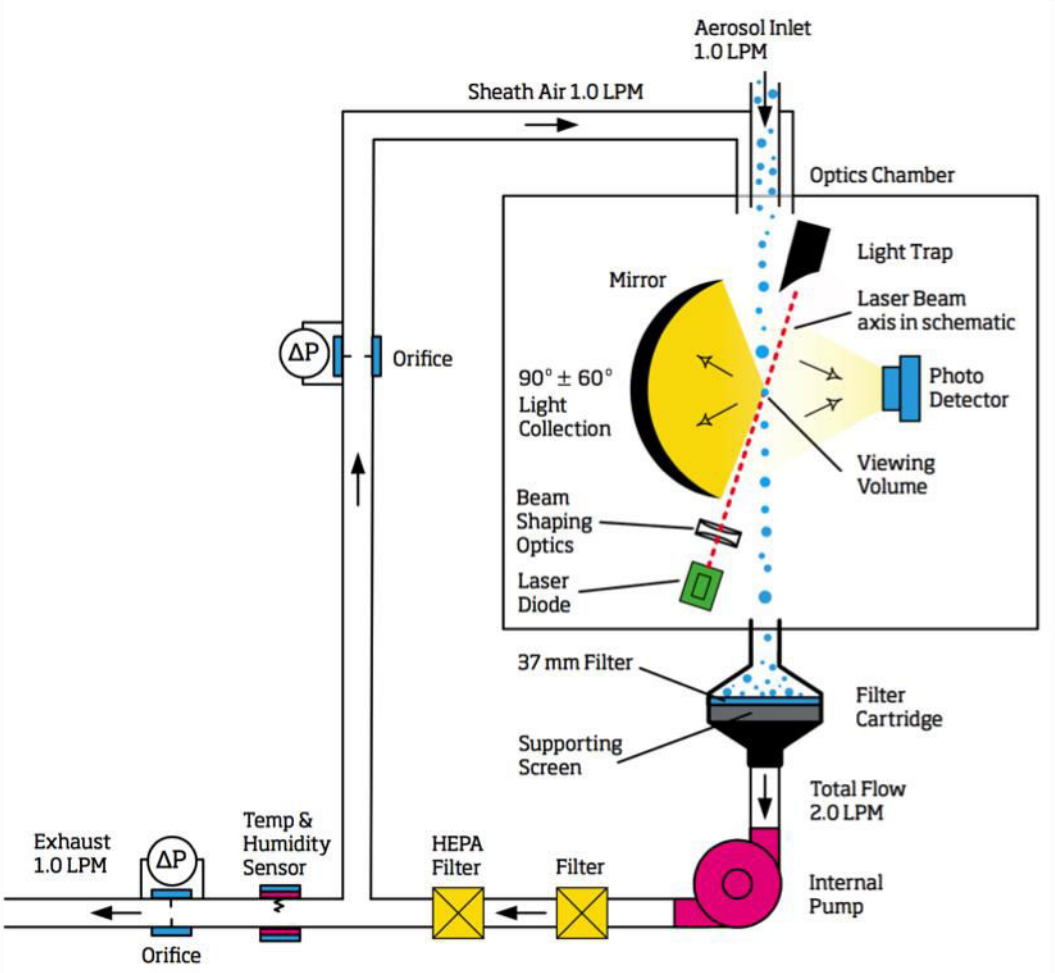

Figure 2.4: Schematics of OPC operation. Image from TSI, 2019.

2.4 Numerical Modeling

In addition to observations and sample analysis, numerical modeling can be used for determining the "lifespan" of volcanic ash on the surface in Iceland. The Weather Research and Forecasting model coupled with Chemistry (WRF/Chem) was used to simulate volcanic emissions of ash into the atmosphere and the suspension of dust at a high resolution.

WRF is a non-hydrostatic terrain following mesoscale model that is used for both forecasting and research (Skamarock et al., 2008). When the meteorological model WRF is coupled with chemistry, the overall air chemistry is considered, as is the emission, transport, transformation, radiative properties and removal of aerosols (Grell et al., 2005; Peckham et al., 2011). Once meteorology and chemistry are inputted into the model code the Advanced Research WRF (ARW) must be implemented. The ARW uses a dynamics solver with the meteorological properties to form a complete simulation of meteorological and chemical conditions (Skamarock et al., 2008). With a completed simulation the meteorology and chemistry parameters interact. The interaction can account for CCN

concentrations, droplet formation and size of droplets, which will then influence precipitation (Barnard et al., 2010). The meteorology and chemistry interaction also account for how clouds, atmospheric gases and aerosols affect incoming and outgoing radiation, as well as photochemical properties. The changes in the radiation budget and photochemical properties then affect meteorological parameters such as temperature, which then affects the setup of thermal circulations (Grell et al., 2005; Peckham et al., 2011).

There have been numerous studies modeling the dispersal of volcanic ash and gases from Iceland using WRF/Chem (Stuefer et al., 2012; Webley et al., 2012; Boichu et al., 2016). However, most of these modeling studies focused on the transport of aerosols away from Iceland and not within Iceland itself. Modeling dust storms in Iceland using WRF/Chem is rather new and uses common global dust parameters that are not optimized for Icelandic dust (Personal Communication O. Rögnvaldsson, 2018). The landuse file for Iceland, that is automatically used by WRF, is incorrect. Glacier coverage is overestimated and some land use classifications are incorrect. Modified landuse for Iceland is available and must be changed within the model for accurate output (UCAR, 2019). Persistent dust sources are not yet recognized by the WRF landuse soil classifications (Personal communication, O. Rögnvaldsson, 2018).

The correction of land use and soil data, inclusion of volcanic emissions and ash deposition, and suspension of dust is time and computationally intensive. The process for modeling the evolution of the ash deposits in Iceland from the Eyjafjallajökull eruption began during this PhD project. As of the writing of the thesis the output from WRF/Chem is not yet available and therefore not included in this thesis.

3 The Effects of Volcanic Eruptions on the Frequency of Particulate Matter Suspension Events in Iceland

This chapter was published in 2019 under the same title in Journal of Aerosol Science, 128, 99 – 113. The co-authors were Sibylle von Löwis, Melissa A. Pfeffer, and Throstur Thorsteinsson.

Abstract

Large quantities of natural particulate matter are generated in Iceland every year. Glaciers, rivers, and explosive volcanic eruptions contribute to the production of suspended material in the air. With frequent high winds and sparse vegetation cover, fine and coarse particles are suspended and transported over land and out to sea. Observations of particulate matter during the period of 1966-2016 were used to determine the impact of explosive volcanic eruptions on the number of observed particulate matter events. Weather observers at synoptic weather stations distributed around Iceland made these observations. Deposits from some explosive volcanic eruptions that produce new source material were found to increase the number of observations of particulate matter at stations relatively close to the volcano (within 125 km) for at least several months after the end of the eruption. This signal is only observed for eruptions that produced enough material to be classified into Volcano Explosive Index (VEI) of 3, or greater, and did not end during the winter, and is only rarely seen at the national scale. Eruptions starting shortly before or during the winter season and ending before the spring melt did not have an impact on the observations of suspended particulate matter due to snow covering the fresh material, reducing the potential for resuspension. The data set is insufficient to explain why only some eruptions fulfilling the criteria produce local effects persisting over multiple months. Seasonality, weather, and wind conditions are much stronger factors for increasing the number of particulate matter (PM) events than the creation of new material provided by explosive volcanic eruptions. A PM event is defined to occur when any type of PM is observed in the atmosphere.

* Errors found in the published manuscript have been corrected in this thesis, corrections were sent to the journal. Errors were in regards to Figures 3.1, 3.2 and Table A.1 in regards to erosion classification and duration of weather station operation. The errors did not effect or change the data presented within the manuscript.

3.1 Introduction

Dust storms are generally associated with hot dry deserts or areas suffering from severe drought (Wheaton, 1990). However, dust storms often occur in the high latitude regions such as Iceland, Alaska, Canada, Russia, Antarctica, New Zealand, and Patagonia (Tarr and Martin, 1913, Prospero et al., 2012, Bullard et al., 2016). Most of the loose material in Iceland comes from glacial sediments carried by glacial meltwater that fills floodplains, from volcanic ash produced during explosive eruptions, and the erosion of old lava fields (Figure 3.1). With a lack of vegetation to hold sediment in place, material is easily suspended into the atmosphere (Arnalds, 2010, Thorsteinsson et al., 2011, Arnalds et al., 2016). Aeolian transport flux of particulate matter (PM) in Iceland ranges from 0.5 - 500 Mg/yr, whereas for comparison the west of the Sahara is at a maximum 10 Mg/km^2/yr; Iceland is a major dust source on Earth (Duce et al., 1991, Arnalds, 2005, Gíslason, 2008).

Glacial floodplains, which serve as established source areas for suspendable material are constantly being resupplied with new material. Typically, 650 Mg/km^2/yr of sediment travel through glacial rivers, some of which is deposited in the floodplain region (Gíslason, 2008). However, during jökulhlaups, i.e. glacial floods, which last on the order of days to weeks, the amount of sediment carried by the rivers is greatly increased to 1200-1400 Mg/km^2/yr, potentially providing even more material able to be suspended (Tómasson, 1990, Hardardóttir and Snorrason, 2002, Hardardóttir et al., 2005, Gíslason 2008).

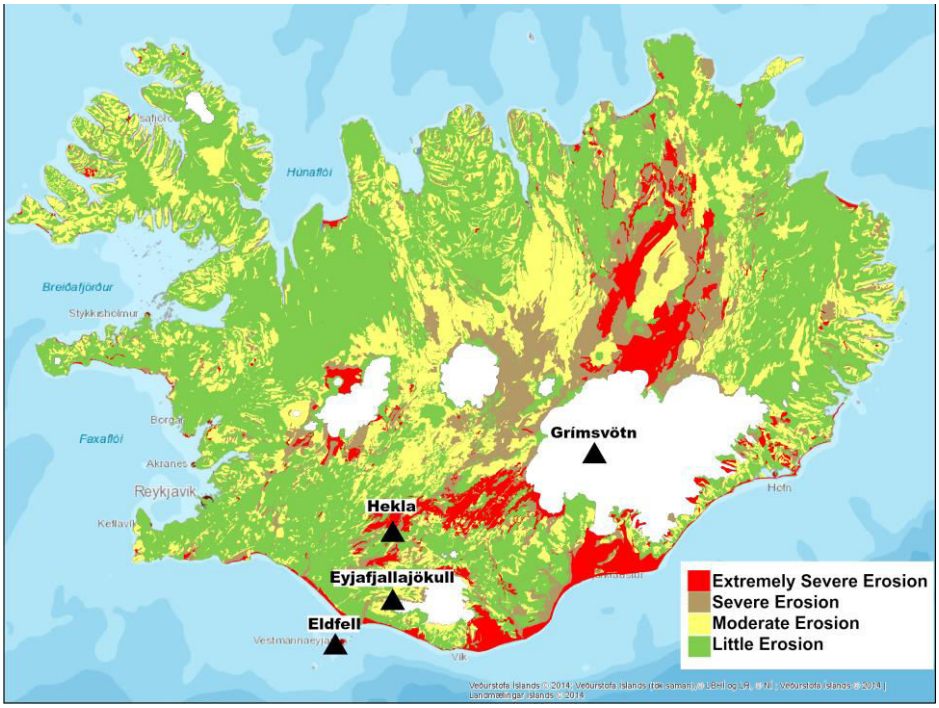

Figure 3.1: Severity of erosion map of Iceland as well as glacier locations marked in white. Original erosion map data provided by the Agricultural University of Iceland and Soil Conservation Service (Arnalds et al., 2001b). Access to dataset provided by the Icelandic Meteorological Office.

The PM from volcanic eruptions can be a part of glacial sediment, as PM deposited on glacial surfaces can be incorporated into the ice through snow or rainfall moving the PM into the glacier surface or burying and incorporating it (Arnalds, 2010; Prospero et al.,

2012; Thorarinsdottir and Arnalds, 2012; Bullard, 2013; Dagsson-Waldhauserova et al., 2013). The source areas for PM events typically are areas that are classified (by severity) to have little (green), moderate (yellow), and extreme (red) erosion (Figure 3.1) which cover roughly half of Iceland (~51,000 km^2) (Arnalds et al., 2001b). The largest source areas for natural PM in the atmosphere over Iceland are mainly along the south coast and west and north of Vatnajökull glacier, the largest ice cap in Iceland (Figure 3.1). These source areas are frequently exposed to strong winds and have very little vegetation to keep the loose material in place (Arnalds et al., 2001b).

Large PM events are possible in Iceland because of frequent high wind speeds due to large pressure gradients as low-pressure systems pass through the area (Einarsson, 1984). Mesoscale features, such as thermal circulations that can form along some mountain sides and land use boundaries, e.g. between cultivated land and glacial outwash plains (sandur areas), are also responsible for producing high winds (Arnalds et al., 2016, Bullard et al., 2016). High winds coupled with loose sediment, create an environment favorable for dust events; i.e. PM suspension.

Airborne particulate matter of any size is a risk to human health, but particles with diameters equal to or less than 2.5 μm ($PM_{2.5}$) are especially harmful (Neuberger et al., 2004, Boldo et al., 2006, Horwell and Baxter, 2006, Kampa and Castanas, 2008, Kinney, 2008, Anderson et al., 2012, World Health Organization, 2013). Due to its chemical and physical properties, such as morphology, volcanic ash can be associated with an increased risk of respiratory illnesses compared to dust or sand (Horwell and Baxter, 2006, Horwell, 2007). The size distribution of volcanic ash typically ranges between 0.3 — 1000 μm with up to 20% of the ash in the size range most able to affect the respiratory system (Horwell, 2007, Gislason et al. 2011, Thorsteinsson et al., 2012). Fresh volcanic ash also can be coated with volatile acids or polycyclic hydrocarbons, as well as other simple organic compounds, which are formed from post-emission reactions of CO and H, adding to the potential health risk due to increased toxicity (Horwell et al., 2003, Geptner et al., 2005, Horwell and Baxter, 2006). Volcanic ash can be in the form of long angular fibers, creating a similar respiratory hazard as asbestos (Horwell and Baxter, 2006, Gudmundsson, 2011, Dagsson-Waldhauserova et al., 2015). While fresh volcanic ash may not initially be in this form, it can evolve into these crystal structures over time due to weathering (Horwell and Baxter, 2006). Volcanic ash can be deposited on the surface and remobilized or resuspended by aeolian processes long after an eruption has ended (Liu et al., 2014, Beckett et al., 2017).

When considering all forms of visible PM in the atmosphere (including suspended dust, volcanic ash, and haze, which can be mostly water droplets with dust mixed in), there are, on average, 135 dust days annually (Dagsson-Waldhauserova et al., 2014b). Where a dust day is defined when any form of PM is observed in Iceland by at least one trained weather observer or by an automatic station that can detect PM. PM observations can range in type from haze, ash, dust whirls, up to extreme dust storms. Most observations of dust are made by the weather observers in South Iceland. In South Iceland, there are more weather observers located close to significant PM source areas, while fewer weather observers live close to significant PM source in other parts of Iceland. In this paper, we identify “dust events” when there is PM in the atmosphere observed by a weather observer. The observations of dust include time periods between and during eruptions (Larsen et al., 2018). Iceland experiences, on average, 20–25 volcanic eruptions per century. Of these

eruptions, 91% are categorized as either "explosive" or "mixed," releasing ash into the atmosphere (Thordarson and Larsen, 2007).

This study provides an analysis of dust event frequency in Iceland, considering the temporal proximity to explosive, ash-producing eruptions, over the fifty-year time period 1966–2016. An explosive eruption is defined as an eruption where the Volcanic Explosive Index (VEI) is greater than zero, meaning the volume of emitted tephra is greater than 10^4 m^3 (Newhall and Self 1982; Houghton et al. 2013). During this fifty-year study period, there were 12 explosive eruptions from four volcanoes, and the VEIs of these eruptions ranged from one to four (Figure 3.1, Table 3.1) (GVP, 2018, Larsen et al., 2018). We utilized fifty years of observations because this length of time allows us to observe 12 volcanic eruptions and is sufficiently long for us to discern seasonal effects on the frequency of dust events. We are interested in the frequency, location, and factors affecting dust events because this knowledge is key for understanding, forecasting, and communicating to vulnerable communities about such socially relevant things such as air quality alerts, poor visibility, aviation hazards from volcanic ash and/or resuspended volcanic material, as well as protection of infrastructure; for example, dust abrasion on buildings, vehicles, or other infrastructure. This analysis can be used by the agencies responsible for monitoring ash and dust to help optimize the distribution of resources, for example it can help provide input for choosing if stations should continue to be manned by weather observers, or where (less resource-consuming) automatic weather stations might be sufficient.

Table 3.1: Explosive eruptions during 1966-2016 with corresponding explosive phase dates and VEI. Total volume of tephra for the Hekla 1980 and Hekla 1981 were combined due to their temporal proximity to each other.

Volcano	Explosive Eruption Start Date	Explosive Eruption End Date	# Days	VEI	Tephra Volume (10^7 m^3)	Reference
Hekla	1970-05-05	1970-07-05	62	3	7	Thordarson and Larsen, 2007
Eldfell	1973-01-23	1973-06-28	157	3	2	Self et al., 1974; Williams et al., 1976
Hekla	1980-08-17	1980-08-20	4	3	6	Thordarson and Larsen, 2007
Hekla	1981-04-09	1981-04-16	8	2		
Grímsvötn	1983-05-28	1983-06-02	6	2	< 0.1	Gudmundsson and Bjornsson, 1991
Hekla	1991-01-17	1991-03-11	54	3	2	Thordarson and Larsen, 2007
Grímsvötn	1996-09-30	1996-11-06	38	3	1	Gudmundsson et al., 1997
Grímsvötn	1998-12-18	1998-12-28	11	3	10-14	Gudmundsson et al., 2000
Hekla	2000-02-26	2000-03-08	12	3	1	
Grímsvötn	2004-11-01	2004-11-04	4	3	4.7	Jude-Eton et al., 2012
Eyjafjallajökull	2010-03-20	2010-06-23	96	4	27	Larsen et al., 2018
Grímsvötn	2011-05-21	2011-05-28	8	4	38	Marzano et al., 2013

3.2 Methods and Data

The PM observations from 61 synoptic weather stations operational during the 1966-2016 study period were used (Figure 3.2a, Appendix A). Twenty-five stations were operational for the entire 50-year period, 25 were operational for at least 20 years, and the remaining 11 stations were operational for at least two years (Figure 3.2A). PM observations were made by weather observers who visually saw any form of suspended material in the air, and classified it as either haze, dust whirls, dust/sandstorms and suspended dust (SYNOP codes 4-9, 30-35; FM 12 SYNOP, WMO, 2015, Table 2.1). Observations include material within the field of view of the weather observer and in the air at the weather station. Observations were typically made every three hours between 0600 and 2400 UTC; some stations started reporting at 0900 UTC. Reports were sporadically made outside of these regular hours; such events were typically larger in size so easily seen. During the 50-year period of this study, over 22,000 PM observations were made in Iceland, with an average of 437 occurring every year. Many observations occurred on the same day) as well as at more than one weather station (which would be grouped together as one dust day).

There has been no long-term monitoring of PM throughout Iceland. PM_{10} and $PM_{2.5}$ measurements have been made for several years in Reykjavík operated by the Environmental agency. The focus of these measurements is urban pollution, while this study is focusing on PM related by natural sources. In the past, instrumentation such as Optical Particle Counters (OPCs), dust filters, and dust traps have been deployed temporarily. These deployments typically occurred during or shortly after an eruption. During the last five years, OPCs were operated from time to time at a few places, but this sporadic monitoring of PM in Iceland is not enough to determine any background levels and to correlate PM concentrations with ash dispersion due to volcanic eruptions.

Because there are many possible sources of particles in Iceland, i.e. dust, ash, sea salt, and anthropogenic PM, it is necessary to include wind direction data in the analysis. The wind direction assists in determining the source of PM. It is assumed that if PM was observed when the wind was coming from inland it was most likely from the source areas of Iceland. This assumption is made because there are very few anthropogenic sources of PM in Iceland (EEA, 2017). In addition, chemical analysis cannot be done for all of Iceland to determine exact sources. A subset (24 stations) of the 61 stations were chosen for wind direction analysis. These 24 stations were along or near the coast, as PM observations from these near-coastal locations are more likely to include non-dust or volcanic ash observations compared to weather stations in interior Iceland (Figure 3.2B). Therefore, in the analysis it was easier to exclude PM observation caused by sea salt because these events are connected to a certain wind direction for each station. This analysis is intended to remove a regional bias in the data analysis due to the proximity to the ocean.

In order to analyze the effects that explosive volcanic eruptions have on the frequency of PM observations, other factors, including time of year, weather, and the amount of material released from each eruption were considered. We calculated the following: a) the average number of PM observations per month for all of Iceland for the entire 50-year study period, b) the average number of PM observations per month for all stations, directly following all 12 eruptions, and c) the average number of PM observations per month for a subset of stations unique to each volcano. a) is helpful for identifying long term average conditions and will reveal impacts due to seasonality and weather conditions; b) is helpful for

identifying national-scale impacts due to additional material provided by volcanic eruptions; and c) is helpful for identifying regional-scale impacts due to additional material provided by volcanic eruptions. The subset of stations that most likely to be impacted by each volcano were chosen for the regional analysis because of their proximity to the volcano (less than 125 km), being within ash deposit areas for eruptions based on isopach maps (Larsen et al., 2018), typical wind directions, and if ash observations were made there. The Moderate Resolution Imaging Spectroradiometer (MODIS) true color and aerosol optical depth (bands 20, 30, 31, and 32) (Hao and Qu, 2007) from 2010-2016 were examined to see if suspended material after the Eyjafjallajökull 2010 and Grímsvötn 2011 eruptions came from new source areas that did not previously exist as identified high erosion areas. Despite MODIS being launched in 1999, the Hekla 2000 and Grímsvötn 2004 eruptions were not included in the satellite portion. This is because the resolution of saved imagery over Iceland is too low to see small scale features such as dust/ash/PM suspension and/or deposition areas.

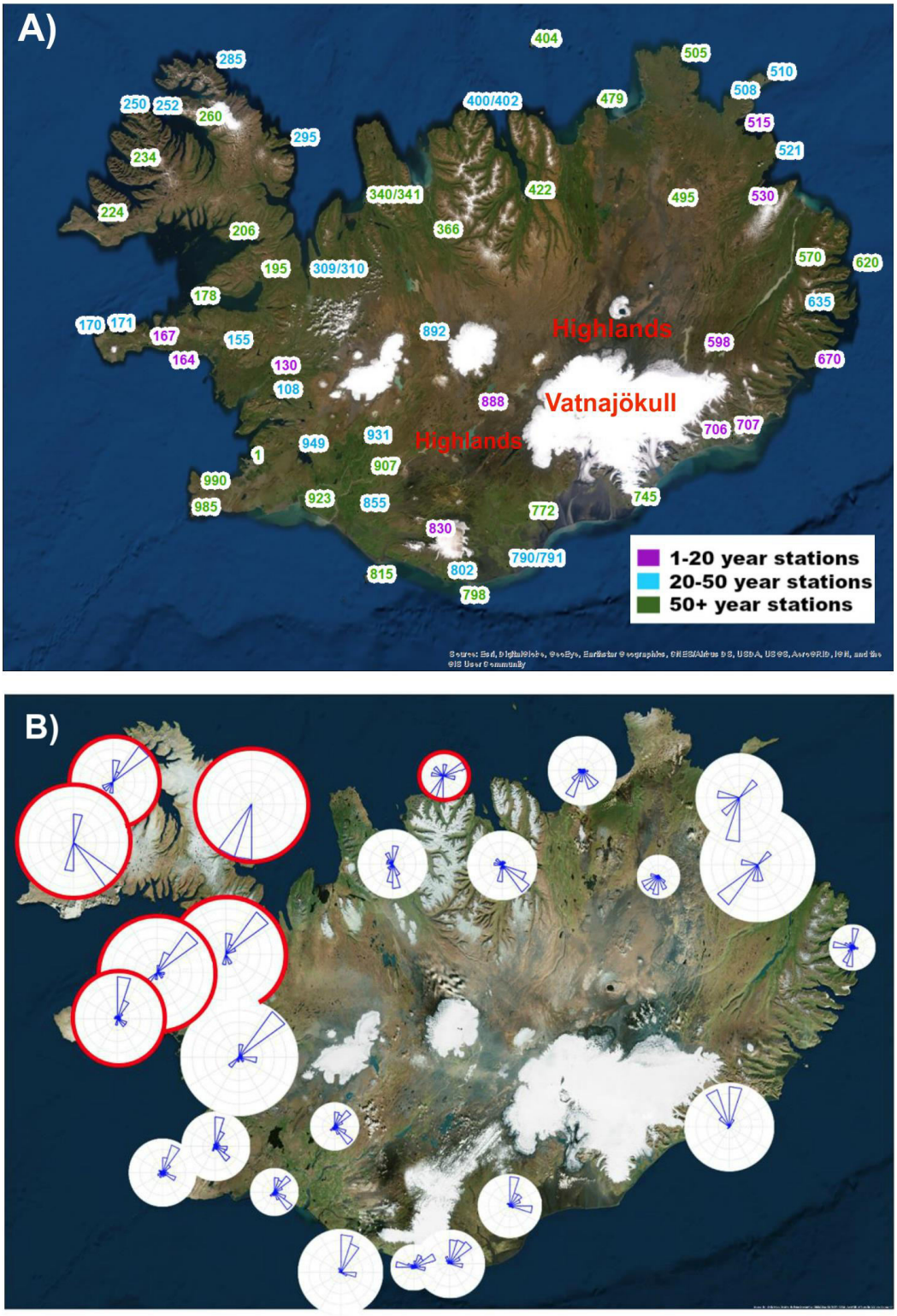

Figure 3.2: A) Map of 61 manned weather stations that were operational for at least two years during the 50-year period of 1966-2016. The color of the station corresponds to the duration the station was operational. B) Windrose map showing frequency of wind direction when PM was observed at 24 manned weather stations in Iceland (sum of frequencies is one). Stations with the majority of observed PM events not coming from a known dust source area (Figure 3.1) are outlined in red.

3.3 Results

3.3.1 Wind Direction and Source Areas

Simple determinations of PM source area and type of PM can be made by analyzing the wind direction. At coastal stations, if the wind came from the sea, then sea salt, or sometimes pollution from Europe, may be the most likely types of PM observed (Prospero et al., 1995, Liang et al., 2016). When the wind direction was directly from a known source area of dust or ash, then it is plausible that the observer was seeing resuspended ash or dust and not some other PM type.

For more than half of the PM observations (54%) at the near-coastal stations, the wind was coming directly from a large known dust source area, but for 46% of the PM observations, the wind was not coming directly from a large known dust source area. Wind roses showing the frequency of wind direction when PM was observed at coastal stations can be seen in Figure 3.2B. At seven stations (highlighted in red in Figure 3.2B), the most common wind direction does not come directly from the large source areas of the Highlands or South Coast. Most of these seven stations are in Northwest Iceland, are near-coastal, and are far from the large source areas. At stations located further inland, PM was observed when the wind was blowing directly from one of the large source areas (stations 495, 530, 772, 931). Stations that are in or next to (0-50 km) one of the large source areas (for example: 598, 888, 931, 495) show the highest variation of wind directions for all PM observations, i.e. PM can arrive to the station from multiple directions due to proximity to the source area. Stations that do not have large topographical barrier such as mountains between them and a large source area also exhibits these characteristics (for example: 1, 366, 570, 772). In this case, the source of PM is viewed as an area, rather than a point source to the observer. The variation in wind direction at these sites is expected and acceptable as the PM can be advected to the station from a larger range of wind directions, and still not come directly from the sea. These stations are unlikely to be biased by sea salt, while the seven stations highlighted in red may be.

3.3.2 Time Series of PM Observations

The monthly average number of observed PM for all stations in Iceland was calculated for the 50-year study period (Figure 3.3A) and an annual summary of the PM observations is provided in Appendix A. A distinct pattern is seen between PM observations and season. The greatest number of observations occurred roughly every spring and fall, and occasionally in summer (Figure 3.3A and 3.3B). Average precipitation for the reporting stations was also calculated. Periods of relatively fewer PM observations (1980s-2000s) occurred when there was an increase in precipitation throughout Iceland (Hanna, Jónsson and Box, 2004). This increase in precipitation is not seen very well in the data set used here because we included only stations with weather observers while the multi-decadal precipitation changes are seen clearly when the automatic stations are also included.

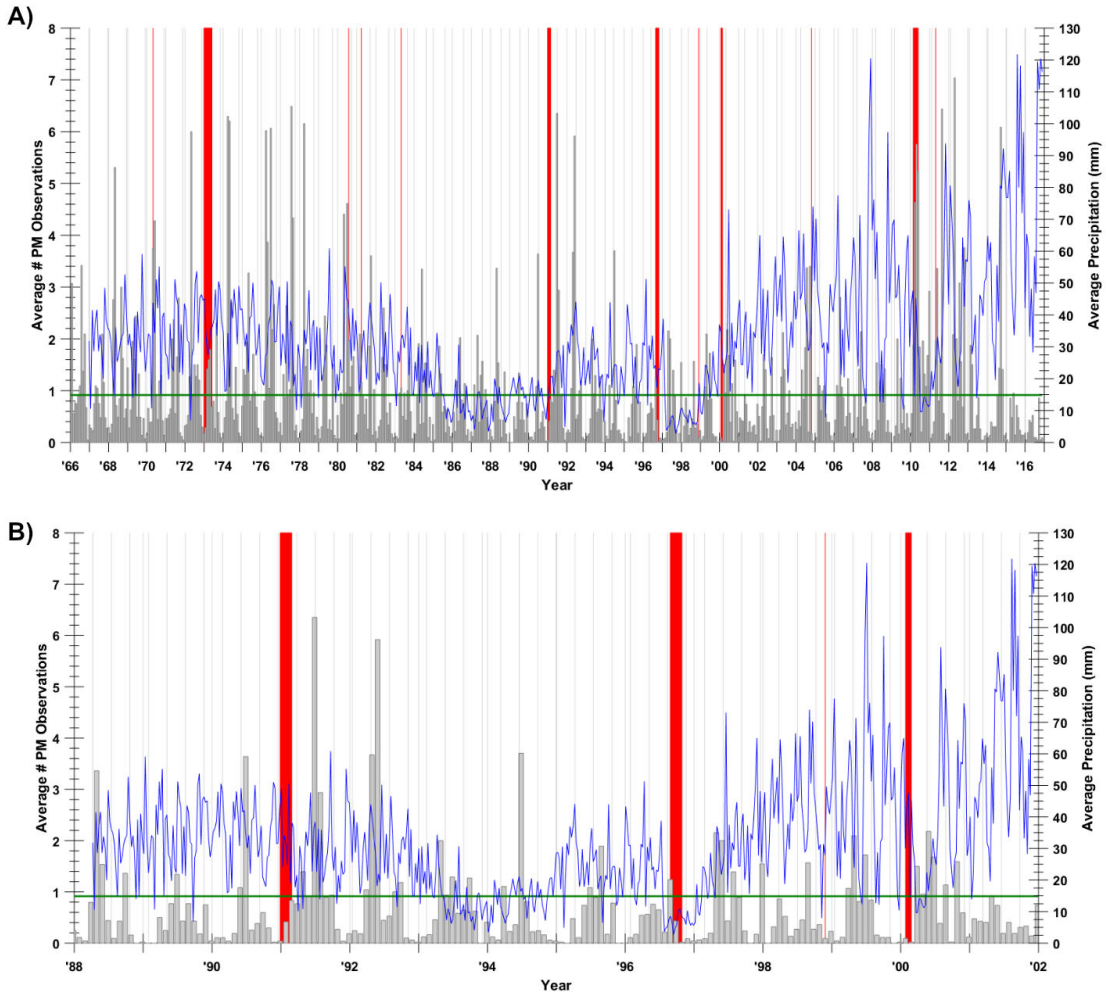

Figure 3.3: A) Monthly average number of PM observations for all manned stations in Iceland over the 50-year period of 1966-2016 (left axis, grey bars) as well as monthly average precipitation (right axis, blue line). Red vertical bars indicate the time period of explosive volcanic eruptions. Green line is the overall average number of PM observations over the entire 50-year period, used to show when observations are above or below 50 year average. B) Zoomed in portion to show seasonal cycle of PM observations.

3.3.3 Seasonal Variability of PM Frequency

The monthly average number of PM observations shows a clear correlation with the seasonal climate in Iceland (Figure 3.4). Fewer PM events occur in the winter months because of snow cover, frozen ground, and generally high amounts of precipitation that keep loose material from being suspended into the atmosphere. There is also the added factor that PM events may be missed by observers in the winter due to the lack of daylight and cloudiness during this season. A rapid increase in the number of observations occurs in the spring, with the greatest number of observations made in May, as it is one of the driest months in the country, snow cover has melted over much of the country (including the South Coast), and the surface material is not completely saturated with water (Einarsson, 1984, Hanna, Jónsson and Box, 2004). June is typically as dry as May (on an Iceland-wide scale), however, there are fewer PM observations in June and the rest of summer than in May. The weakening of the Icelandic Low brings a shift in the jet stream and storm tracks,

resulting in lower wind speeds in Iceland during summer. On the national monthly scale, mean wind speeds decrease from 6-7 m s^{-1} (May) to 4-6 m s^{-1} (June, July, August), and as a result, less surface material is picked up by the wind (Einarsson, 1984, Serreze et al., 1997). An increase of precipitation in July and August also occurs in the north eastern part of the Highlands, further decreasing PM events (Einarsson, 1984; Hanna, Jónsson and Box, 2004). An increase in observations is seen in September as winds strengthen during the fall. The average number of observations is lower in the fall than in the spring, as fall is the wettest season in Iceland (Hanna, Jónsson and Box, 2004).

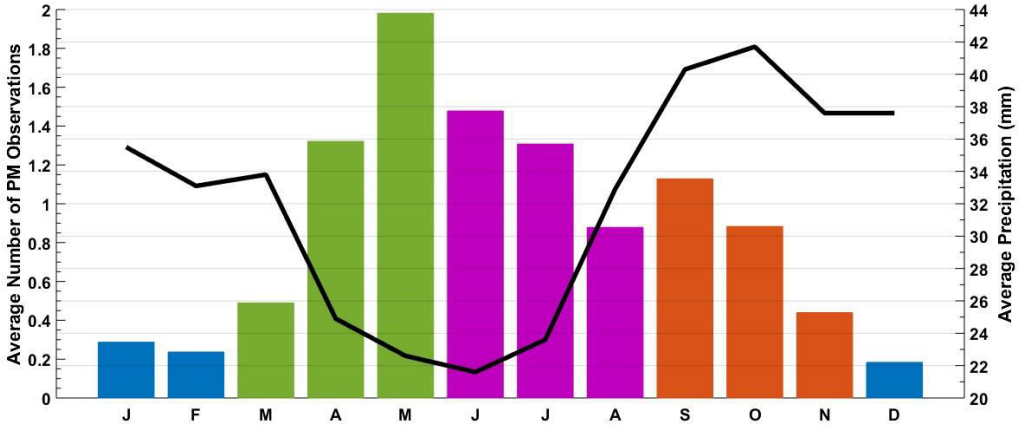

Figure 3.4: Average number of PM observations by month for all manned stations in Iceland 1966-2016. Colors denote season, blue: winter, green: spring, purple: summer, and orange: fall. Average precipitation is also included for each of these months (right y-axis).

3.3.4 Frequency of PM Immediately Following Eruptions

Explosive volcanic eruptions occur approximately every three to four years in Iceland (Table 3.1). Within the 50-year study period, 6 of the 12 eruptions ended in either spring or fall, the peak seasons for suspension of material; five eruptions ended during the summer, and only one ended in winter. After all eruptions, the expected seasonal variation of PM observations is seen with the highest number of observations occurring in snow-free and windy periods (Figure 3.3). In Figure 3.5 the average number of PM observations that occurs in a given time since an eruption over all of Iceland is shown, as well as the number of eruptions that have a given number of months until the next eruption. Six eruptions (Eldfell, Grímsvötn ‘83, Hekla ‘91, Grímsvötn ’00, Grímsvötn ‘04, Grímsvötn ‘11) were followed by 57 months before the next eruption began (Figure 3.5). The anomalously high number of observations made in month 86 is due to observations made in a single month of particularly windy and dry conditions in parts of Iceland (August 1990) (Figure 3.5) (Hanna et al., 2004). On the basis of including all manned weather stations (61 stations) across the country, no trend in the number of observations can be attributed to an enhancement in available material sourced by an eruption.

In order to examine if there is a detectable increase in the number of PM observations following an eruption on a regional scale, rather than considering nation-wide observations, a subset of stations was chosen for each of the four volcanoes active during

the study period. Five stations were chosen for each volcano based on their proximity to the eruptive volcano and the most common wind directions (Figure 3.6).

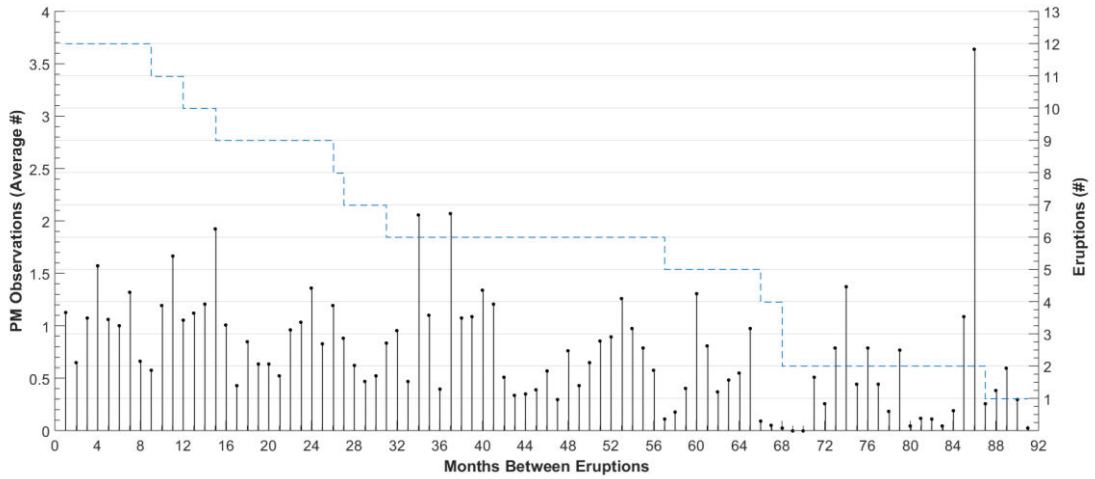

Figure 3.5: Cumulative number of months between eruptions (blue line, right y-axis). Average number of PM observations for each month after the end of all 12 eruptions for all of Iceland (grey bars, left y-axis).

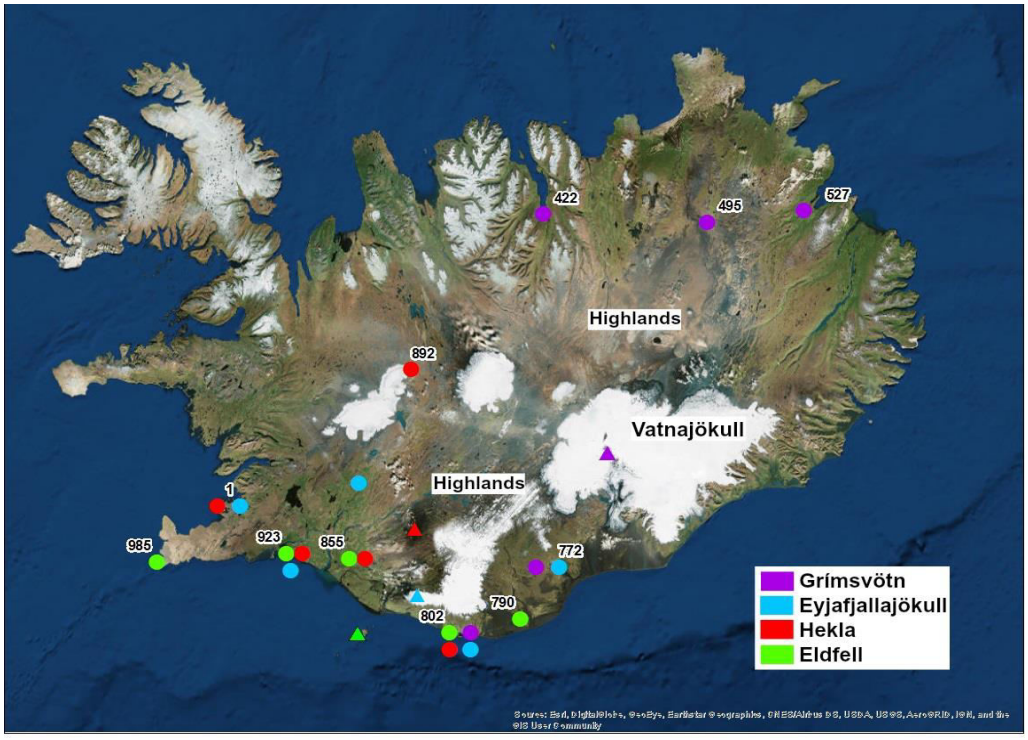

Figure 3.6: Stations used for the regional-scale analysis directly following individual eruptions. Triangles indicate volcanoes. Circles in each color indicate the stations included in the analysis for each volcano.

Increases in the number of observations following an eruption are defined to be when the average number of observations for a month (bars in Figure 3.7), averaged for the subset of stations most sensitive to a volcano´s deposits, is at least double the fifty-year average for those stations (vertical lines in Figure 3.7). Such increases in observations are identified for six eruptions: Hekla 1970, 1980, 1981, 1991, Eyjafjallajökull 2010, and Grímsvötn 2011 eruptions. All except one (Hekla 1981) of these eruptions had VEI 3 or greater, and the post-eruption periods did not begin during winter. These eruption characteristics, however, are insufficient to forecast if ash from an eruption may lead to an increase in the number of particulate matter observations. Six other eruptions had VEI 3 or greater and the post-eruption periods did not start during winter, however, in the number of PM observations did not increase. We suggest as possible explanations, which are not verifiable given our dataset, for why some eruptions show an increase and others do not: 1) weather conditions on a smaller than reported scale; 2) small-scale ground features where ash is deposited (e.g. is on cliffs that are generally protected from precipitation, compared to areas in the open and exposed to the weather), 3) observations being missed due to PM transported through uninhabited areas where there are no observation stations, 4) observations being missed due to darkness. For all of the eruptions, some of the increases in observations following the eruption can be attributed to the non-eruption-related variations in wind speeds or wind directions, and not unambiguously attributed to an increase in material being able to be suspended from ash from the eruptions.

There is an increase in PM observations after the Eldfell 1973 eruption, which was not twice as high as the background, and therefore does not meet the criteria established for this work to be considered a post-eruption increase. We will discuss this smaller-than-the-criteria increase, however, because it clearly exemplifies one of the reasons that there is ambiguity in attributing post-eruption PM increases to an increase in available material. Following this eruption, greater numbers of observations were made when winds were more frequently coming from the Highlands and the sandur plains of the South Coast, large source areas on mainland Iceland (north and northeasterly winds). Winds coming from the Eldfell eruption site would have been southerly. A post-eruptive increase in PM observations is not unambiguously attributable to the eruption as weather features still have a strong role in changing the number of PM events.

Following the Hekla 1970 eruption, the months with typically high wind speeds (September, June, and May) had the highest average number of PM observations as compared to months when an increase in PM observations was not observed.

Hekla 1981 was the only eruption in which the VEI was less than three, and had an increase in observations, but due to the temporal proximity of the Hekla 1980 eruption, this increase could be attributed to ash produced during Hekla 1980.

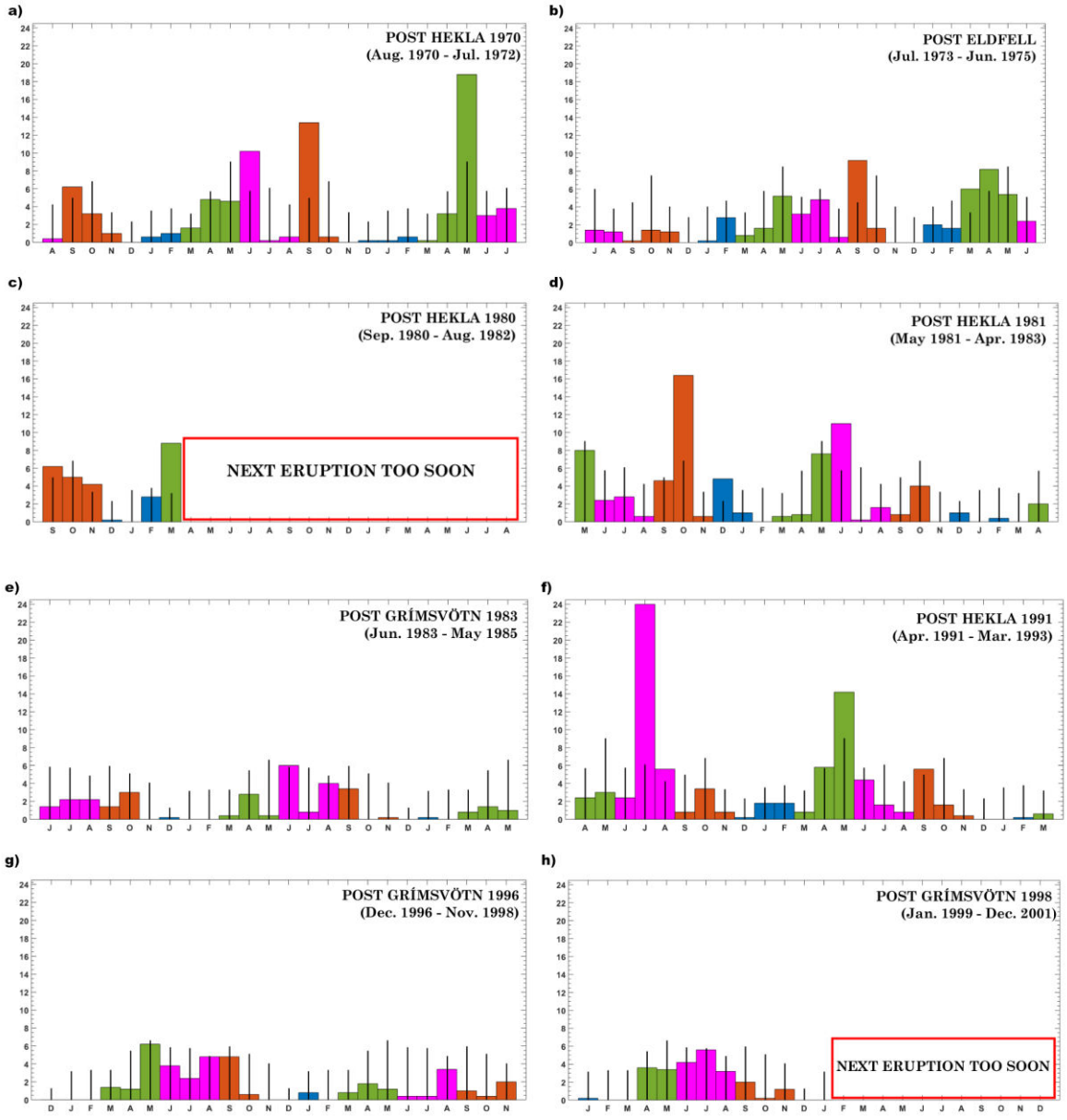

Figure 3.7 (part 1): Number of PM observations for the two years directly following each of the 12 eruptions for the subset of stations shown in Figure 3.6. The color of each bar indicates the season as in Figure 3.4. The vertical black lines are the fifty-year average number of observations for the subset of stations for each volcano. "NEXT ERUPTION TOO SOON" indicates when the following eruption began within two years (i.e. the country-wide repose time was less than two years).

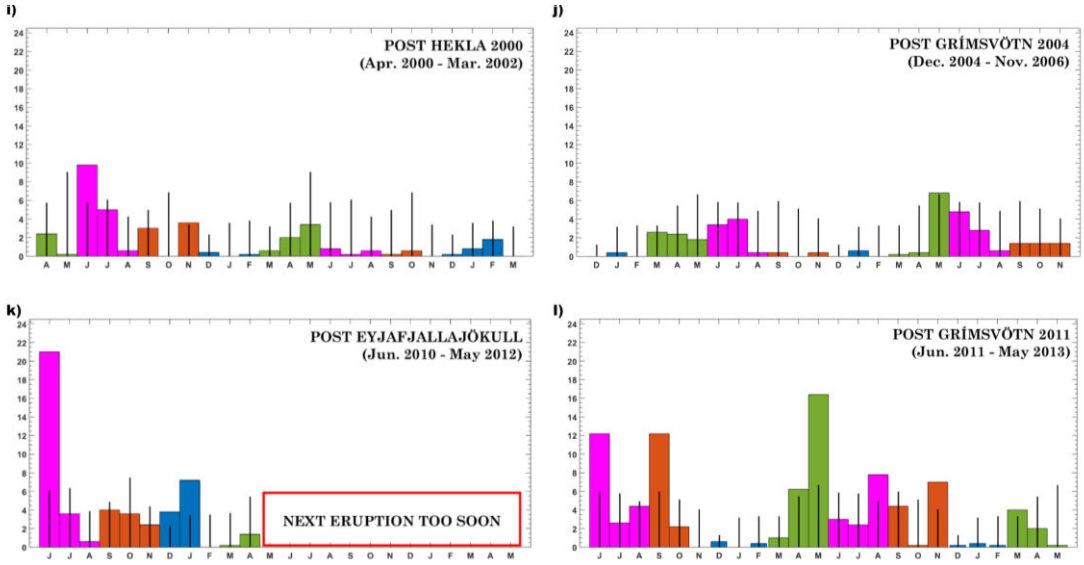

Figure 3.7 (part 2): Number of PM observations for the two years directly following each of the 12 eruptions for the subset of stations shown in Figure 3.6. The color of each bar indicates the season as in Figure 3.4. The vertical black lines are the fifty-year average number of observations for the subset of stations for each volcano. "NEXT ERUPTION TOO SOON" indicates when the following eruption began within two years (i.e. the country-wide repose time was less than two years).

3.3.5 Satellite Confirmation of Source Areas

With close examination of satellite data, it was found that new source areas of PM following explosive eruptions were gone within two years following the two considered eruptions (Eyjafjallajökull and Grímsvötn '11) (Figure 3.8). Vegetation grew back, washout of the surface occurred, and seasonal snowfall covered and incorporated ash layers into the glaciers. Suspension of material after this point came from areas known for dust suspension.

A post-eruptive increase in the number of PM observations could be attributed to new source material provided by ash generated during the eruptions. For a few months following Eyjafjallajökull 2010, material was sporadically suspended from the surface of the glacier, detectable by satellite during cloud free days (Figure 3.8A). However, after the seasonal snow cover formed, material was no longer seen in the satellite images as coming from the glacial surface. During the spring and summer of 2011, material that appeared to have a source area on the glaciers and icecaps was a result of the Grímsvötn 2011 eruption, but not Eyjafjallajökull 2010 (Figure 3.8B). Once snow began to cover ash deposits on the glaciers and the Highlands, material from these new source areas was no longer suspended (Figure 3.8C). The satellite image for August 2012 (Figure 3.8D) shows the material embedded into the near surface of outlet glaciers from Vatnajökull, but this material is very unlikely to become suspended in the atmosphere directly from the glacier. Suspension is unlikely because it would require a layer of ash to be exposed on the surface and simultaneously dry enough to be suspended by the wind (Liu et al., 2014). It is more likely that this material will be removed from the glacier through melt water and then potentially suspended later from a dried flood plain. All other source areas seen from the 2012-2016

satellite images already existed as known dust source areas prior to the 2010 and 2011 eruptions.

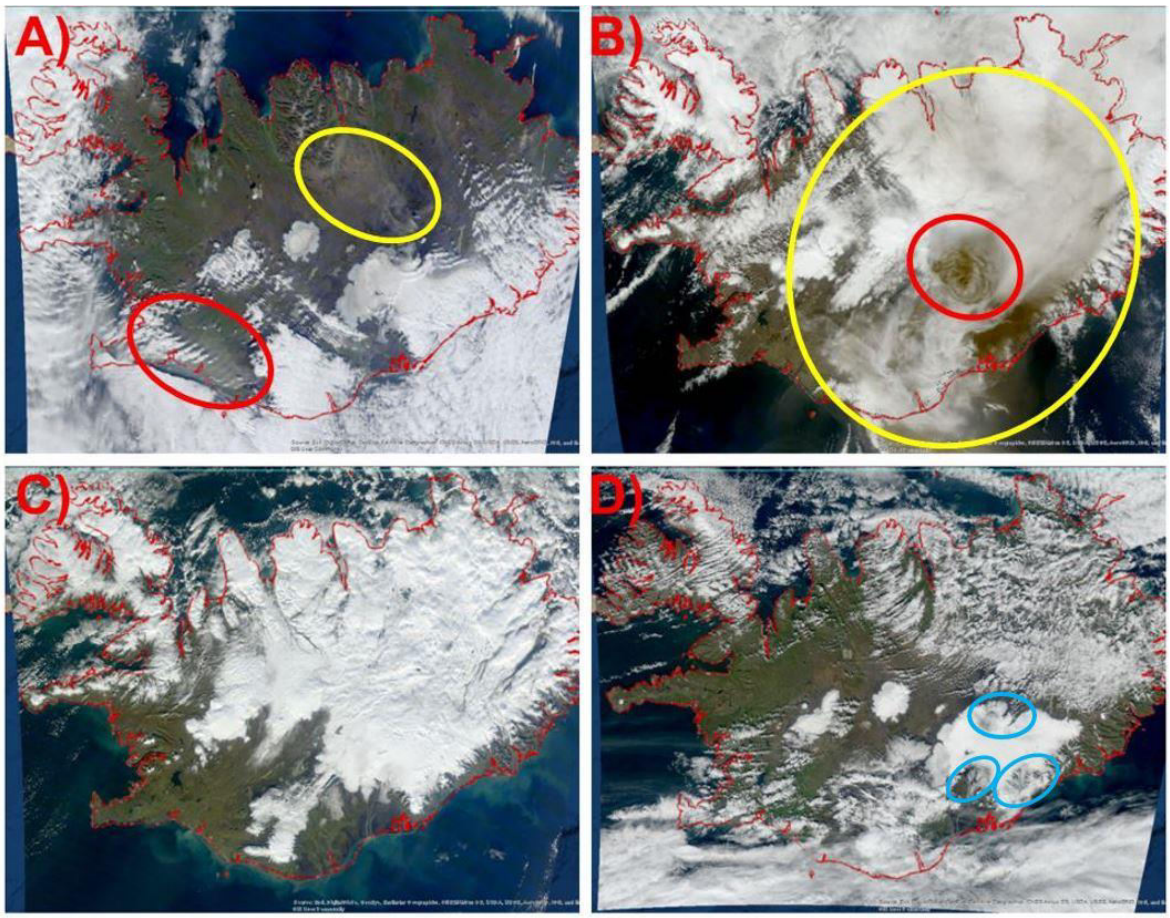

Figure 3.8: True color MODIS satellite imagery over Iceland (courtesy of the Icelandic Meteorological Office). A) September 2010, five months after the end of the Eyjafjallajökull 2010 eruption. All icecaps and glaciers as well as surrounding area around eruption site are seen to be darkened by ash deposits. A dust storm is seen in the highlands (yellow circle) as well as coming off the Eyjafjallajökull glacier (red circle). B) May 2011, during the Grímsvötn 2011 eruption. The volcanic eruption can be seen (red circle) as well as the dispersion of ash and possibly dust throughout Iceland (yellow circle). C) October 2011, five months after the end of the Grímsvötn 2011 eruption. Snowpack covers the highlands and ice caps hiding any evidence of fresh ash deposits. D) August 2012, over a year after the end of the Grímsvötn 2011 eruption. The only evidence of a recent eruption is visible ash on the surface of the ice caps and glaciers (blue circles).

3.4 Discussion and Conclusions

On an Iceland-wide scale, the availability of recently produced ash does not have a detectable impact on the number of observations of particulate matter. This is due to the enormous availability of loftable material from the known inland source areas. This is supported by the finding that most of the PM observed at near-coastal weather stations with a weather observer in Iceland comes from inland, as opposed to particles coming from

the ocean, such as sea salt or aerosol. Additionally, stations that are near the known inland source areas, or have an unobstructed path from a source area, exhibit the most variability in wind directions during PM observations (Figure 3.2). Stations located near the edges of source areas have much more consistent wind directions during PM observations with the most common wind directions during observations at these stations being directly from a source area. This, however, does not prove that PM observed while winds were not coming directly from a source area was definitely not from a major source area. The observed PM could have been lofted and looped around in circulation patterns. However, we do assume the simplest directional transport in our analysis for determining source area.

The greatest numbers of PM observations are made in spring and summer. Seasons are the driving factor for PM observations. The timing of snowmelt, surface dry out, and strong winds from persistent weather patterns are all visible in the monthly meteorological patterns and reflected in the of numbers of PM observations. Dust events occurring during summer are often spatially localized, as they are dominated by mesoscale wind circulations and influenced by downslope winds. There is a small increase in observations at the beginning of fall as winds strengthen and synoptic scale wind storms approach Iceland (Serreze et al., 1997). This increase does not persist, as fall, on average, has the greatest amount of precipitation. Major source areas, especially in the Highlands, become covered with snow early in fall. Despite the high winds that can occur during the winter months, there are few PM observations during this time because of snow and ice covering the loose surface material. Moreover, the prolonged darkness of winter may make some PM events impossible for observers to see, and, as a result are not recorded. Past meteorological studies have shown that for about a 20-year period (1980-2000) more precipitation was falling in all of Iceland (Einarsson, 1984). Our data shows that this caused a decrease in the number of PM observations made during this time. During drier periods, the number of dust observations increased.

The additional material available to be suspended provided by recently produced ash has less of an effect on the number of PM events than seasonal and climatological conditions. When considering all manned weather stations in Iceland, there is no detectable increase in PM observations immediately following eruptions, and no detectable diminishment in PM observations in the months following an eruption, as this additional material could be presumed to decrease in availability. However, examining the impact of individual eruptions on a regional (125 km) scale revealed that some eruptions with VEI 3 or greater, not ending in winter, had increased PM observations in some individual months within two years post-eruption. Not all eruptions of this size and timing had an increase in PM observations; and the increase is not seen consistently for more than one month at a time. Stations that are near, or that are in the most common downwind direction of the volcanoes, may see a higher than average number of PM observations at least once during the following spring, summer, or fall, for example, station 798 after the Eyjafjallajökull eruption in 2010. The intensity and timing of the increase is largely dependent on weather conditions following the eruption. Dry windy months following an eruption are the most conducive to enhancing the number of PM observations relative to the long-term average (e.g. Hekla 1991, Eyjafjallajökull 2010, Grímsvötn 2011) (Figure 3.7). An increase in PM observations can be attributed in some months to the volcanic eruptions, however, no new long-term source areas were formed from the eruptions in this fifty-year study period, as seen through satellite images, personal communications, and field observations. As seen from satellite images of ash deposits from the 2010 and 2011 eruptions (Figure 3.8),

deposits on not already existing source areas dissipate within a few months after the eruption. Suspension events from these short-term source areas do not occur as frequently as events from the known, persistent source areas, which may include volcanic ash. Deposits on glaciers need to be dry enough for suspension to occur directly from the glacier surface. Due to orographic precipitation that occurs over the glaciers and icecaps, sufficiently dry conditions can be hard to achieve (Liu et al., 2014). The deposits are readily buried by snow and even if they become exposed at the surface the following summer, they are saturated with water from snow and ice melt and precipitation, and are more likely to be washed away with melt water than to be lofted into the air. Material that leaves the glaciers via melt water can later be suspended from dried riverbeds and floodplains (i.e. the known dust source areas).

The number of observations of PM suspension events may be a minimum value, as events may have occurred which were missed by the observers. The events may have been missed due to their distance from the observers, or because they occurred during darkness when they would not be visible. An additional factor is the decrease in the number of manned weather stations in Iceland over the study period, especially during the most recent ten years. However, there is no indication that the missed events due to decrease in observers would bias the results of this study. In the future, similar studies could potentially be made with data collected by automatic visibility sensors and ceilometers, allowing for full time monitoring. Such monitoring and studies have already been done in larger dust source areas (e.g. Sahara, Asia, Middle East) (Washington et al., 2003, Pérez et al., 2006, Wang et al., 2008).

Explosive volcanic eruptions create new loftable particulate matter, thereby increasing the amount of material available to be suspended in Iceland. This is, however, too small a signal to be seen on a national scale. These new source areas do not persist for a long period of time, but the produced material does add to preexisting source areas.

4 Influence of the Weather Conditions for Particulate Matter Suspension following the 2010 Eyjafjallajökull Volcanic Eruption

This chapter is in preparation and will be submitted to the Bulletin of the American Meteorological Society in 2019. The co-authors are Sibylle von Löwis, Melissa A. Pfeffer, and Throstur Thorsteinsson.

Abstract

The 2010 eruption of Eyjafjallajökull produced volcanic ash that was mostly deposited to the south and east of the volcano with the thickest deposits closest to the main eruption vents. For months following the eruption there were numerous reports of resuspension of volcanic ash made by weather observers on the ground. An Optical Particle Counter (OPC) located to the south of Eyjafjallajökull measured post-eruptive particulate matter (PM) suspension events, some of which were also observable by satellite imagery. Visible satellite images show that PM measured by the OPC originated mostly from the slopes of Eyjafjallajökull where ash from the 2010 eruption was deposited. PM events were only detected by this OPC when winds had a northerly component or coming from the slopes of Eyjafjallajökull towards the instrument. These PM events were likely dominated by the recently deposited volcanic ash and are therefore considered to be ash resuspension events. During the detected ash resuspension events, most of the particles were 1 µm and smaller. During the largest observed events, particles of up to 10 µm were also suspended but in extremely low concentrations (< 1 particle/cm^3). The weather conditions during the observed PM events were typically windy and dry. During the largest events, winds were at least 5 m/s with a relative humidity < 70%. Ground conditions in Iceland quickly change from unfavorable to favorable for the suspension of particles. It is hypothesized that this is due to the overall porosity of the surface material allowing water to filter through quickly, as well as the fast drying time of surface material. The moist conditions of Iceland in terms of the atmosphere and the ground do not appear to be a deterrent for large PM events to occur, as they are in other locations.

4.1 Introduction

The 39-day long eruption of Eyjafjallajökull started on 14 April 2010. The eruption emitted 270 $\cdot 10^6$ m^3 of airborne tephra, with daily maximum plume heights ranging from 3 - 10 km (Gudmundsson et al., 2010; Gudmundsson et al., 2012; Stevenson et al., 2012). Half of the airborne tephra (140 ± 20$\cdot 10^6$ m^3) was deposited on Iceland (Gudmundsson et al., 2012). Deposits ranged from a dusting to over 30 meters thick layer at the rims of the ice cauldrons that formed above the two main subglacial vents (Gudmundsson et al., 2012). The depth of the tephra deposits decreased rapidly with increasing distance from the vents. At 2 km from the vents the depth was measured to be 1 m (Gudmundsson et al., 2012). At least a dusting of ash was reported everywhere in Iceland except for in the West Fjords (Gudmundsson et al., 2012). Most of the ash measurements were made to the south and east of the vent, where ash deposits were initially between 1 - 15 cm (Figure 4.1) (Gudmundsson et al., 2012; Arnalds et al., 2013).

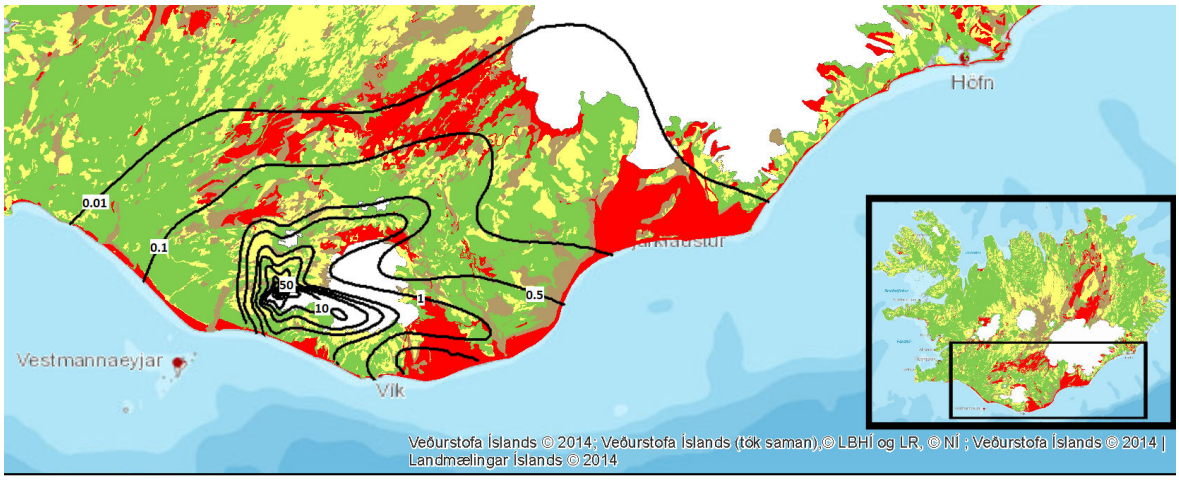

Figure 4.1: Isopachs of tephra thickness from Eyjafjallajokull 2010 eruption in cm over the dust source map of Iceland. Dust source map shows area of low erosion (green) to extremely severe erosion (red). (Erosion data: Agricultural University of Iceland and the Soil Conservation Service of Iceland. Basemap data: National Land Survery of Iceland. Cartography: Icelandic Meteorological Office. Isopachs courtesy of Magnus Tumi Gudmundsson.)

After the Eyjafjallajökull eruption ended on 22 May 2010, dust storms and resuspended ash events were observed frequently by weather observers throughout Iceland. Both dust storms and resuspension of ash are defined here as particulate matter (PM) events. Particulate matter is composed of any solid suspended material in the atmosphere. These particles could come from smoke, dust, and volcanic ash (AMS, 2012). The amount of time following an Icelandic eruption that PM events occur that contain mostly resuspended ash as opposed to the bulk material available for dust storms, is primarily dependent on the weather conditions and secondarily on the amount of material produced by the eruption (Butwin et al., 2019a) Typically, ash provided by an eruption can increase the number of PM events above the background levels for less than one year (Butwin et al., 2019a). Ash can be resuspended for longer than one year but is generally accompanied by so much other available material that the PM event is not mostly composed of resuspended ash. May, the month the 2010 eruption ended, is generally the month with the most frequent PM observations in Iceland when there are dry surface conditions due to little precipitation

and high winds, regardless of whether ash has recently been deposited by an eruption (Dagsson-Waldhauserova et al., 2014a; Butwin et al., 2019a). In 2010, southern Iceland experienced drier conditions than average, warmer temperatures, and below average wind speeds (Petersen, 2010; IMO, 2011). With the dry conditions and warm temperatures, there was also unusually little snow cover in the south, allowing PM, including the recently deposited ash, to be easily suspended despite lower than normal wind speeds. The PM events in late spring 2010 were especially strong and frequent along the South Coast (Thorsteinsson et al., 2012; Arnalds et al., 2013). Suspension events are also observed during wetter and calmer periods (Dagsson-Waldhauserova et al., 2014b).

In other regions in the world that regularly experience dust storms, such as China and the Southwest United States, the meteorological conditions that create favorable conditions are often driven by synoptic scale systems such as the passing of cold fronts or low pressure systems (Chen et al., 2003; Lei and Wang 2014). Dust events can also be started by mesoscale weather systems such as downdrafts from thunderstorms, katabatic or foehn winds (McGowan et al., 1996; Chen et al., 2003; Lei and Wang 2014). Typical wind speeds for initiation of dust suspension occurs between 5-10 m/s at the dust source (McGowan et al., 1996; Song et al., 2019). Additionally, relative humidities are typically not higher than 40% during the onset of large dust events outside of Iceland (Natsagdorj et al., 2002; Csavina et al., 2014).

In this study we analyze a set of PM events following the 2010 Eyjafjallajökull eruption in Southern Iceland, determine if the events were likely dominated by freshly deposited ash or by the bulk available dust, ascertain the properties of the PM events, and consider the meteorological conditions that led to them. We apply the results of this analysis to provide thresholds that can be used for forecasting ash resuspension events following future eruptions in Iceland and for regular dust suspension events.

4.2 Methods and Data

A mobile environmental dust monitor EDM365 was installed on a farm in Drangshlíðardalur near Skógar, South-Iceland, in September 2010, four months after the end of the 2010 eruption, and operated until 1 May 2011 (Figure 4.2 and 4.3). This is after the three-month long post-eruptive period when the ash provided by the eruption clearly increased the number of PM observations, and the number of PM events detected in Iceland by weather observers had returned to the 50-year average (Butwin et al., 2019a). The farm is approximately 15 km SSE from the eruption vents. The EDM365 is an optical particle counter (OPC) which measures particles in the size range 0.25-32 µm in 31 size bins using the scattering of light to count the number of particles in each size bin over one-minute intervals. Particles > 10 µm were excluded from this study because number concentrations were consistently < 1 particle/cm^3 in the study period. The OPC has a drying system to reduce a bias towards particles being measured as larger than they are due to enhancement by condensation during high humidity.

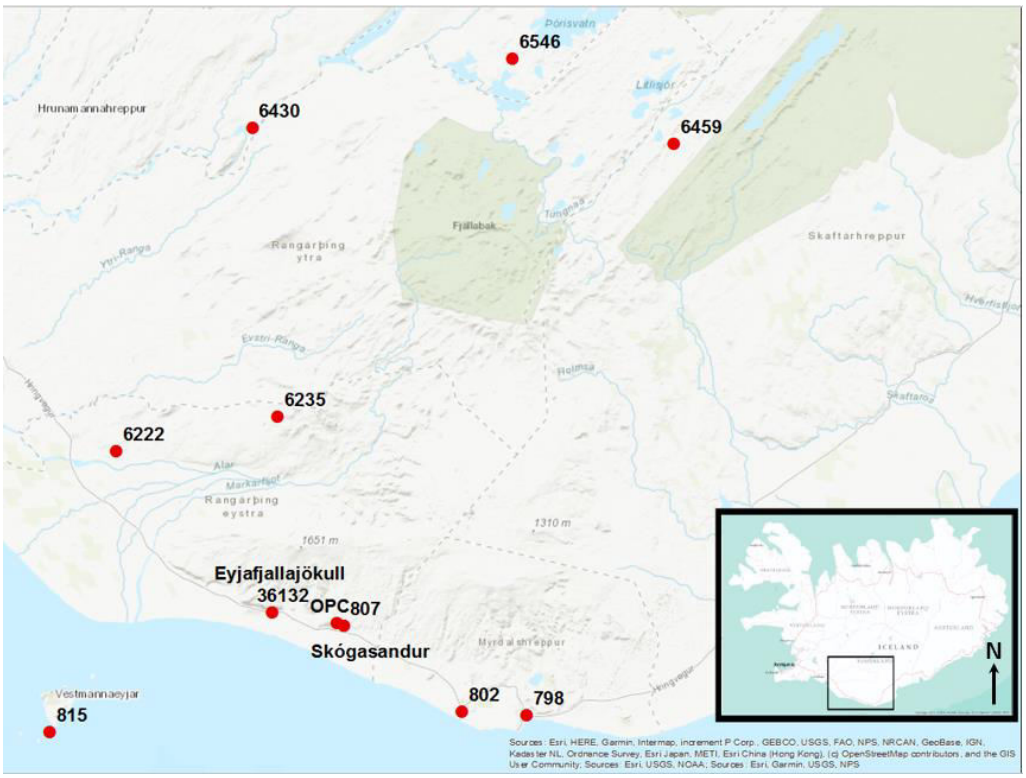

Figure 4.2: Map of weather stations (automatic, manned, and precipitation) with station number and OPC locations in Southern Iceland. See Table 4.1 for station type and exact location.

Weather data, including wind, precipitation, ground conditions, and humidity from six nearby automatic weather stations (AWS), three nearby manned weather stations (MWS), and one manned precipitation station, were used to assess the weather conditions down and upwind from the OPC (Table 4.1, Figure 4.2). OPC measurements and reports from weather observers at MWS were used to identify PM events onset, duration and severity. The weather station location and its spatial relationship to the OPC are important when integrating the weather data with respect to the weather's impact on PM events. The AWS Steinar (36132) operated by the Road Authority is the closest AWS to the OPC. Steinar is the same distance from the ocean as the OPC is and is the most representative station for atmospheric moisture content and ground conditions. Steinar is located close to the slopes of Eyjafjallajökull and as a result frequently experiences decreased wind speeds due to being in the wind shadow, which is particularly evident when winds have some northerly component. Wind speed and direction are measured at 6 m elevation instead of 10 m as recommended by World Meteorological Organization (WMO) at Steinar, which enhances the frictional drag of the surface. This means it is not the most representative station for wind measurements. The other nearby AWS are at higher elevations (stations: 6546, 6235, 6222, 6430, 6459, 815), and/or are in more open locations away from mountain sides (stations: 6546, 6235, 6222, 6430, 6459, 6045/802, 798, 815),), compared with the location of the OPC. The MWS and AWS in Vatnsskarðshólar (802/6045) and the MWS in Vík (798) most likely have similar wind conditions as where the OPC is located. These stations are also set up according to WMO standards. We have plotted multiple stations to choose the optimal weather station for analyzing the wind conditions during each PM event. We used the full suite of nearby stations to determine the overall conditions of Southern Iceland, particularly over the persistent and temporary source areas for PM.

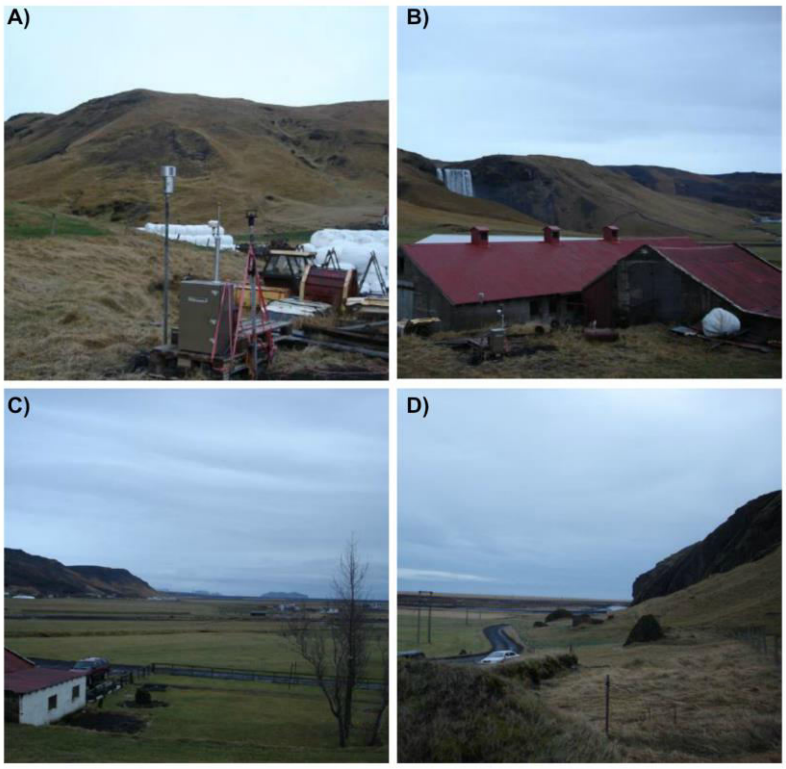

Figure 4.3: A) OPC set up at the farm in Drangshlíðardalur looking northward. B) View from farm looking towards the NE. C) View to the east from farm. D) View to SW from farm. Photos by Sibylle von Löwis

Table 4.1: Measurement sites

Station Type	Station Number	Name	Latitude	Longitude	Height Above Sea Level (m)	Distance from OPC (km)
OPC	-	Drangshlíðardalur	63.53°	-19.52°	36	-
Manned precipitation station	807	Skógar	63.53°	-19.50°	36	1
AWS	36132	Steinar	63.54°	-19.69°	20	9
AWS	6546	Vatnsfell	64.20°	-19.05°	540	78
AWS	6235	Tindfjöll	63.78°	-19.68°	870	29
AWS	6222	Sámsstaðir	63.74°	-20.11°	90	37
AWS	6430	Búrfell	64.12°	-19.75°	249	66
AWS	6459	Lónakvísl	64.10°	-18.61°	675	77
AWS	6045	Vatnsskarðshólar	63.42°	-19.18°	20	20
MWS	798	Vík í Mýrdal	63.42°	-19.01°	15	28
MWS	802	Vatnsskarðshólar	63.42°	-19.18°	20	20
MWS	815	Stórhöfði	63.40°	-20.29°	118	41

From 21 September 2010 – 1 May 2011, there were eight PM events reported by weather observers in Vatnsskarðshólar, Vík, and Stórhöfði (Table 4.2). Only six of these events were detectable in the OPC data based on number concentrations elevated above the background number concentration of 10 particles/cm^3 that is consistently present. The background concentration was calculated over all times in the measurement period when the number concentration of PM was consistent with no changes in number concentrations > 5 particles/cm^3 over three or more hours over all particle sizes. During all these periods no PM was reported by the weather observers at all three MWS in the area. During background number concentrations, the weather was cool, calm, and typically cloudy, or heavily precipitating. The size of PM events detected by the OPC were classified by relative intensity at the OPC location into categories of Type I, Type II, and Type III (Table 4.2). These classifications do not take into account the spatial expanse of the event or event intensity at other locations. Type I events contain only particles of 1 µm in diameter and smaller and number concentrations of 10–100 particles/cm^3. Type II events last less than one day and only particles smaller than 5 µm are above the background concentration with overall number concentrations of 100-500 particles/cm^3. Type III events last longer than one day and particles larger than 5 µm are above background concentrations. Overall number concentrations for Type III events are above 500 particles/cm^3. These values are considerably lower than number concentrations of particles from dust sources outside of Iceland, where small dust storms would have number concentrations of at least 1000 particles/cm^3 (Gillies et al., 1996; Jayarante et al., 2011; Shao and Mao, 2015). Background number concentrations in areas prone to dust storms outside of Iceland are often higher than what is being classified as a Type III event in Iceland (Gillies et al., 1994; Shao and Mao, 2015).

The start of a PM event is defined as when particle concentrations have exceeded 10 particles/cm^3 for longer than three hours. The end of a PM event is more gradual and is more difficult to define. We have defined the end of a PM event to be when number concentrations return to 10 particles/cm^3 for 12 hours. This accounts for temporary lulls in PM event detection by the single OPC despite an ongoing PM event due to shorter-lived changes in wind direction and/or speed. One event was detected by the OPC that was not reported by at least one of the three weather observers in the area. The typical particle size distribution for different size events can be seen in Figure 4.4.

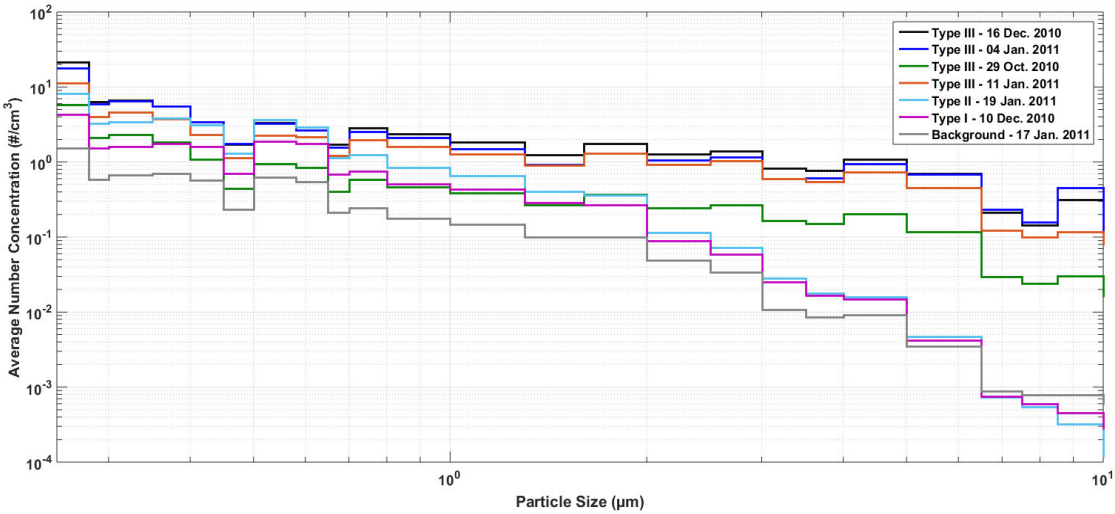

Figure 4.4: Average number concentration during PM events of varying magnitudes occurring in 2010 and 2011.

Table 4.2: PM event intensity classification with comparable number and mass concentrations.

Intensity	Total Number Concentration (#/cm^3)	Total Mass Concentration (µg/m^3)	Particle Size Range (µm)	Duration
Background	< 10	< 10	≤ 1	-
Type I	10-100	10-2200	≤ 1	-
Type II	100-500	2200-14000	≤ 5	< 1 day
Type III	≥ 500	≥ 14000	all	≥ 1 day

Three of the six events that were detected by the OPC were chosen for in depth analysis. These three events were selected because in addition to detection by the OPC there was also data available from weather observers, AWS, and they were categorized as Type III. Because of the short daylight period during wintertime, composite visible satellite images from NASA Worldview could only partly be used to supplement the surface data, and they were used to assist in determining the source area. From the station analysis favorable weather conditions for Type III PM events in this location were evaluated and the size distributions of particles during these events were analyzed. How conditions differ during other PM event intensities is also discussed. Additionally, the mass concentrations for PM_{10}, $PM_{2.5}$, and PM_1 during the Type III events were calculated using the density measured in Butwin et al. (2019b), the conversion between number concentration and mass concentration can be seen in Equation 4.1 where the density of the particle (ρ) is in kg/m^3, and V is the volume of an assumed to be spherical particle.

$$\frac{\mu g}{m^3} = \frac{\#}{L}\left(\frac{1L}{1000\ cm^3}\right)\left(\frac{1\ cm^3}{1 * 10^6\ m^3}\right)(\rho)\left(\frac{1 * 10^9\ \mu g}{1\ kg}\right)(V) \qquad (4.1)$$

Table 4.3: PM events that were observed by weather observers or detected by the OPC during the study period. See Figure 4.4 for overall average particle size distribution for different intensity level events. Bolded events are the events discussed in detail in this paper.

Start Time	Duration (hrs.)	Wind Direction	Precipitation on day of event	Classification	Weather Observer Classification
29 October 2010, 1400 UTC	**100**	**N, NE**	**No**	**Type III**	**Widespread Dust Suspension**
10 November 2010, 1500 UTC	29	E, NE	No	Type III	Dust storm
10 December 2011, 0900 UTC	36	W	Yes	Type I	Haze
16 December 2010, 1415 UTC	**125**	**W, N, E**	**No**	**Type III**	**Dust storm, Widespread Dust Suspension**
04 January 2011, 0000 UTC	**72**	**N**	**No**	**Type III**	**Dust storm, Widespread Dust Suspension and Whirls**
11 January 2011, 0400 UTC	84	E	No	Type III	Dust storm and Widespread Dust Suspension
17 January 2011, 0230 UTC	24	W	No	Background	No PM Observation
19 January 2011, 0000 UTC	175	W, NW	Yes	Type II	No PM Observation
04 February 2011, 1200 UTC	4	E	Yes	Background	No PM Observation

4.3 October 29-31, 2010 (Five Months After the End of the Eruption)

4.3.1 Synoptic Situation

At the start of the dust event in Southern Iceland on 29 October 2010 there was a low-pressure system to the SE, with the 970 hPa center over the Faroe Islands (~500km away). There was also a high-pressure system centered over Northeast Greenland with a center pressure of 1020 hPa approximately 2000 km from the south coast of Iceland. The

following day, 30 October 2010 (Figure 4.5A), the low-pressure system moved north, and the center was located approximately 500 km to the east of Iceland. In addition, the high-pressure system over NE Greenland strengthened slightly and extended even further south. There was also a secondary low centered ~2000 km to the SSE from Southern Iceland. By the 31st of October 2010 the initial low and high pressure systems had moved to the north as a result of the incoming low from the southeast (Figure 4.5B). With the movement of these systems winds all over Iceland began to die down.

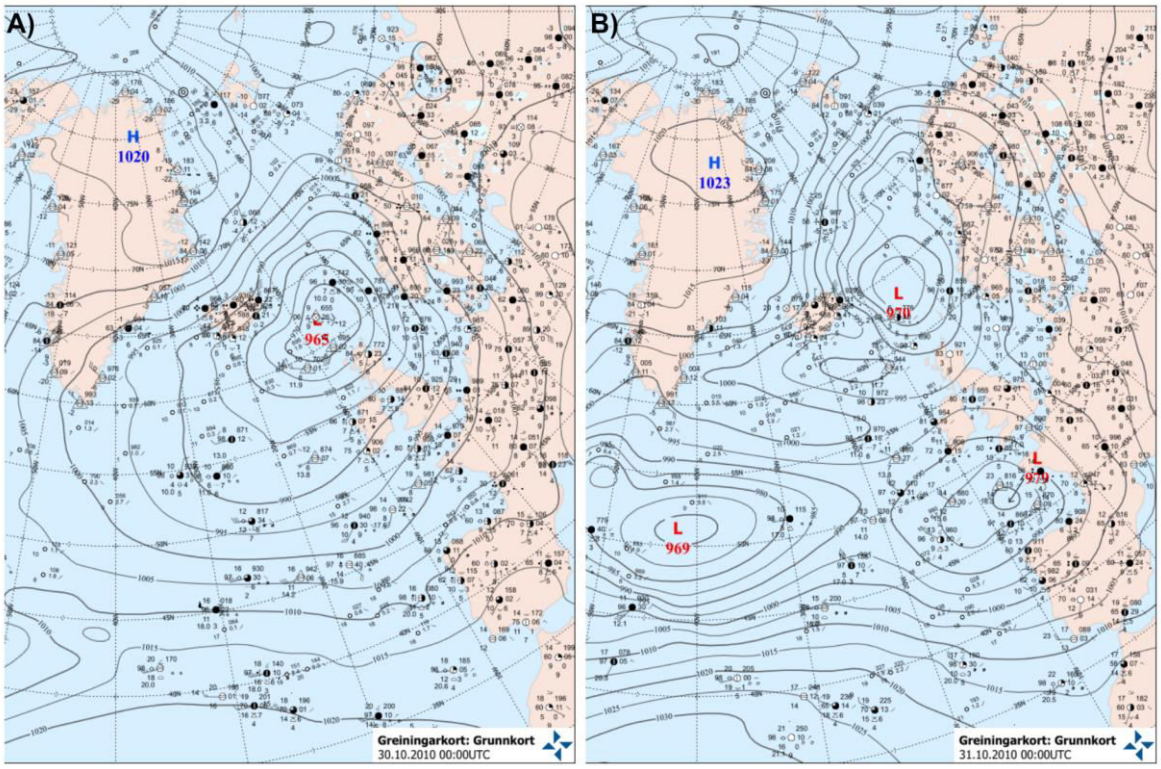

Figure 4.5: Synoptic overview for the North Atlantic, valid for A) 30 October 2010 at 00 UTC and B) 31 October 2010 at 00 UTC. Both maps are products from the Icelandic Meteorological Office.

4.3.2 Local Weather Conditions

For most of October 2010, precipitation was measured almost every day until the 19th. Days that did not experience precipitation still had consistent high relative humidity (> 70%) at all the examined weather stations. Following the 19th relative humidity at all the stations fluctuated more, between 25-100%, depending on station location and time. This pattern is most evident at Steinar (Figure 4.6B). Wind speeds after the 19th are no higher than during the earlier part of the month at each of the stations. However, during this latter part of the month there was little precipitation. These conditions resulted in multiple PM events (Figure 4.6A), with the largest starting the 29th and lasting until the 31st of October 2010 (Figure 4.7A).

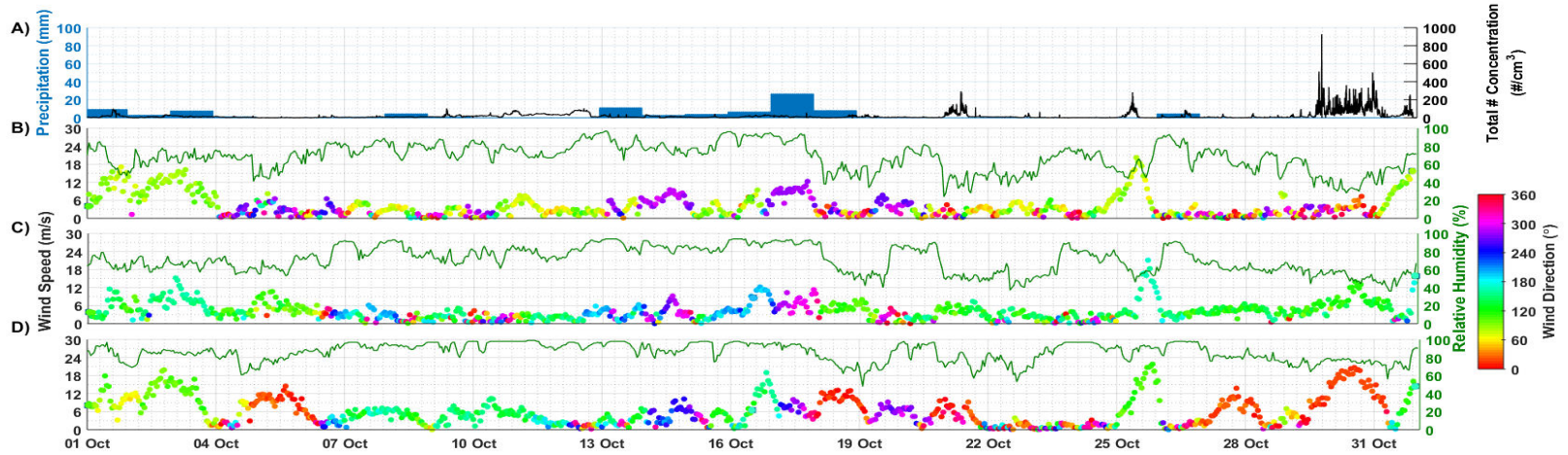

Figure 4.6: October 2010 A) Precipitation (24-hour sum, blue) measured at Skógar (807) and total number concentration of PM measured by the OPC (one-minute sum, black). Wind speed (left axis), direction (color bar) and relative humidity (green) measured at B) Steinar (36132), C) Sámsstaðir (6222), and D) Lónakvísl (6459).

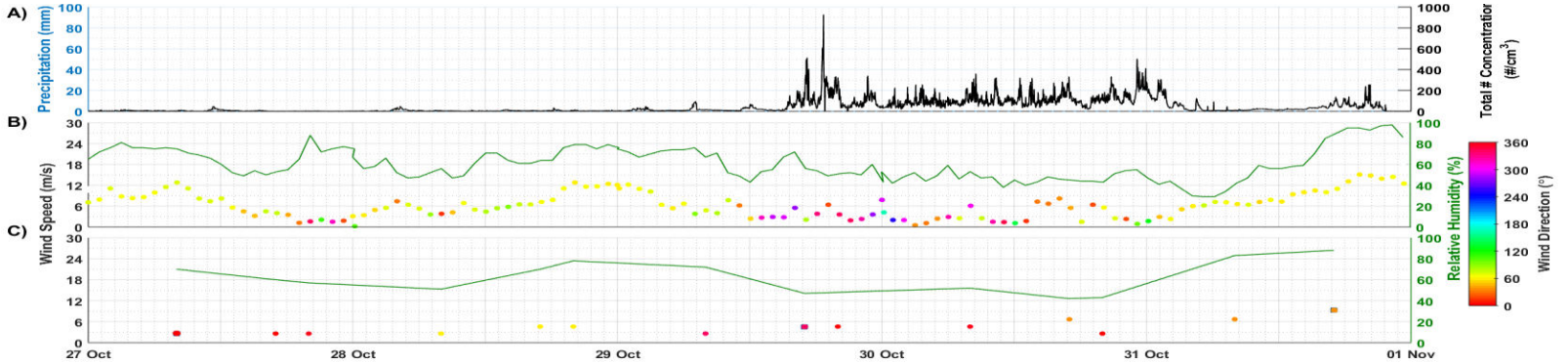

Figure 4.7: Type III PM event October 2010 A) Precipitation (24 hour sum, blue) measured at Skógar (807) and total number concentration of PM measured by the OPC. Wind speed (left axis), direction (color bar) and relative humidity (green) measured at B) Vatnsskarðshólar (6045), C) Vík (798).

The wind directions at the stations of interest were consistently northerly leading up to the PM event at the end of October at all stations except Sámsstaðir (Figure 4.6C). Sámsstaðir's differing wind direction is most likely due to local effects as winds throughout Iceland were northerly. Wind speeds during the PM event were greater than 5 m/s at both Vatnsskarðshólar and Vík during most of the event, with only brief periods of lower wind speeds. The relative humidity at the two manned stations are 3-15% higher than what was recorded at the Steinar location (36132) possibly due to the proximity to the ocean. Composite satellite imagery shows airborne PM originating from the slopes of Eyjafjallajökull and Mýrdalsjökull that were not at the time covered in snow (Figure 4.8). Additionally, PM is seen originating from the sandy source area to the north and west of Eyjafjallajökull (Figure 4.8). This suspended PM does not go south over the mountains and is more transparent than the PM south of Eyjafjallajökull that is measured by the OPC which is more opaque. By 1200 UTC, 31 October 2010 winds begin to shift to more southerly as the low-pressure system moves to the north (Figure 4.5B). As a result, wind directions shift to be easterly then westerly with heavy precipitation beginning after midnight, resulting in a drop in PM concentrations.

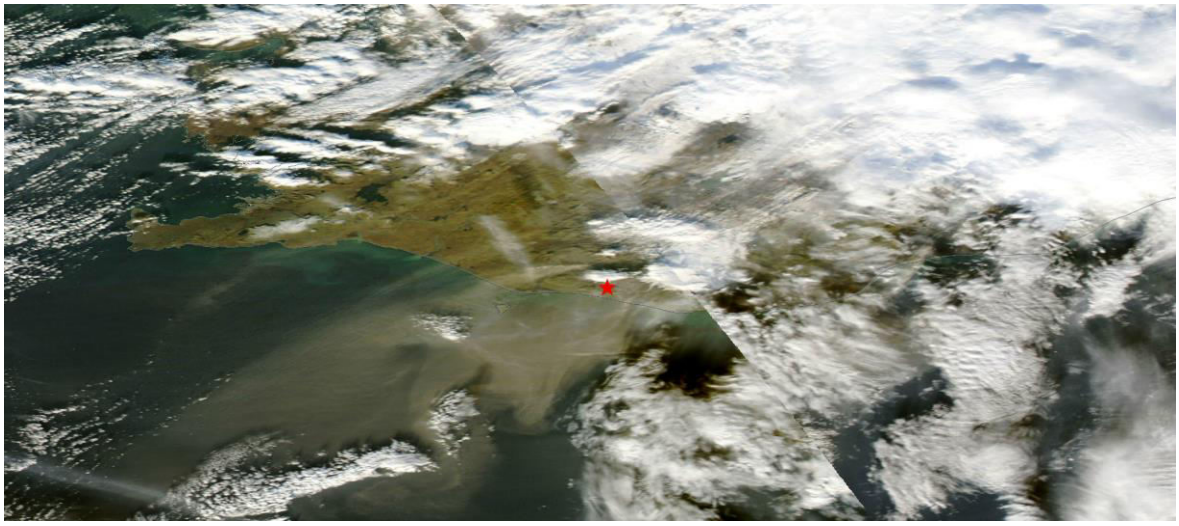

Figure 4.8: Composite true color visible satellite image of southern Iceland on 30 October 2010. The red star represents the location of the OPC. Image curtesy of NASA Worldview.

4.3.3 PM Size and Concentration

The background number concentration of particles is about 10 particles/cm^3, seen both before and after the event (Figure 4.9). This is typical, and number concentrations less than 10 particles/cm^3 can be observed during any weather conditions experienced at this site during the measurement campaign, with the lowest concentrations observed during precipitation. During the 29-31 October 2010 Type III event, the highest number concentrations were measured for particles < 1 µm in diameter. Number concentrations of the fine particles exceeded 80 particles/cm^3. Larger particles were also greatly enhanced during the event, mostly up to size 8.5 µm. The highest number concentrations happened with low relative humidities and a range of wind speeds at all the weather stations, Steinar and Vatnsskarðshólar values are shown in Figure 4.10.

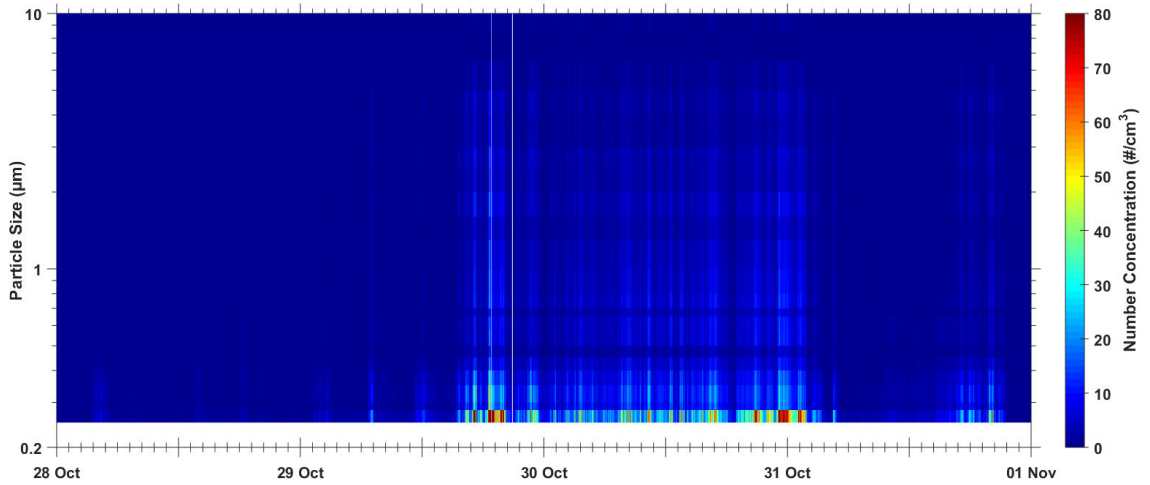

Figure 4.9: Number concentration by size for the PM event at the end of October 2010. There is no data below 0.25 µm.

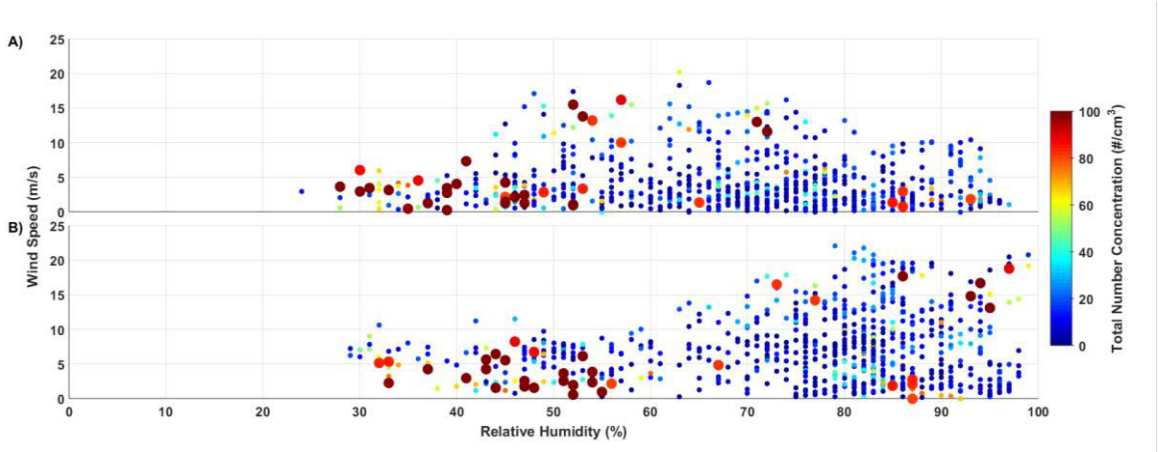

Figure 4.10: Total number concentration of PM (color scale) measured by the OPC during October as a function of wind speed (y axis) and relative humidity (x axis) measured at A) Steinar (36132) and B) Vatnsskarðshólar (6045). Larger dots represent total number concentrations greater than 80 particles/cm^3.

4.3.4 Source of PM

Based on the composite satellite image of 30 October 2010 (Figure 4.8) the PM being measured by the OPC during this event came from the flanks of the mountain which were currently coated in ash, but typically covered in vegetation at lower elevations and solid rock at higher elevations before the icecap edge. PM suspension is seen also originating in the persistent PM source areas north and west of Eyjafjallajökull. This PM would contain mostly bulk Icelandic dust with a minor contribution from the 2010 ash. With the northerly wind direction during the event, it is unlikely that PM measured at the OPC had been transported from the sandy areas north and west of Eyjafjallajökull, as the mountain blocks the transport. The PM measured by the OPC was most likely dominated by resuspended volcanic ash while the event itself is a combination of both resuspended ash and Icelandic dust.

4.4 December 16-23, 2010 Event (Seven Months After the End of the Eruption)

4.4.1 Synoptic Situation

During the month of December 2010, the Icelandic low was well established, with low pressure systems circling the country. On 18 December 2010, a low pressure system moved to the northeast of Iceland, resulting in northerly winds in southern Iceland (Figure 4.11A). Weather observers at MWS reported that the ground conditions in southern Iceland were frozen at the surface without snow cover (Figure 4.11B). Weather reports outside of this research area but in southern Iceland also reported numerous PM events during the period of December 16-23, 2010.

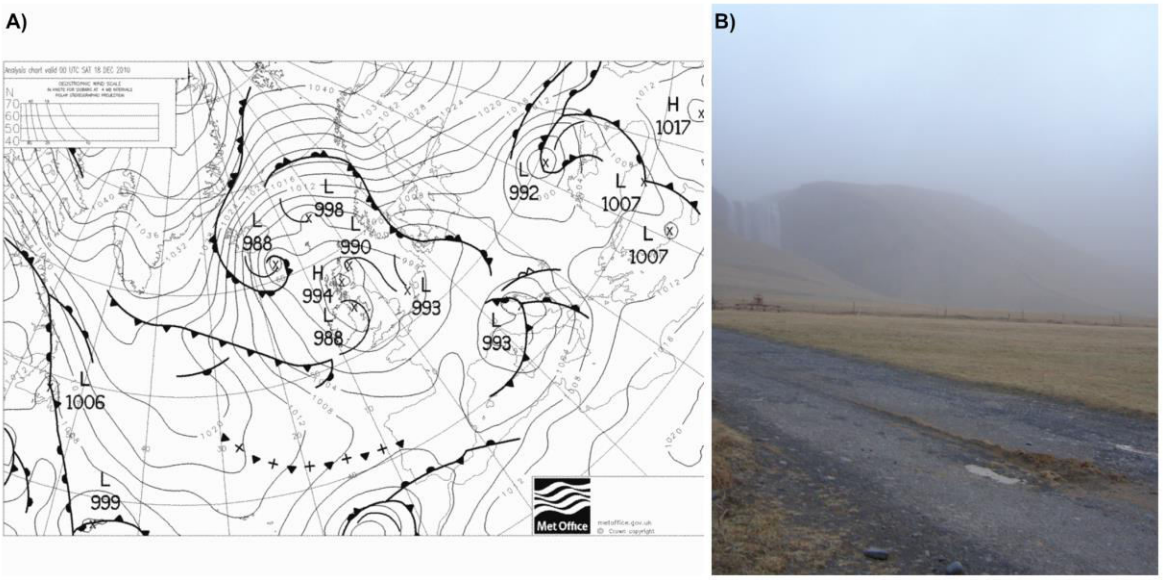

Figure 4.11: A) Synoptic scale conditions for the North Atlantic, valid for 18 December 2010 00 UTC. Courtesy of the UK Met office. B) PM event looking NE from the OPC station. Image taken on 17 December 2010 by Magðalena Jónsdóttir, Drangshlíðardalur

4.4.2 Local Weather Conditions

Precipitation at Skógar was recorded on the 9-12th, 15th, and the 24-28th of December 2010. During these periods no PM events were measured by the OPC (Figure 4.12A). During the first half of the month wind speeds were on average less than 10 m/s at all stations in this study. Stations that were located further inland and at higher elevation (Búrfell (6430), Vatnsfell (6546), Lónakvísl (6459)) had an average relative humidity > 60% during the beginning of the month. At the start of the PM event, relative humidity dropped to ~60% as measured at Vatnsskarðshólar, Vík and Steinar, and then slowly began to rise over the course of the event.

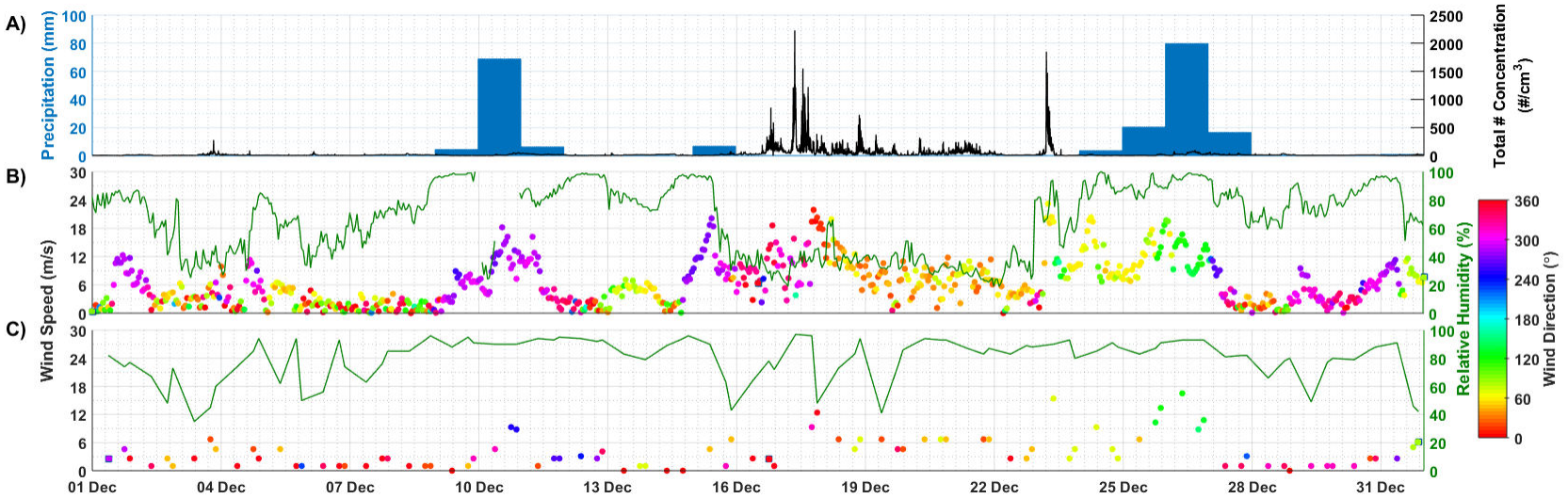

Figure 4.12: A) Precipitation (24 hour sum, blue) and total number concentration of PM (one minute sum, black) during December 2010. B) Wind speed (left axis), direction (color bar) and relative humidity (green) at Vatnsskarðshólar (6045) and C) Vík (798).

At all stations other than Lónakvísl (6459) and Sámsstaðir (6222) wind directions throughout the month were variable, because of the passing of low-pressure systems. Lónakvísl predominantly experienced northerly winds, and Sámsstaðir predominantly experienced south easterly winds. The differing wind directions at Lónakvísl and Sámsstaðir during the month of December 2010 is due to their location and the location of the center of low-pressure systems that pass through. At the start of the PM event winds were northerly at all locations other than Steinar which is due to the wind shadow. Wind speeds during this time were typically between 8 – 24 m/s depending on the station. At the end of the PM event the wind directions shifted to southerly, humidity rose, and precipitation began early on the 24th (Figure 4.12). Weather observers noted that as soon as wind directions began to shift precipitation began, greatly decreasing the intensity of the PM event.

4.4.3 PM size and concentration

During the month of December 2010, the size distribution of particles during events was much more variable over time than in the other months analyzed. Outside of periods during precipitation there was number concentrations above the background of 10 particles/cm^3. During times when no PM event was recorded measured particles were less than 5 µm. During PM events particles 10 µm and less were measured, with the highest number concentrations occurring with particles 1 µm and less (Figure 4.13). The Type III event that occurred 16-23 December 2010 had frequent peaks every 2-10 hours. Number concentrations > 80 particles/cm^3 were measured for particles ≤ 2.5 µm during the peak of the event (Figure 4.13). It was observed that the lower the humidity the higher the number concentrations regardless of the wind speed. When the humidity is higher, higher wind speeds are needed to observe similarly high number.

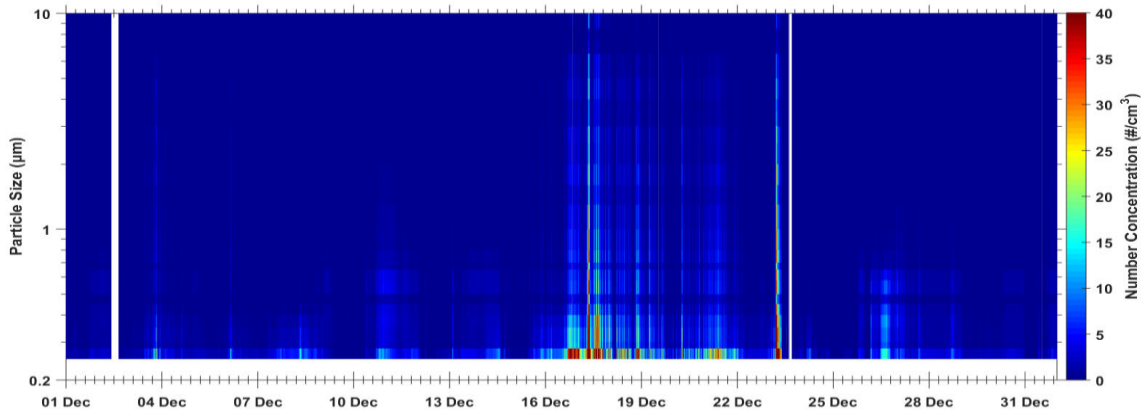

Figure 4.13: Total number concentration and size distribution during the December 2010. No data below 0.25 µm.

4.4.4 Source of PM

There were no useful visible satellite images during this event because of wintertime darkness, so we use only wind directions to assess the most likely source for the lofted PM. All the weather stations in the research area measured north-northwesterly winds during the first two days of the event, indicating that the material measured by the OPC most likely came from the sides of the mountain and not from a persistent source area, meaning

the PM measured by the OPC was resuspended ash. However, on 18 December 2010 winds began to shift and become more easterly. During this time dust from the Skógasandur plain (< 10 km) may have also been suspended. The latter part of the December 2010 PM event may have been mixed resuspended volcanic ash and bulk Icelandic dust.

4.5 January 4-8, 2011 Event (Eight Months After the End of the Eruption)

4.5.1 Synoptic Situation

The conditions at the start of January 2011 were very similar to those of December 2010, with low pressure systems either approaching Iceland from the south and then traveling to the northeast or traveling to the south of Iceland and continuing east (Figure 4.14A).

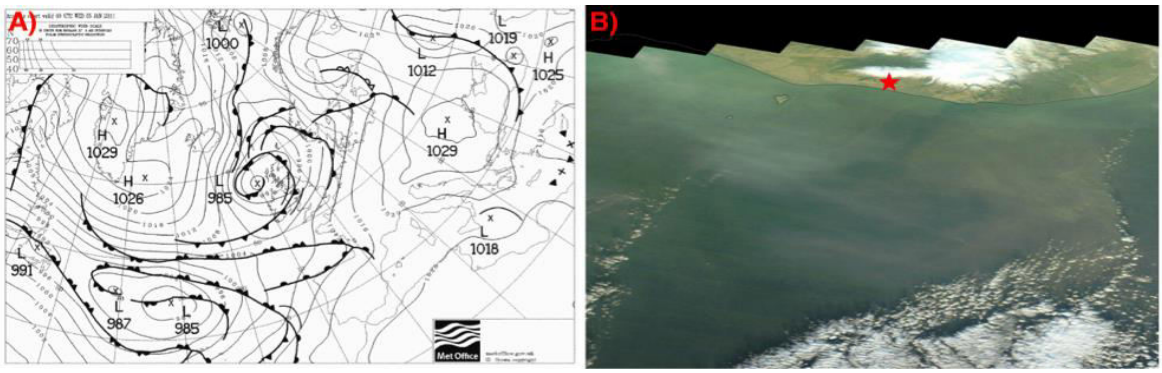

Figure 4.14: A) Synoptic scale conditions for the North Atlantic, valid for 05 January 2011 00 UTC. Courtesy of the UK Met office. B) Composite true color visible satellite image of southern Iceland on 05 January 2011. The red star represents the location of the OPC. Image curtesy of NASA Worldview.

4.5.2 Local weather conditions

The relative humidity was greater than 80% prior to and after the 4-8th of January 2011 PM event (Figure 4.15). During the event the humidity dropped in all locations, with the greatest drop occurring in Vatnsskarðshólar and Steinar which went from > 90% to < 40%. Following the 8th the weather pattern remained steady and two more PM events occurred which were classified as Type II and III. Starting the 15th, humidity was once again high at all stations, and precipitation was recorded at Skógar (807) every day in January 2011 except the 23rd and 26th.

Starting 3rd of January 2011 winds were consistently northerly for stations other than Sámsstaðir and Steinar. Sámsstaðir experienced more easterly winds, whereas, Steinar experienced a fluctuation of westerly and northerly winds. This also occurred to a lesser degree at Vatnsskarðshólar. Wind speeds at Vatnsskarðshólar peaked at 29 m/s on 7 January 2011 during the event (Figure 4.15). Steinar's wind speeds fluctuated between 2 and 20 m/s, showing that despite the shelter of the mountain there were still intermittent strong winds close to the OPC.

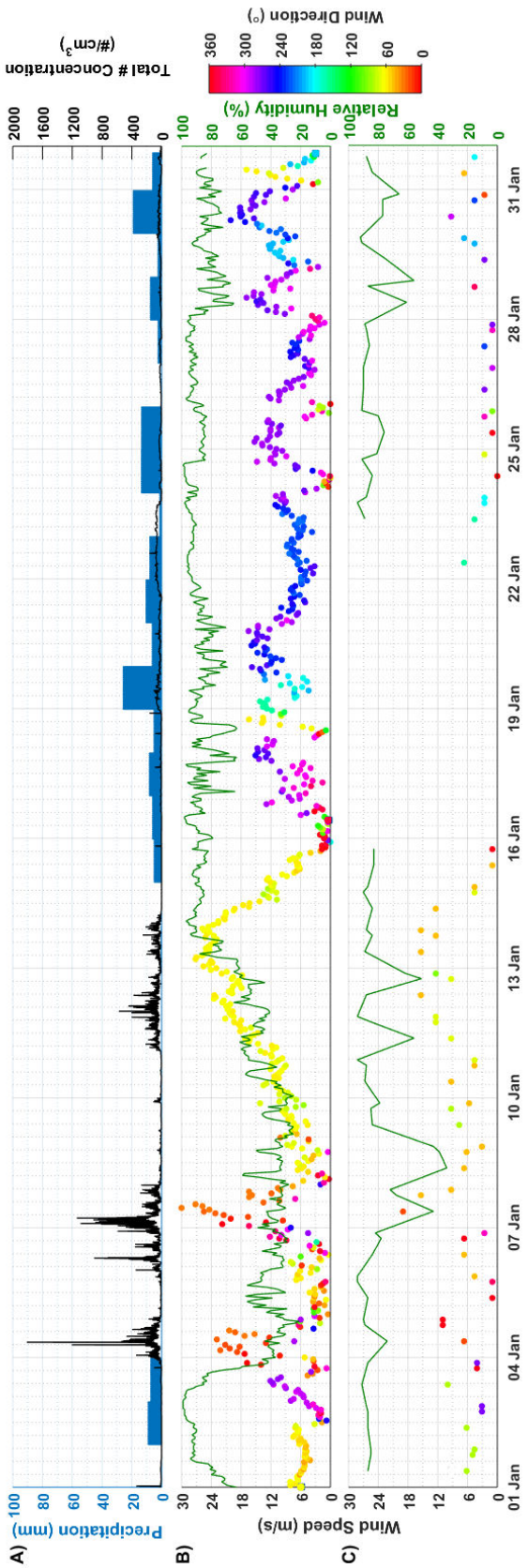

Figure 4.15: PM event January 4-9, 2011. A) Precipitation from Skógar and total number concentration of PM recorded by the OPC. Wind speed (left axis), direction (color bar) and relative humidity (green) from B) Vatnsskarðshólar, C) Vík. Missing data occurred 16-23 January at Vík.

4.5.3 PM concentrations

Even with precipitation, number concentrations of particles were above the background of 10 particles/cm^3. During the Type III event that began on the 4 January 2011 there were two main peaks of particle number concentrations. The peaks in PM concentration coincide with peaks in wind speed at Vatnsskarðshólar. Following the end of the first peak in particle concentrations wind speeds decreased, and humidity rose upwind from the OPC. When wind speeds began to increase upwind from the OPC, the number concentrations began to rise once again.

During this Type III event the size distribution was very similar to the event that occurred in mid-December, except it was shorter lived (Figures 4.13 and 4.16). Figure 4.16 shows the influence of precipitation before the event as the OPC was measuring well within the background levels.

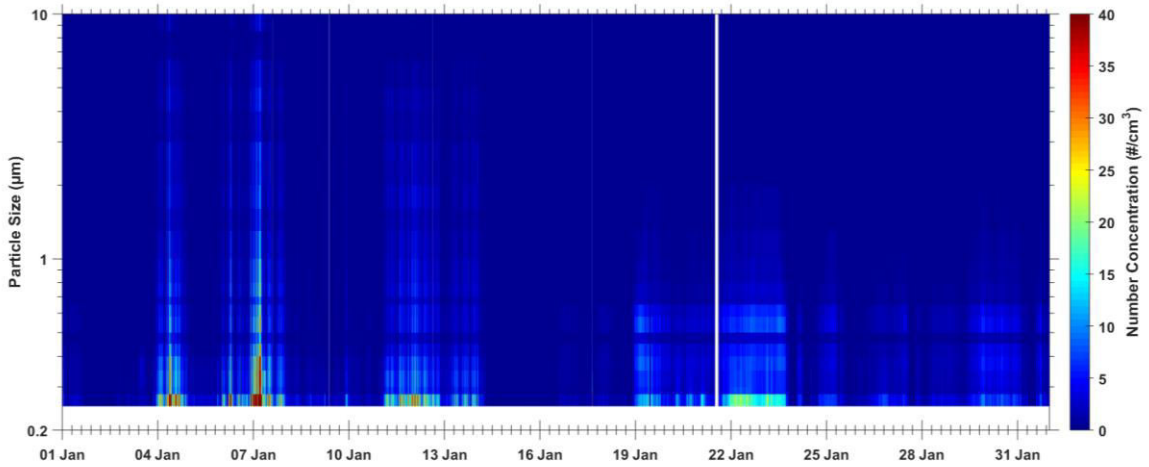

Figure 4.16: Total number concentration and size distribution during the January 2011. There is no data below 0.25 µm.

4.5.4 Source of PM

At the start January 2011 there is enough light to create a composite visible satellite images that cover the south coast of Iceland and just north of Eyjafjallajökull. The image produced for 5 January 2011 (Figure 4.14B) shows PM coming directly off the south coast of Iceland. The dust appears to be from the slopes of Eyjafjallajökull and from the sandur plains to the east. The PM continues to move south off the coast of Iceland until about ~30 km offshore when wind direction shifts from northerly to easterly. The measured wind directions are mostly northerly. The PM measured by the OPC during this event is most likely resuspended ash.

4.5.5 Mass Concentrations during Type III Events

The European Environment Agency's hourly health limit for PM_{10} (PM with diameter < 10 µm, and in mass concentrations) is 50 µg/m^3 (EEA, 2019). Assuming a density of 2.36 g/cm^3 that was calculated by Butwin et al., (2019b) for suspendable PM in Iceland the mass concentration of PM_{10}, $PM_{2.5}$, and PM_1 were calculated for October, December 2010

and January 2011. During the three Type III events discussed, the PM_{10} concentrations at the OPC were above the hourly limit for 90% of the duration of the events, for almost 700 hours (689 hr) during these three months (Figure 4.17). Mass concentrations during the peaks of these events were above 10^3 $\mu g/m^3$, with the highest hourly-average mass concentration of 27,200 $\mu g/m^3$ measured in December (Figure 4.17).

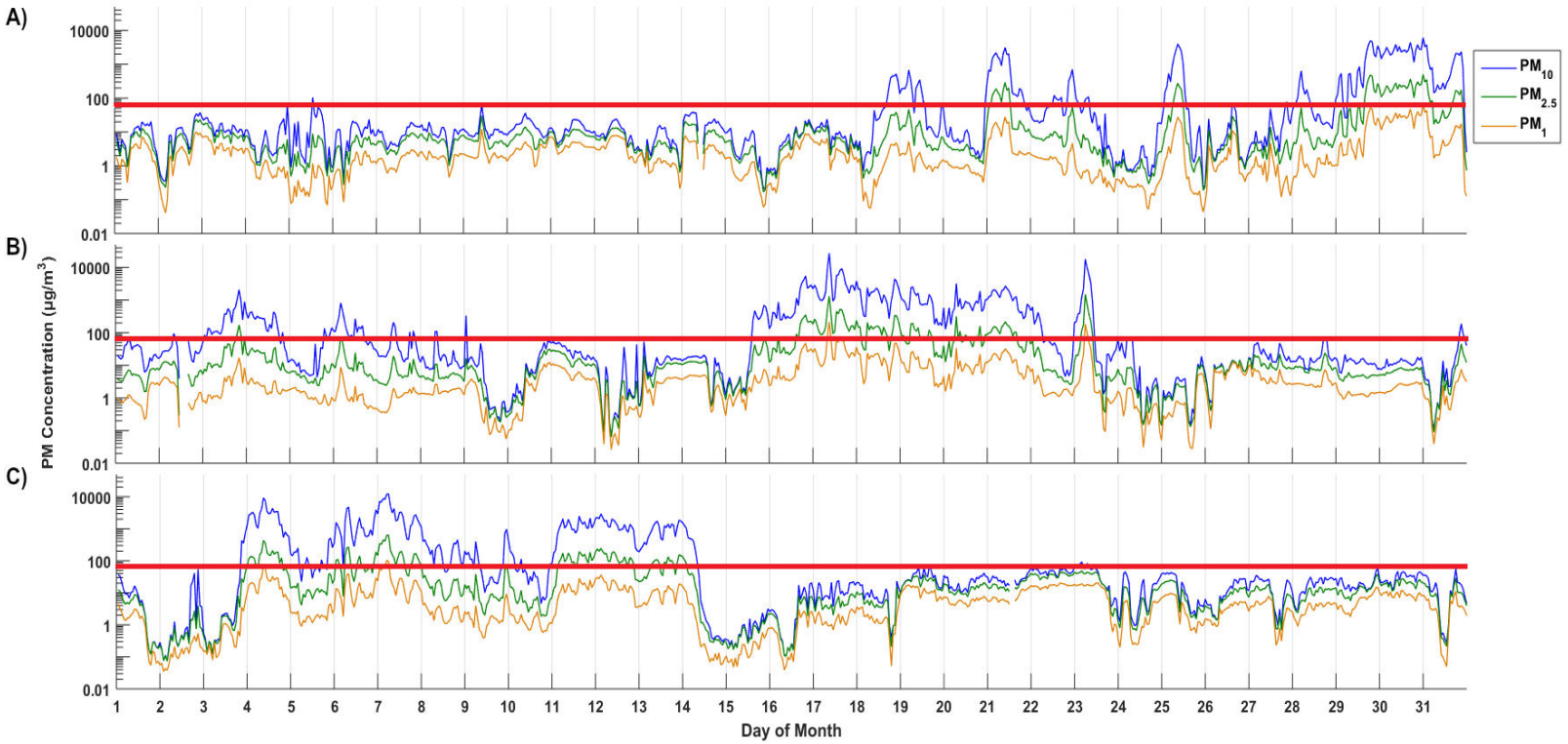

Figure 4.17: Calculated mass concentrations during the months of A) October 2010, B) December 2010 and C) January 2011 for PM_{10}, $PM_{2.5}$, and PM_1. The horizontal red line represents the hourly health limit of PM_{10} (50 µg/m^3) according to the European Environment Agency (EEA, 2019).

4.5.6 Conditions During Weaker PM Events

The presence of moisture becomes a stronger prohibitor of PM suspension resulting in weaker events. During the 19 January 2011 Type II event, winds were westerly and above 5 m/s during the time PM concentrations were above background levels. When winds dropped below 5 m/s so did PM concentrations. However, wind speeds increased to ≥ 5 m/s within two hours, resulting in the Type II event lasting 175 hrs. During this entire event relative humidity remained above 75% at all stations in the study (Figure 4.15). If there was less moisture it is hypothesized that this event would have been Type III.

Type I events typically can occur in two kinds of conditions. The first being dry but calm conditions, where wind speeds are too low for PM to easily become suspended but are likely suspended due to small thermals. The second being during times of high winds, and humidity > 90%, including periods of precipitation. The Type I event that occurred on 10 December was one of high winds, but also high relative humidity and measured precipitation during the day (Figure 4.12). Wind directions were north, northwesterly, with speeds > 5 m/s at all stations. Due to the moist atmosphere and surface, only the finest grains could become suspended, and even then, they were not at high concentrations (Figure 4.13). These types of conditions are typical for all the Type I events that were observed during the study period. Additionally, snow cover and precipitation do not seem to prohibit Type I events from occurring.

Background concentrations typically occurred when the winds had a southerly component, and exceeded background concentrations with winds with a northerly component. Southerly winds do not pass over a PM source between the ocean and the OPC. Background concentrations occur during periods of heavy precipitation (25 December), or when there is precipitation over the course of many days (Figure 4.12 and 4.13).

4.6 Discussion

Precipitation was not present during the largest, Type III events examined in this study. Precipitation may have occurred as recently as one day prior as was the case in the January event (Figure 4.15A). Total particle number concentrations greater than 1000 particles/cm^3 were typically measured when relative humidity was less than 70% and the wind direction was north to northeasterly, directly over a source, most likely the 2010 ash deposit, towards the OPC (Figures 4.12 and 4.15). PM coming from the persistent dust source area would need to pass over the mountain to be measured by the OPC, which is less likely than that PM measured during north to northwesterly winds was resuspended ash that had not yet been blown or washed away or integrated into the environment.

Smaller Type I and II events often occur during periods that have more moisture in the atmosphere and/or the surface (Figure 4.15). Soil moisture diminishes the likelihood of particles to be suspended, resulting in lower PM concentrations in all sizes, even when strong winds went directly from a source area to the OPC. Additionally, the time it takes for material to be dry enough to become suspended is not currently known, but it could be on the scale of hours (Figure 4.15). Note that the magnitude classification is based on a single measurement location. The Type I and II events may have had higher concentrations elsewhere in the plume, and had the OPC been located elsewhere, may have been classified

as Type III, but this is not possible to speculate on due to the lack of other instrumentation. Magnitude classifications of events should include the spatial scale of an event, but to accomplish this, multiple measuring stations are necessary.

The PM events of this study are within the time frame when the ash provided by the 2010 eruption are observed to increase the number of PM events recorded by weather observers locally (Butwin et al., 2019a). During the months in which the OPC was deployed, only January 2011 had more PM events than the 50-year average number of January PM events for stations near Eyjafjallajökull. Volcanic ash from the 2010 eruption was still being resuspended, without increasing the overall number of PM events in the other months, as PM from the persistent source areas was being suspended simultaneously. Eyjafjallajökull 2010 ash deposited on the flanks of the volcano continued to be resuspended into January 2011 because of the lack of snow cover at the time. If winter 2010/2011 had been a heavier snow winter, we hypothesize that the December and January events would have been dampened, or prevented entirely, by the snow.

The particle size distribution measured by the OPC during the different PM events is more dependent on weather conditions rather than if the source of the material was resuspended ash or bulk dust. The size distributions measured by the OPC of 10 μm and smaller during the three Type III events discussed here were very similar to each other (Figure 4.4) regardless of if the source was identified as the ash deposit or a blend of ash with the bulk dust. The size distribution rather changed as a function of the magnitude of the event, which was dictated by the environmental moistness. This coincides with the similar size distributions of particles ≤ 10 μm found in volcanic ash and surface material of Iceland (Butwin et al., 2019b). Because of the similar size distributions, PM source cannot be determined by PM_{10} size distribution alone, either wind direction or physical properties of the suspended material need to be known to identify if the material is most likely resuspended ash or bulk dust. This is important for determining the potential hazards of PM events to infrastructure, transportation and health which can differ if the material is ash or bulk dust (Horwell and Baxter, 2006; Hong et al., 2010; Horwell et al., 2013; Leiva et al., 2013; Xing et al., 2016; Zhang et al., 2016).

4.7 Conclusions

The conditions needed for suspension of PM discussed here are very similar to that of PM suspension in other areas of the world: wind speeds ≥ 5 m/s, no precipitation and relatively low humidity. As wind speed increases and humidity decreases, the measured particle number concentrations increase. The time needed for the surface material to become dry enough after precipitation is less than that in other dust source regions. Additionally, humidity during PM events in Iceland is higher than during typical PM events outside of Iceland.

In this study, northerly winds from the 2010 Eyjafjallajökull ash deposits to the OPC produced the largest measured PM events that were composed predominantly of resuspended volcanic ash. After the ash is blown and washed away from the mountainside this wind direction would not produce PM events of this magnitude at the OPC location. The exact timing for all fresh volcanic ash to be removed from surface is dependent on the

weather conditions. With combining the Butwin et al. (2019a) study and this one, it is likely that volcanic ash was still being resuspended eight months after the eruption but would have been removed by the two-year mark.

During all measured PM events, particles < 1 µm have the highest number concentrations. Particle number concentrations decrease with increasing particle diameter, in all measured PM events.

We don´t find a difference in weather conditions needed for resuspension of ash and suspension of other surface material. The size distribution of the resuspended volcanic ash and bulk Icelandic dust are very similar when suspended, so imagery and observations of surface conditions are key when trying to classify events as resuspended volcanic ash or dust. For future eruptions, it is recommended to have multiple measuring stations and, if possible, sample collection. This would allow for a better constraint on how long recently deposited volcanic ash remains available for resuspension.

5 Properties of Dust Source Material and Volcanic Ash in Iceland

This chapter was submitted under the same title to the Journal of Sedimentology on 28 June 2019. The co-authors were M. A. Pfeffer, S. von Löwis, E. W. N. Støren, E. Bali, and Th. Thorsteinsson

Abstract

The volcanic origins, primarily basaltic, of most of the surface material in Iceland influences its physical properties and appearance. Size distributions, shape analyses, and melting experiments were made for surface material collected in high-erosion dust source areas and fresh volcanic ash deposits to determine if they differ from each other and from dust from other major dust sources. The major differences found between Icelandic dust and dust from other major dust sources in the world, such as the Sahara, are in the particle shapes, its lower density, and its darker color. Icelandic dust particles greater than 20 µm retain volcanic morphological properties that are also found in fresh volcanic ash. Dust and fresh volcanic ash particles less than 20 µm are crystalline and blocky in nature, similar to the dust from other global source regions. The finer grained (< 20 µm) Icelandic particles will have similar suspension and transport behaviors and be similarly hazardous to health and infrastructure as non-Icelandic dust. The coarser particles (> 20 µm) will have different suspension and transport behaviors than other dusts due to the volcanic morphology. Icelandic surface material has between 5-30% glassy particles compared to fresh volcanic ash which has more than 50% glassy particles. Glassy particles were observed to melt at a lower temperature than the mineral grains; and as a result, volcanic ash is found to be more threatening to aircraft engines than the typical dust from Iceland. Icelandic dust was observed to be blocky, or plate like in the respirable size fraction, suggesting similar health hazards as dust from other regions.

5.1 Introduction

The definition of dust varies by discipline and by geographical location but can be defined as dry particles suspended in the atmosphere (Leathers, 1981; American Meteorological Society, 2019). Many studies on the suspension of dust have focused on the world's large deserts, such as those within the dust belt (North Africa, the Middle East, Central and South Asia), Patagonia, Australia, and SW North America (Tarr and Martin, 1913, Prospero et al., 2012, Bullard et al., 2016), but the large Icelandic deserts are less researched (Arnalds et al., 2001a). More than 20,000 km^2, (19%), of Iceland is classified as sandy desert and are major source areas for dust (Arnalds et al., 2001a). Iceland's deserts are different from most of the major dust sources in the world in the respect that they are mainly formed through the erosion of basaltic lava (Sigmarsson and Steinthórsson, 2007; Arnalds, 2010, Moroni et al., 2018). The Icelandic dust is darker in color, is more porous and angular in shape, and has lower particle densities that differ from what is found in other major dust sources in the world such as the Sahara (Thorarinsdottir and Arnalds, 2012; Dagsson-Waldhauserova et al., 2013). The other major dust sources in the world are predominately composed of quartz, clay minerals and feldspars, and are typically lighter in color than the material of Iceland (Lawrence & Neff, 2009; Arnalds, 2010; Atkinson et al., 2013; Scheuvens et al., 2013; Iwata and Matsuki, 2017; Ryder et al., 2018). These physical properties are key when it comes to accurately monitoring and modeling the suspension of dust, as well as understanding the impacts of the dust on climate and on the health of people and animals living in dusty areas (Laurent et al., 2008; Wittmann et al., 2017).

Explosive volcanic eruptions occur on average every three to four years in Iceland (Thordarson and Larsen, 2007) producing ash, which is an additional solid suspendable material, the other being the material in the persistent high-erosion source areas. In the atmospheric sciences, volcanic ash is defined such that the source of the particles is an eruption that occurred within approximately 100 years, and is a portion of atmospheric dust (AMS, 2019; WMO, 2019). The geological sciences define volcanic ash to be all particles ejected from a volcano with diameters ≤ 2000 μm of any age (Cashman and Rust, 2016; USGS, 2019). These definitions of volcanic ash are not usable for determining the difference between volcanic ash and bulk Icelandic dust after an eruption has ended. The morphology and size of volcanic ash is dependent on the environment in which it is formed (Smellie, 2000). Glass particles lacking vesicles are formed due to the rapid cooling of magma, which occurs when the environment is rich in water, which is typical for subglacial eruptions that occur with Eyjafjallajökull, Grímsvötn, and Katla volcanoes (Smellie, 2000; Dellino et al., 2012; Gudmundsson and Höskuldsson, 2016; Gudmundsson and Larsen, 2016a; Larsen and Gudmundsson, 2016b). During eruptions from subglacial volcanoes, the magma is in direct contact with water and blocky, step like features form in the ejecta due to brittle magma fragmentation (Büttner et al., 1999, 2002; Dellino et al., 2001, 2012). Ash in the form of fibers, often referred to as Pele's hair, can form during subaerial explosive eruptions with low viscosity basaltic melt (Heiken and Wohletz, 1985; Dellino et al., 2012). Fibers can also be formed, once ejected into the atmosphere; through the deformation of low viscosity magmas by air friction (Heiken, 1972; Shimozuru 1994; Moune et al., 2007; Dellino et al., 2012). These fibers were produced during fissure eruptions such as Laki 1783-1784 and a very few were observed during the Holuhraun eruption 2014-2015 (Hamilton et al., 2010; Civil Protection and Emergency Management, 2014). Ash with morphological properties such as vesicles, bubbles, and bubble walls are

formed due to the presence of volcanic gases, with little to no water interactions, which can occur with all the volcanoes in Iceland (Dellino et al., 2012).

Loose material can easily be suspended in Iceland due to frequent high winds and sparse vegetation (Einarsson, 1984; Arnalds et al., 2001b). The persistent source areas for dust in Iceland are also areas where volcanic ash is often deposited during eruptions (Arnalds et al., 2016). Volcanic ash deposited in these source areas remains suspendable for a longer period of time compared to ash that is deposited directly on glaciers or in vegetated areas (Arnalds, 2010; Thorsteinsson et al., 2011; Thorsteinsson et al., 2012; Arnalds et al., 2016, Butwin et al., 2019). As a result of volcanic ash being deposited in preexisting source areas for dust, volcanic eruptions have little effect on the overall annual average of 135 days in which suspended solid particulates are observed in Iceland (Dagsson-Waldhauserova et al., 2014b; Butwin et al., 2019a). It is not presently known how long the fresh volcanic ash remains on the surface as a distinct component of the surface material before being blown away or worked into the pre-existing surface material, ice, snow, or soil. It is important to note that weather observers typically report the suspension of volcanic ash only during an eruption: once the eruption is over, dust events dominated by recently deposited ash would typically be classified by the weather observers as dust (WMO, 2015; Butwin et al., 2019a). By characterizing the properties of Icelandic dust, with particular attention paid to the fresh volcanic ash component of the dust, uncertainties in direct and remote sensing measurements can be reduced and forecasts of Icelandic dust events can be improved.

The size, shape and density of the dust particles are important factors for their suspension, transport, and deposition. These factors are used to calculate surface roughness and threshold wind velocity for suspension (Chepil, 1951; Tsoar, 1994; Laurent et al., 2008). Grains smaller than 60 µm are light and small enough to be suspended into the atmosphere and transported long distances regardless of shape (Marticorena and Bergametti, 1995). Grains ranging from 60 - 2000 µm can become suspended when wind speeds are high enough. Grains of this size usually undergo saltation, where they skip over the surface, but are not lifted more than 1 m above the ground and are not suspended. Grains greater than 2000 µm experience surface creep where they do not leave the surface, but move along it (Marticorena and Bergametti, 1995). However, because grains are not evenly sorted along the surface, threshold wind velocities and roughness lengths can vary throughout a single source area (Marticorena and Bergametti, 1995; Laurent et al., 2008). Grains as large as almost 180 µm from the Grímsvötn 2011 eruption have been transported over 100 km; meaning larger Icelandic grains can be suspended and transported farther distances than theory expects (Liu et al., 2014). Studies from the other dust sources have shown that these "giant" dust particles (> 75 µm) can travel thousands of kilometers (van der Does et al., 2016). The mechanisms that allow these "giant" particles to be transported such long distances are not yet fully understood. Knowing the shape of the particles is crucial when it comes to knowing how the particles will behave once suspended in the atmosphere regardless of size. For example, the more spherical a particle is the higher the fall velocity (Haider and Levenspier, 1989; Saxby et al., 2018). Whereas the fall velocity of particles that are more rod or plate like will depend on the orientation of the particle while falling. When the long axis is oriented perpendicular to the force of gravity, the aerodynamic drag will keep the particle suspended for a longer period of time (Vainshtein et al., 2004). In addition, the shape of particles affects the accuracy of particle size measurements and monitoring (Nousiainen, 2009). Due to the differences in shape and color of Icelandic dust, the light scattering properties are different from other dusts (Torres et al., 1998;

Kalashnikova and Sokolik, 2004; Kahnert and Nousianinen, 2005; Nousiainen, 2009). Volcanic material can vary in shape due to the differing formation conditions due to the type of eruption, making shape assumption difficult (Liu et al., 2015a; Saxby et al., 2018). Shape characteristics can also be used to assist in determining the source of the material, especially with volcanic ash. Each volcanic eruptions' ash has distinct characteristics depending on the environment it was formed in (Schmith et al., 2018; Liu et al., 2018; Shoji et al., 2018).

The potential hazards of suspended dust differ based on the properties of the dust. The typical hazards from dust storms are decreased visibility, abrasion of infrastructure and agriculture, failure of electrical equipment as well as engines, and harm to animal and human health. In extreme cases visibility can be decreased to zero, creating problems for both vehicular and air traffic (Chepil and Woodruff, 1957; Buritt and Hyers, 1981; Laity, 2003; Miller et al., 2008; Baddock et al., 2013; Ágústsdóttir, 2015). Infrastructure as well as crops are often damaged during dust storms because of the sandblasting effect (Chamberlain, 1975; Wilshire et al., 1981; Pye, 1987; Stefanski and Sivakumar, 2009). Over time, this abrasion causes damage to engines in both automobiles and aircrafts, leading to higher rates of replacement, and in extreme cases engine failure. For aircrafts it also has the added risk of pitot tube malfunction from dust creating static charges possibly leading to incorrect flight speeds (Clements et al., 1963; Carter, 1979; Pye 1987; Lekas et al., 2011; Alexander, 2013).

Suspended volcanic ash creates similar hazards to that of suspended dust, like decreases in visibility, abrasion of windows and engines, and reduction of engine power, but with greater efficiency when compared to overall dust (Casadevall et al., 1996; World Meteorological Organization, 2007; Prata and Tupper, 2009; Alexander, 2013; Wilson et al., 2014). Due to the glass content volcanic ash's melting temperature is lower than that of typical dust, and typically lower than the operating temperature of airline engines, with typical jet engine temperatures operating at 1200-2000°C (Perepezko, 2009; Eliasson et al., 2016; Song et al., 2016). With sintering of ash beginning at 850-900°C, while with other dusts, sintering begins closer to 1200-1400°C (Kueppers et al., 2014). The exact temperatures depend on the composition, morphology and particle size of the ash and/or dust (Kueppers et al., 2014). The amount of time a particle spends in the engine effects how much the particles sinter or melt. With the lower sintering/melting temperatures of ash, the time needed is shorter than that of other dust (Kueppers et al., 2014). As a result, the glass in volcanic ash in an aircraft engine can melt, forming a glassy coating within the engine, and at high enough concentrations, lead to engine failure (Eliasson et al., 2016). The volcanic ash hazard does not end with the eruption as preserved ash can be repeatedly resuspended, even for over a century such as is seen with the deposits from the 1912 Novarupta volcano in Katmai National Park, Alaska, USA (Hadley et al., 2004; McGimsey et al., 2005). E.g., the most recent SIGMET (significant meteorological information statement) issued by the US National Weather Service about resuspended ash from the 1912 eruption was released in November 2017 (AVO, 2017). The huge deposit from the 1912 eruption and the lack of other persistent dust sources in the region have enhanced the preservation of suspendable ash in this place. One month following the 2010 eruption of Eyjafjallajökull a volcanic ash resuspension event reached the capital city of Reykjavík, with ten-minute average particle concentrations exceeding 2000 $\mu g/m^3$ (Thorsteinsson et al., 2012). Despite the high concentrations of resuspended volcanic ash, the Reykjavík Airport did not close because resuspension events were not included in operational

volcanic ash forecasts models and the event was treated as a dust storm composed of typical Icelandic surface material (Thorsteinsson et al., 2012). One reason for resuspension events not being included in operational models is that it is not known how long ash deposits remain suspendable on the surface.

The impact of dust storms on animal and human health depends on the proximity to the source area: the more active the source area and the closer a population is to the source area the greater their exposure (Goudie, 2014). Particles ≤ 10 μm can be inhaled and cause aggravated breathing, and irritation to the respiratory tract (Mészáros et al., 2014). Particles smaller than 4 μm can reach the lungs, depending on their shape and compositions, but do not reach the smallest branches of the respiratory track (Beckett; 2000; Fedorovitch, 2019). Particles 2.5 μm or less can reach alveoli, the smallest branches of the respiratory tract (Zhang et al., 2016). Inhaling large amounts of particles ≤ 2.5 μm, or repeated exposure to lower concentrations, leads to asthma attacks, respiratory inflammation, heart attacks and even death, for people with preexisting respiratory conditions, with the young and elderly the populations most susceptible to these adverse health effects (Hong et al., 2010; Leiva et al., 2013; WHO, 2013; Xing et al., 2016; Zhang et al., 2016).

Volcanic ash may be more hazardous to human health than mineral dust due to morphology and chemical coatings when it is fresh. Volcanic ash may be in the form of fibrous material, similar to that of asbestos. Not all volcanic eruptions produce directly this fibrous material, but with time weathering and hydration may alter the morphology forming this fibrous material, typically occurring on the order of thousands of years (Horwell and Baxter, 2006). For most eruptions in Iceland, fibrous material is very rarely created and is dependent on the type of and conditions during an eruption (Horwell et al., 2013; Dellino et al., 2012; Damby et al, 2017). Angular, blocky ash is more common in Iceland, which can be inhaled when the diameter is < 10 μm (Horwell et al., 2013). Fresh volcanic ash can carry volatile acids, polycyclic hydrocarbons and trace metals which potentially increases the toxicity to humans when inhaled (Horwell et al., 2003; Geptner et al., 2005; Horwell and Baxter, 2006). These compounds will remain on the particle until washed away by precipitation or from surface water, which due to the wet conditions in Iceland, will be a short-lived hazard (Jenkins et al., 2015).

This study characterizes the properties, including size, shape, and morphology of Icelandic dust and freshly deposited volcanic ash. The persistent dust source areas of Iceland are routinely being resupplied from glacial, fluvial and aeolian processes in addition to ash provided by explosive volcanic eruptions. We will show new measurements of how Icelandic dust is physically different from other dusts in the world. In addition to distinguishing the properties of the Icelandic dust, we also will show how fresh Icelandic volcanic ash differs from the bulk of Icelandic dust. We conclude with an assessment of how the physical differences imply different hazards to aviation and health. This work deals with surface-atmosphere interactions and the geological approach used here gives applicable findings for sedimentology and the atmospheric sciences.

5.2 Methods

In August and September 2016 and September 2017 twenty-six surface samples were collected in persistent dust source areas and locations where ash from the Eyjafjallajökull 2010 and Grímsvötn 2011 eruptions were deposited (Figure 5.1). Additionally, volcanic ash samples that were deposited and collected during the Eyjafjallajökull and Grímsvötn eruptions at two locations were also analyzed. Dust storms are frequently observed at all sample collection sites when exposed to winds capable of suspending the material (Dagsson-Waldhauserova et al., 2014a). Wind speeds during these so-called dust events in the source areas are typically at least 8 m/s, however, wind speeds > 20 m/s frequently occur in the source areas (Einarsson, 1984; Dagsson-Waldhauserova et al., 2013). The surface samples were taken from the top five centimeters of the surface. Samples were then dried at 50 °C to remove moisture and then dry sieved at half phi intervals from 0.5-4 ϕ (710-63 μm) and then once more with a 5.5 ϕ (20 μm) sieve to isolate the particles that are the most easily suspendable, transported the farthest, and pose a greater hazard to health and aviation relative to larger particles. The percent error for all sieved samples was 3%, based on mass lost during the sieving process. However, accuracy of sieving decreases with grain size. To better assess the size distribution of material < 125 μm, this material was also measured using a Malvern Panalytical Mastersizer 3000 at the University of Bergen, Norway. The Mastersizer measured particles 0.01-125 μm in 75 size bins. The volcanic ash samples only underwent sizing with the Mastersizer, and were not sieved, due to the sieved size distribution of the ash being already known (Gudmundsson et al., 2012; Gudmundsson and Larsen, 2016b). The volcanic ash was measured with the Mastersizer for particles 0.01-3500 μm in 101 size bins. The 26 surface samples and 2 volcanic ash sample locations were analyzed. The size distribution results were averaged into regionally representative values. Sample sites 1-11 (Figure 5.1B) were averaged to be representative of the Western Highlands; sites 12-20 (Figure 5.1C) of the Northern Highlands; and sites 21-26 (Figure 5.1D) of the South Coast Region. During sample collection an assessment of the amount of sorting of the surface material was done based on sediment grain size sorting charts. During surface sample collection weather conditions were mostly calm, with scattered precipitation occurring before and during collection in some locations. Site 27 was Eyjafjallajökull 2010 ash that was collected during the eruption and site 28 was Grímsvötn 2011 ash that was collected during the eruption. During ash collection in both 2010 and 2011 weather conditions were clear, calm, with no recent precipitation.

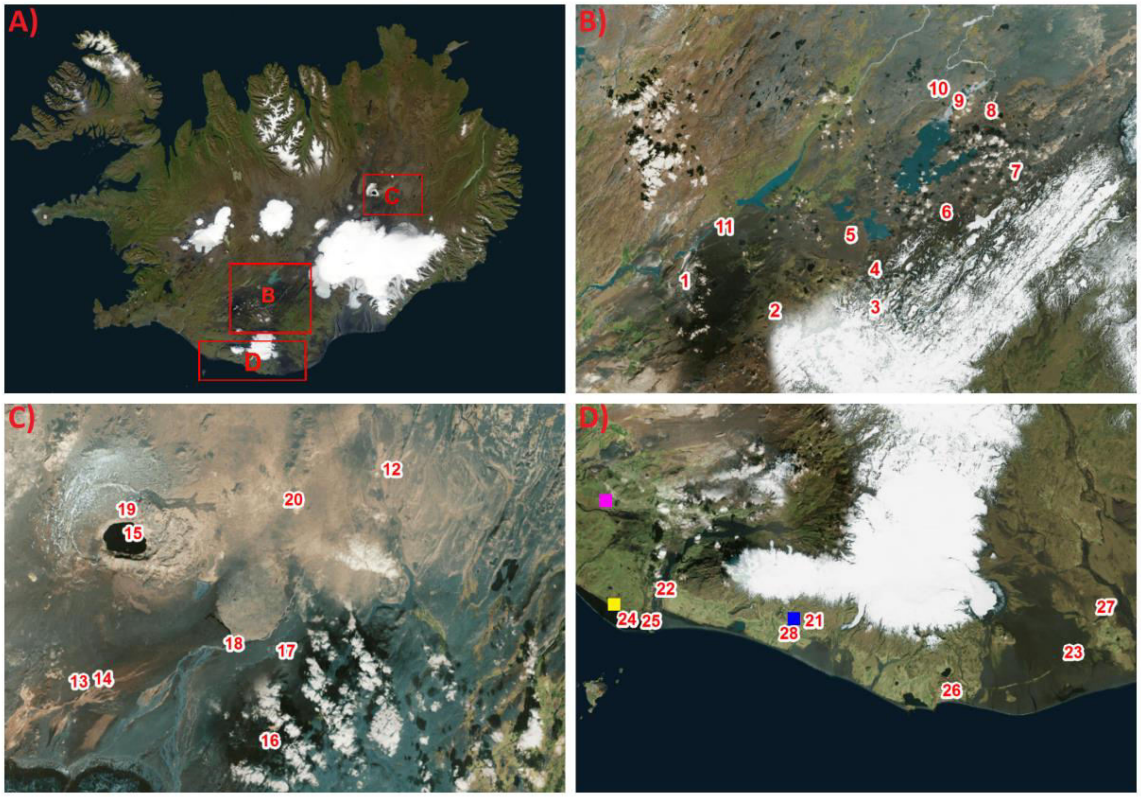

Figure 5.1: A) Surface sample collection location overview B) the Western Highlands, C) the Northern Highlands, and D) the South Coast. See Table 2 for properties of fine-grained particles from each location. Colored squares are Optical Particle Counter (OPC) locations, with pink operated: September – December 2010, yellow: April – October 2016, blue: December 2010-August 2012. Ash samples are sites 27 (Grímsvötn 2011) and 28 (Eyjafjallajökull 2010) respectively.

The finest sieved surface material, less than 20 µm, as well as the bulk volcanic ash samples were analyzed using a Hitachi TM3000 Scanning Electron Microscope (SEM) operating in secondary electron mode. The SEM samples were placed on carbon tape and then gold coated. Images were taken at 2000x magnification, with a pixel size of 0.07344 µm (13.6 pixels per µm). The samples' physical characteristics were noted for comparison with shape and texture characteristics recorded in the literature of mineral dust (e.g. Alastuey et al., 2005; Wang et al., 2011; Buck et al., 2013). Uncertainty arises as particles could not be rotated for a complete observation on all sides.

Shape analysis of 300 particles with a diameter of approximately 2.5 µm and less was done with the ImageJ image processing software for each sample (Rasband, 2012). The shape analysis was done on only the finest grains as they pose the greatest health hazard and remain in the atmosphere the longest. The software measured the particles' dimensions (Figure 2) which were then used to calculate: equivalent diameter (d_{eq}), elongation (e), flatness (f), circularity (X), sphericity (Φ), shape factor (Ψ), drag coefficient (C_d), and settling velocities (w). Similar methods were used in Dellino et al. (2005) and Blott and Pye (2008) to characterize particle shape. Using the methods described in Blott and Pye (2008) elongation and flatness ratios were also calculated for further particle shape classification. These measurements follow techniques described by Sneed and Folk (1958)

and Blott and Pye (2008), which measured particles in three dimensions. Due to the non-uniformity of particles and inability to rotate the particle to observe all sides it is possible that the short, intermediate, and long dimensions have errors, resulting in dimension errors that can change the overall shape of the particle. The particles that were measured in three dimensions were situated on the sample plate or on top of larger grains so that length, width and height could be seen (Figure 5.2). In the case of platy particles, the errors will be the greatest because of the difficulties associated with measuring the height dimension. Uncertainty arises in this technique, as the angle at which these particles are oriented is not known so geometry cannot be applied to correct for this. Measuring the angle in reference to the sample plate would only increase errors at this resolution. Two-dimensional analysis as done in Liu et al. (2015) would have produced similar uncertainties. The extent of the uncertainty is dependent on the angle the particle is oriented, with the greater the angle the greater the uncertainty.

Table 5.1: List of symbols used in this paper.

Symbol	Description	Units
d_{eq}	Equivalent Diameter	µm
e	Elongation	-
f	Flatness	-
X	Circularity	-
Φ	Sphericality	-
Ψ	Shape Factor	-
C_d	Drag Coefficient	-
w	Settling Velocity	m/s
ρ_f	Atmospheric Density	g/cm^3
ρ_s	Particle Density	g/cm^3
g	Acceleration of Gravity	m/s^2
µ	Atmospheric Viscosity	µPa s
S	Short Dimension of Particle	µm
I	Intermediate Dimension of Particle	µm
L	Long Dimension of Particle	µm

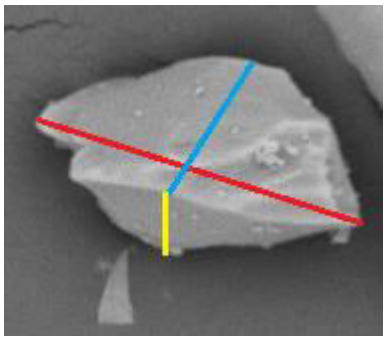

Figure 5.2: Dimensions of particles measured using ImageJ software. Long axis is in red (L), intermediate in blue (I), and short axis yellow (S).

Material in sieve bins ≤ 125 μm were recombined and went through laser diffraction measurement with a Malvern Mastersizer 3000 using a Hydro Large Volume dispersion unit at 2500 rpm stir speed. Refractive index (RI) was set to 1.543 and absorption index (AI) to 0.01, which are the values often used for quartz grains. Other RI were tested but did not fit the Mie scattering calculations as well as the values used for quartz. These tests minimized the error in size measurements due to the optical properties of the Icelandic material. All samples were sonicated for 60 seconds prior to measurements to break up any aggregates, and five measurements were averaged to calculate each result. The Mastersizer uses laser diffraction to measure the optical particle diameter for particles ranging from 0.01 – 3500 μm (but only particles smaller than 125 μm were analyzed in the surface samples). Overall, the Malvern Mastersizer 3000's measurement error is at least 0.6 % (Malvern Panalytical, 2019). The accuracy of measurements is dependent on the sample and sample preparation methods (Malvern Panalytical, 2019). The use of specific optical properties minimized the errors in size measurements. However, for sizing, the particles are assumed to be spherical, and non-porous, while we know Icelandic dust is not spherical and is porous. The volume percent size distribution measured by the Mastersizer was assumed to be equal to the mass percent size distribution, assuming density remained constant for all sizes. Standard deviations were calculated for the material measured by the Mastersizer and the maximum standard deviation was 2% by volume, however, the standard deviation for most size bins was less than 1%.

Optical Particle Counters (OPCs) were deployed at various times and differing locations in the South Coast region during the period of 2010-2016 (Figure 5.1). Due to the sporadic nature of the OPC deployment in the same geographical region, the size distribution of suspended material was assumed to be homogeneous amongst the OPC measuring sites and averaged in order to have a comprehensive picture of the observed suspension events. A Grimm EDM 365 OPC, on loan from the University of Applied Science, Dusseldorf, Germany was used for the 2010-2012 period. For the 2014-2016 period the TSI OPS (Optical Particle Sizer) 3330 was used. For the Grimm OPC, particles of 0.25 - 10 μm were counted in 24 size bins, the TSI OPC measured particles 0.3-10 μm in 16 size bins. For both OPCs the measuring accuracy is within 5% when run with uniform silicate particles. Measurement errors occur due to non-uniform densities, shapes, and color of the sampled particles. Similar to the Mastersizer the OPCs measured the optical diameter of the particles. However, the refractive index is not optimized for Icelandic dust particles. The shape factor was also not modified from the default value for Icelandic particles. These settings increase the error in the particle sizing done in Iceland. In addition, there is the potential for aggregation of particles to occur within the atmosphere, which would alter the measured size distribution.

Density of particles ≤ 125 μm in diameter at each sample location was measured using a standard Gay-Lussac pycnometer. Due to the minimal variance in density in all samples, the average density was calculated and used for all formulas involving particle density, including the conversion from mass to volume percentage. Uncertainties occur because materials are not homogeneous resulting in densities for bulk material rather than for individual grains as well as assuming density remains constant with grain size.

The average dimensions of $PM_{2.5}$ were used to determine the computable shape variables. For calculating the drag coefficients and settling velocities standard atmospheric conditions were used which are: air temperature of 15°C, air density of 0.001225 g/cm^3, and an atmospheric dynamic viscosity of 17.89 µPa s (Diehl, 1924; Green and Lane, 1964; Pye, 1987). The flatness (S/I) and elongation (I/L) variables are key to characterizing three-dimensional particle shape as defined by Blott and Pye (2008) and Bagheri and Bonadonna (2016) (Figure 5.3). Sphericity Φ (Equation 5.1) for volcanic material is approximated by the sphericity of an ellipsoid of the same dimensions (Bagheri et al., 2015; Bagheri and Bonadonna, 2016),

$$\Phi = \ (SIL)^{2/3}\left[\frac{3 - 0.0942(1 - 27LIS(L + I + S)^{-3})}{(LI)^{1.5349} + (LS)^{1.5349} + (IS)^{1.5349}}\right]^{1/1.5349} \tag{5.1}$$

Sphericity is used to estimate how close to a sphere a particle is, values range from 0-1 with 1 being a perfect sphere. Circularity, X (Equation 5.2), was also determined for all samples as shown in Riley (1941) and Blott and Pye (2008),

$$X = \sqrt{\frac{L}{S}} \tag{5.2}$$

The shape factor Ψ is used to estimate the drag coefficients (Equation 5.3) (Corey, 1949; Blott and Pye, 2008; Kuhn, 2015), the larger the Ψ the closer to a sphere the particle is,

$$\Psi = \frac{S}{(LI)^{0.5}} \tag{5.3}$$

The drag coefficients of the particles (C_d) is calculated to quantify the resistance of the particle in the atmosphere (Equation 5.4), and settling velocities (w) assuming the dynamic viscosity µ of air at 15°C to be 17.89 µPa s (Equation 5.5),

$$C_d = \frac{0.69gd^3\rho_f\left(1.33\rho_s - 1.33\rho_f\right)}{\mu^2\left(\frac{g\Psi^{1.6}d^3\rho_f\left(\rho_s - \rho_f\right)}{\mu^2}\right)^{1.0412}} \tag{5.4}$$

$$w = \sqrt{\frac{4gd(\rho_s - \rho_f)}{3C_d\rho_f}} \tag{5.5}$$

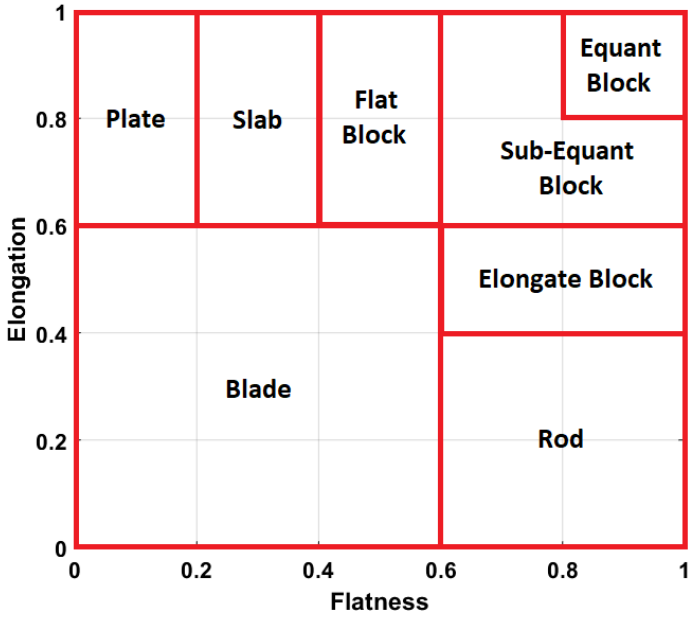

Figure 5.3: Dimensional particle shape as defined by Blott and Pye (2008) and Bagheri and Bonadonna (2016).

In addition to size and shape analysis, the hazard to aviation from particle melting was assessed by melting small portions of one surface sample and one volcanic ash sample. The two samples that were chosen for the melting experiment were fresh ash collected during the Grímsvötn 2011 eruption (sample #28) and a surface sample from Markarfljótsaurar (sample #22). These two samples were chosen because the Grímsvötn ash was more basaltic/mafic than the rhyolitic/andesitic ash from Eyjafjallajökull (Davies et al., 2010; Thorsteinsson et al., 2012; Liu et al., 2015b; Gudmundsson and Larsen, 2016a) and had high angularity (Liu et al., 2015b) and the Markarfljótsaurar sample had the lowest fraction of mafic particles of the surface samples. All the other samples were somewhere between these two end members of the sample set. The range of possible melting temperatures of the particles can be assessed by looking at these two end-member samples. The samples were first examined under a microscope, checking the angularity and basaltic glass to mineral ratio. Based on mineral grain percentage charts, the Markarfljótsaurar sample was made up of approximately 5% of glass, whereas the Grímsvötn ash was composed mostly by glass grains (> 50%). They were then placed into graphite crucibles and heated at 50°C intervals between 800-1000°C using a Zicar high temperature furnace. The temperature in the Zicar furnace was calibrated based on the melting points of NaCl, Ag and Au and the accuracy of the measured temperature was within 5°C. Samples were left in the furnace for 5 minutes for the temperature to equilibrate after the cooling that occurs when opening the furnace, as well as to allow the sample to reach the correct temperature. The samples were then rapidly cooled in water with care to not get the sample wet. The cooling process ends the sintering/melting process, allowing temperature specific changes to be preserved. Each of the samples that underwent heating were then re-examined under a microscope to determine if any melting occurred and if so to what extent and to how much of the material.

5.3 Results

5.3.1 Size Distribution

Sieved surface samples from the South Coast, Western Highlands and Northern Highlands all have two peaks in their size distribution (Figure 5.4A) with most of the volume being composed of particles greater than 600 µm in size and the secondary peak differing among locations. Samples from the Western Highlands and Northern Highlands have approximately the same size distribution except for the Western Highlands having the greatest amount of coarse material with approximate 17% by volume of the sampled material being greater than 710 µm. The Northern Highlands and Western Highlands have their secondary peak at 125 µm while the South Coast has a larger secondary peak with coarser material at 330 µm (6% by volume).

Size distribution measured by the Mastersizer of the recombined sieved surface material ≤ 125 µm (31% of total sieve size bins) shows a single peak in the size distribution (Figure 5.4A). The surface samples all peaked at 110 µm while the ash samples peak with a slightly larger value of ~150 µm. Note that the volcanic ash samples were never sieved. The decrease in particle sizes in the surface samples is much more rapid than for the ash samples. The ash samples have fewer particles between the particle sizes of 35-110 µm. Ash from Eyjafjallajökull had more particles ≤ 20 µm when compared to the surface samples as well as the Grímsvötn ash.

Ash from Eyjafjallajökull has a similar size distribution as the surface samples. Whereas, the Grímsvötn ash from location 28 did not have any material ≤ 10 µm from this sample location taken during the eruption. The lack of material < 10 µm is reasonable as the total size distribution during Grímsvötn 2011 was relatively coarse and particles < 10 µm were only formed during certain times during the eruption and not found at all deposit areas in Iceland (Höskuldsson et al. 2018). Overall, the Mastersizer showed at maximum a 2% standard deviation between the regional/ash averages and the individual measurements. The size distribution of the finer, airborne particles measured by the OPC shows three peaks in the size distribution (Figure 5.4B) with peak concentrations at 2.5, 4.5 and 9 µm.

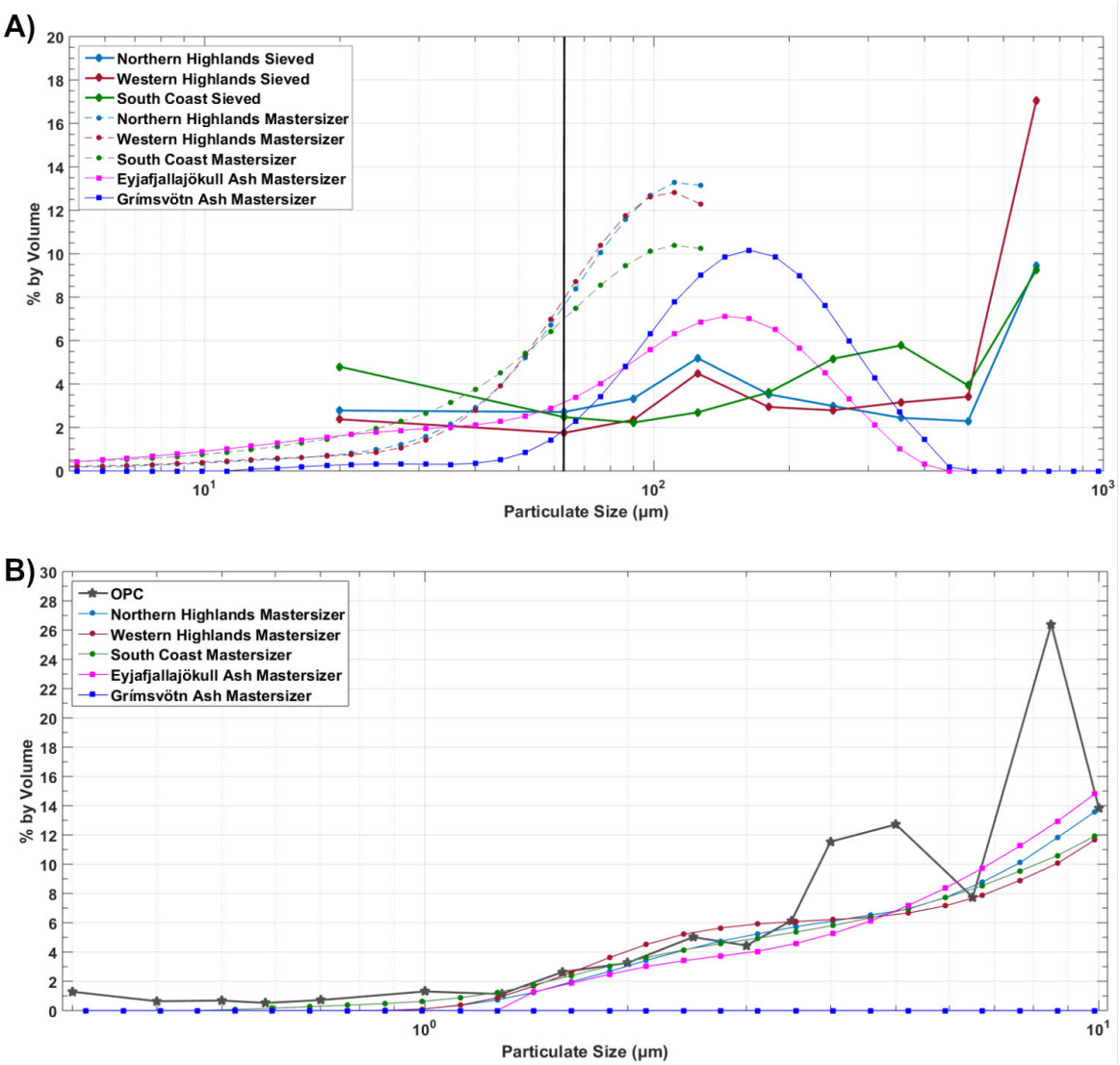

Figure 5.4: Size distribution as fraction (%) by volume of material for all measuring techniques, using overall density for all particle sizes. A) Average size distribution of surface material, and volcanic ash. Solid colored lines correspond to material that was sieved; colored dashed lines are measured with the Mastersizer 3000. Due to the overall fine texture, ash samples were not sieved. The solid vertical line is at 63 µm shows the typical division between suspension and saltation (Pye, 1987). B) Average size distribution of suspended material measured by an OPC and Mastersizer data for the surface and volcanic ash samples.

5.3.2 Particle Properties

Table 5.2 shows the measured and calculated particle properties of: density, long, intermediate, short dimensions, flatness, elongation, equivalent diameter, sphericity, particle perimeter, equivalent circle perimeter, circularity, shape factor, drag coefficient and settling velocity, which were calculated using measurements from SEM images for particles with geometric diameters of 2.5 µm or less. The particles in this size range are 16% by number concentration of the particles measured by OPC, and approximately 4% of

the total surface material, so they represent only a small fraction of the airborne or potentially airborne particles in Iceland.

*Table 5.2: Sorting Classification for the bulk material, properties of particles with geometric diameter ≤ 2.5 µm. Sample location numbers refer to Figure 1. Sample region is denoted as Western Highlands (W. H.), Northern Highlands (N. H.), and South Coast (S. C.). * densities are based on particles ≤ 125 µm.*

Sample Region	Sample Location	Sorting Classification	ρ_s* (g/cm^3)	L (µm)	I (µm)	S (µm)	d_{eq} (µm)	f	e	Φ	*X*	Ψ	C_d	*w* (m/s)
W. H.	**1**	Moderate	2.12	2.1±1.0	1.2±0.6	0.7±0.4	1.1±0.5	0.6	0.6	0.9	0.6	0.5	1.6	0.1
W. H.	**2**	Well	2.40	2.0±1.1	1.2±0.6	0.7±0.4	1.0±0.5	0.6	0.6	0.9	0.6	0.4	1.7	0.1
W. H.	**3**	Poor	2.41	2.2±1.5	1.3±0.6	0.7±0.3	1.2±0.5	0.6	0.6	0.9	0.6	0.4	1.7	0.1
W. H.	**4**	Very Poor	2.49	2.1±1.4	1.1±0.6	0.7±0.4	1.1±0.5	0.6	0.6	0.9	0.6	0.5	1.6	0.1
W. H.	**5**	Moderate	2.47	2.1±1.1	1.2±0.8	0.7±0.4	1.1±0.6	0.6	0.6	0.9	0.6	0.4	1.8	0.1
W. H.	**6**	Moderate	2.74	1.6±0.9	0.9±0.7	0.5±0.4	0.8±0.6	0.6	0.6	0.9	0.6	0.4	1.7	0.1
W. H.	**7**	Very Poor	2.55	1.5±0.8	0.8±0.9	0.5±0.5	0.8±0.8	0.7	0.6	0.9	0.6	0.5	1.5	0.1
W. H.	**8**	Poor	2.62	1.7±1.1	0.9±0.9	0.5±0.6	0.8±0.8	0.6	0.6	0.8	0.6	0.4	2.1	0.1
W. H.	**9**	Very Poor	2.23	1.4±0.8	0.7±1.0	0.4±0.6	0.7±0.8	0.6	0.6	0.8	0.6	0.4	2.0	0.1
W. H.	**10**	Poor	2.52	1.6±0.9	0.8±0.8	0.5±0.5	0.8±0.6	0.6	0.5	0.8	0.5	0.4	2.2	0.1
W. H.	**11**	Moderate	2.25	1.4±0.8	0.7±0.7	0.4±0.4	0.7±0.5	0.6	0.6	0.8	0.5	0.4	2.2	0.1
N. H.	**12**	Moderate	2.35	1.2±0.6	0.7±0.7	0.4±0.4	0.6±0.5	0.6	0.6	0.8	0.5	0.4	2.2	0.1
N. H.	**13**	Well	1.84	1.1±1.	0.6±0.6	0.4±0.3	0.6±0.5	0.6	0.6	0.8	0.6	0.4	2.1	0.1
N. H.	**14**	Very Well	2.32	1.0±0.7	0.6±0.5	0.3±0.3	0.5±0.4	0.6	0.6	0.8	0.5	0.4	2.3	0.1
N. H.	**15**	Moderate	2.00	1.0.±0.7	0.5±0.5	0.3±0.3	0.5±0.4	0.6	0.6	0.8	0.5	0.4	2.3	0.1
N. H.	**16**	Poor	2.56	1.1±1.1	0.6±0.5	0.2±0.3	0.5±0.4	0.5	0.6	0.7	0.4	0.3	4.1	0.1
N. H.	**17**	Moderate	2.46	1.3±0.7	0.7±0.5	0.3±0.3	0.6±0.4	0.5	0.6	0.8	0.5	0.3	3.2	0.1
N. H.	**18**	Moderate	2.76	1.3±0.5	0.7±0.4	0.3±0.3	0.6±0.4	0.5	0.6	0.8	0.5	0.4	2.6	0.1
N. H.	**19**	Well	2.03	1.2±1.0	0.7±0.4	0.3±0.3	0.6±0.3	0.5	0.6	0.8	0.5	0.3	3.0	0.1
N. H.	**20**	Well	2.30	1.2±1.4	0.7±0.3	0.3±0.2	0.7±0.3	0.5	0.6	0.8	0.5	0.4	2.3	0.1
S. C.	**21**	Poor	2.12	1.5±1.3	0.9±0.4	0.4±0.2	0.7±0.3	0.6	0.6	0.8	0.6	0.4	2.2	0.1
S. C.	**22**	Moderate	2.33	1.6±1.1	0.9±0.5	0.3±0.2	0.7±0.4	0.5	0.6	0.7	0.5	0.3	3.6	0.1
S. C.	**23**	Moderate	2.55	1.3±1.2	0.7±0.5	0.3±0.2	0.6±0.4	0.5	0.6	0.8	0.5	0.3	3.0	0.1
S. C.	**24**	Very Well	2.78	1.5±1.2	0.8±0.4	0.4±0.2	0.7±0.3	0.6	0.6	0.8	0.5	0.4	2.5	0.1
S. C.	**25**	Well	2.27	1.2±1.1	0.7±0.4	0.4±0.2	0.6±0.3	0.6	0.6	0.8	0.5	0.4	2.1	0.1
S. C.	**26**	Moderate	2.15	1.5±0.9	0.8±0.5	0.3±0.2	0.6±0.4	0.5	0.6	0.8	0.5	0.3	3.1	0.1
S. C.	**27 (Volcanic Ash 2010)**	Very Well	2.27	1.1±0.8	0.6±0.5	0.3±0.5	0.6±0.4	0.6	0.6	0.8	0.6	0.4	2.1	0.1
S. C.	**28 (Volcanic Ash (2011)**	Very Well	2.20	1.2±0.7	0.6±0.5	0.3±0.3	0.5±.0.3	0.6	0.6	0.8	0.5	0.4	2.5	0.1
W. H.	**Average**	-	2.44	1.8±1.0	1.0±0.8	0.6±0.4	0.9±0.6	0.6	0.6	0.9	0.6	0.4	1.8	0.1
N. H.	**Average**	-	2.33	1.2±0.9	0.6±0.5	0.3±0.3	0.6±0.4	0.6	0.6	0.8	0.5	0.3	2.6	0.1
S. C.	**Average**	-	2.31	1.4±1.1	0.8±0.5	0.3±0.2	0.6±0.4	0.5	0.6	0.8	0.5	0.3	2.9	0.1
	Volcanic Ash Average	-	2.24	1.1±0.8	0.6±0.5	0.3±0.4	0.5±0.4	0.6	0.6	0.8	0.5	0.4	2.3	0.1
Overall	**Average**	-	2.37	1.5±0.9	0.8±0.6	0.4±0.3	0.7±0.4	0.6	0.6	0.8	0.5	0.4	2.2	0.1

Of the 300 randomly selected fine particles (~ 2.5 μm) from each location, the particles from the Northern Highlands are smaller than any other sample locations, with the particles being at maximum 2.6 times smaller. The South Coast and both the volcanic ash samples had diameters similar to that of the overall Icelandic average of 0.7±0.4 μm. Particles in the Western Highlands were found to be the most spherical, whereas the South Coast had the least spherical particles. A 19% difference exists between the most and least spherical particles in Iceland. When examining the shape in only two dimensions, the most circular particles were in the Northern Highlands and the least circular in the South Coast, with a 21% difference between the least and most circular particles. Particles that may appear circular on two dimensions can be more cylindrical in nature and as a result will change the particles behavior in the atmosphere (Kalashnikova et al., 2005). The differences in sphericity and circularity is a product of the errors in measuring as discussed in section 5.2.

Density measurements ranged from 1.84-2.78 g/cm^3 with an average value of 2.37 g/cm^3. The density values were then used to calculate the drag coefficient and settling velocities. The particles with the highest drag coefficient, as a function of sphericity and circularity, were found in the South Coast, and the lowest drag coefficients in the Northern Highlands. The average settling velocities, as a function of drag coefficient, for particles (≤ 2.5 μm) in Iceland is 0.1 m/s. Uncertainties that occurred due to measurements is propagated into the settling velocity calculation.

Volcanic ash is typically less dense and less elongated compared to the surface material, regardless of source region. The flatness and elongation of volcanic ash has similar values to that of all preexisting surface material. As a result, volcanic ash has similar sphericity and circularity as the surface particles, which results in similar settling velocities for particles ≤ 2.5 μm.

5.3.3 Morphological Characteristics

The typical structure of the Icelandic surface material differs from the surface material of most major dust sources, like the Sahara, which are typically made up of quartz, clay minerals and feldspars. Icelandic surface particles greater than 20 μm in diameter, which makes up 90% by volume of the total sieved samples and 40% by volume of the suspendable material between 20-63 μm, exhibit distinct volcanic properties including vesicles, river line fractures showing brittle fracture processes, bubble imprints, and bubble wall pieces (Figure 5.5). Surface samples of particles less than 20 μm in diameter, 11% of the sieved samples, have similar physical characteristics (blocky, plate, and crystalline like structures) to the dusts found commonly outside of Iceland (Coude-Gaussen et al., 1987; Reid et al., 2002; Alastuey et al., 2005; Wang et al., 2011; Atkinson et al, 2013; Buck et al., 2013; Scheuvens et al., 2013). These finer grains are crystalline like in nature and have little variation in their blocky nature. The volcanic properties mentioned above are no longer present in the surface material nor in the volcanic ash.

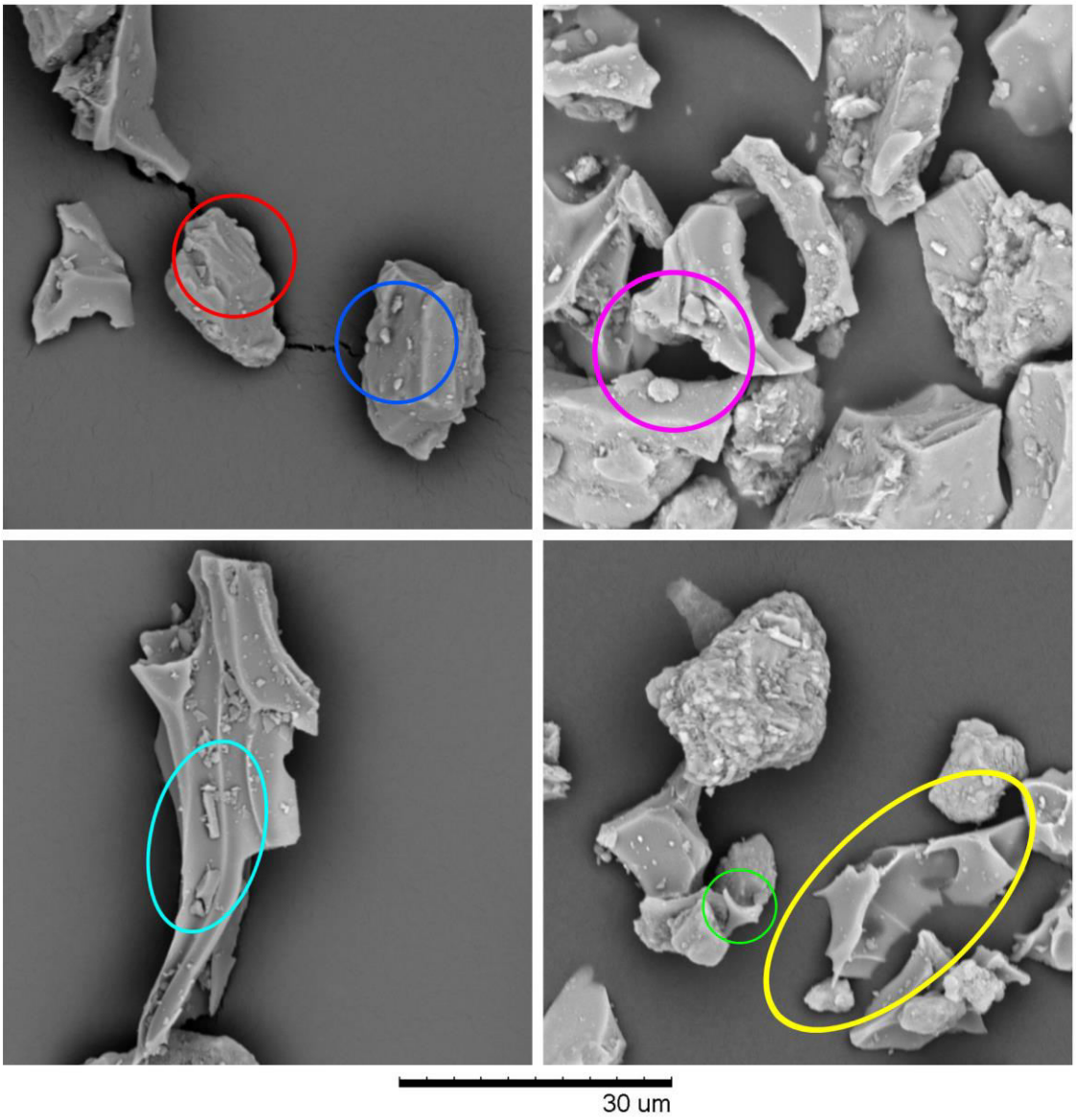

Figure 5.5: Morphological characteristics of suspendable material in Iceland. Each colored oval highlights a different physical property. Red: river line fractures. Blue: ultrafine particles (≤ 1 μm) slightly elongated grains. Pink: fine grained crystalline like and blocky particles. Light blue: fine grained elongated blocky crystals. Green: bubble walls. Yellow: bubble wall imprints and vesicles.

Based on the flatness and elongation, most of the fine material (≤ 2.5 μm) has close to equal dimensions and is crystalline like in nature (Figure 5.6). The bulk of the particles are some form of blades and blocks, followed by slab and rod like particles. Plates and equant blocks are the least common shape form.

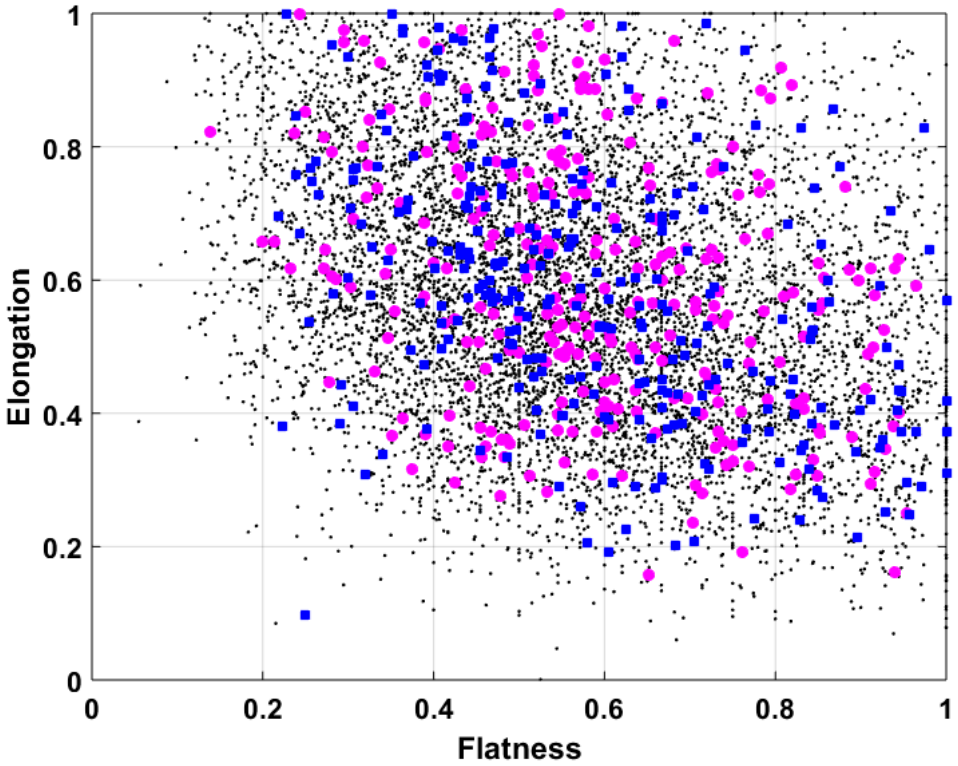

Figure 5.6: Shape of particles measured in Iceland. Black dots: surface samples, Pink circles: Eyjafjallajökull ash, Blue squares: Grímsvötn ash.

5.3.4 Melting Experiments

The finest material (≤ 2.5 μm) in the Grímsvötn ash sample (#28) and Markarfljótsaurar (#22) sample, had similar characteristics in two dimensions, i.e. flatness, elongation, circularity. As a result, the rate of heating of the grains will be similar between the samples.

The original Grímsvötn ash (sample #28) had defined angular edges, had high glass content, and contained a few mineral grains (Figure 5.7). After heating to 800°C there was very little to no rounding of the edges of non-glass grains. Bubbles formed from larger pieces of glass, but the smaller grains of glass were still present and unchanged (Figure 5.7). At 850°C the material began to sinter together in the crucible. Very little rounding was observed in any of the material. There were no more glass bubbles present (Figure 5.7). At 900°C the material had coalesced together, and grains were beginning to become rounded. At 950°C all the material began to become conjoined together. At the highest temperature of the experiment at 1000°C all grains were either rounded or had evidence that the edges began to become soft or melt. Most grains were glued together with the glassy material (Figure 5.7).

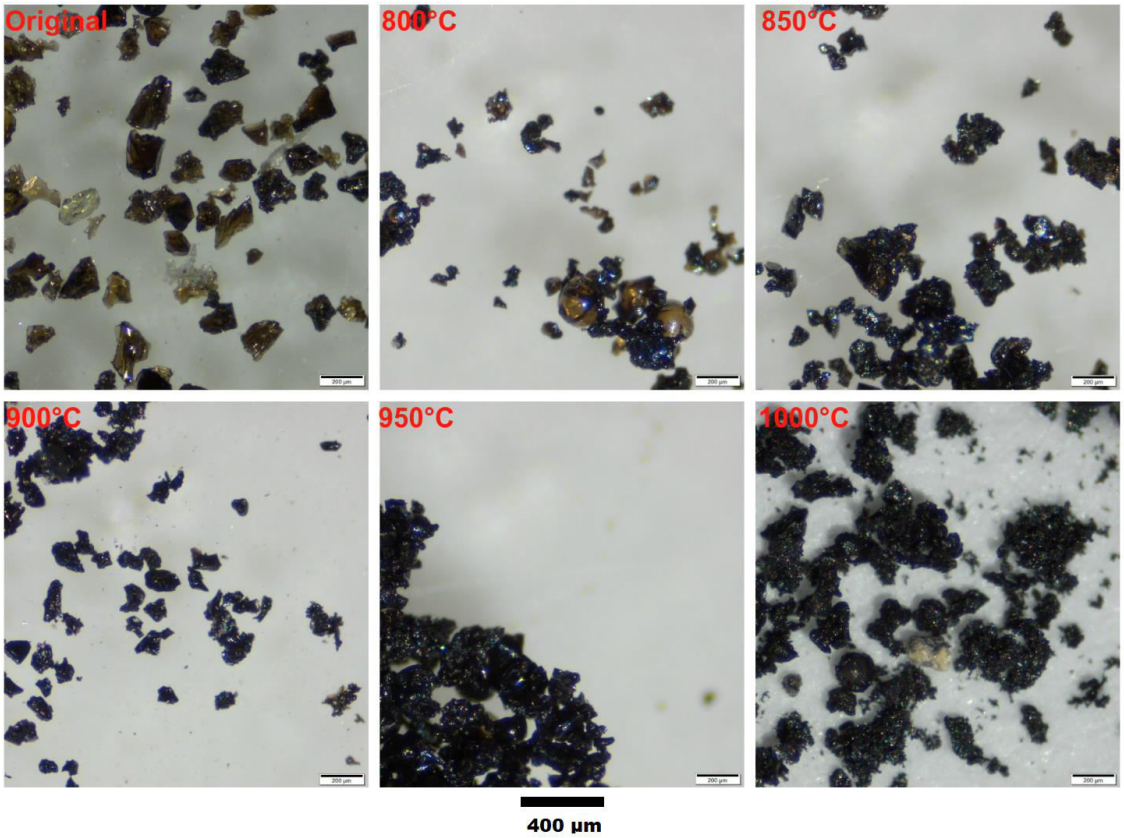

Figure 5.7: Grímsvötn 2011 volcanic ash (sample #27) in its original state and as heated at 50°C intervals 800°C - 1000°C.

The Markarfljótsaurar sample (sample #22) was much sandier in texture with rounder edges and uniform grain sizes and shape, it was also mineral rich (Figure 5.8). At 800°C no change in the grains was observed. At 850°C a few glassy bubbles were associated with material that began to stick together. Overall the grains were mostly separated. At 900°C more grains were conjoined and more glass bubbles were formed than at 850°C, however, there was less than in the ash at this temperature (Figure 5.7 and 5.8). Some of the grains began to have edges rounding. At 950°C most of the grains had sintered together and more bubbles were present. Rounding did not change much from 900°C. Finally, at 1000°C the grains had definite rounding, which is most evident when in contact with other grains. All the heated sample had become glued together at this temperature (Figure 5.8).

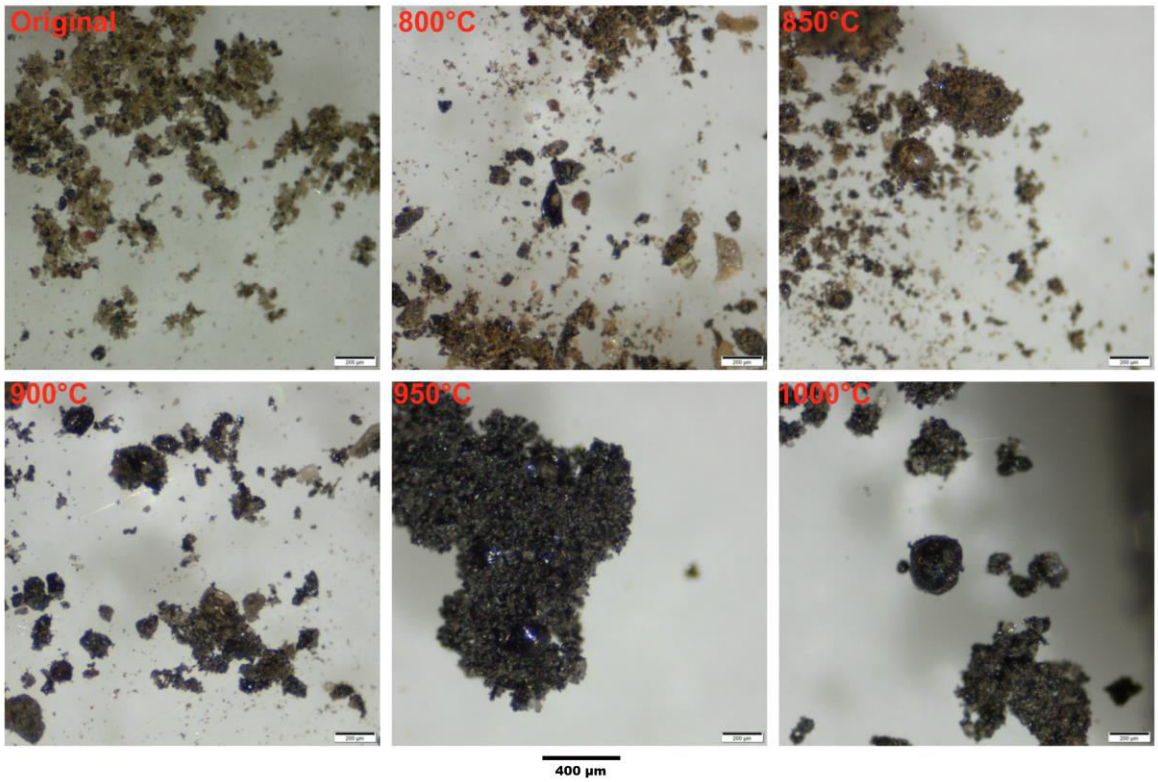

Figure 5.8: Markarfljótsaurar < 125 µm (sample #22) surface sample in its original state and as heated at 50°C intervals 800°C - 1000°C.

5.4 Discussion

Based on the field and lab analysis it is likely that the samples collected for this research are representative of their respective areas. Additionally, when averaged to create the overall Iceland values it probable that the characteristics are representative for suspendable material throughout Iceland.

The size distribution of surface material shows that the particle size distribution is mostly the same for both the Northern and Western Highlands (Figure 5.4), differing mainly with the largest grains (≥ 710 µm). Based on field and lab analysis it is thought that the reason for the Western Highlands having a larger percentage of grains in this larger size range is that the area does not undergo as much flooding as the Northern Highlands and as a result, the grains are not exposed to as much fluvial erosion to break up the grains (Johannesdottir, 2011). This may contribute to the more gravely texture of the Western Highlands (Figure 5.1B). The South Coast has a similar percent of grains ≥ 710 µm as the Northern Highlands, but a higher percentage of the finest (≤ 50 µm) material. The South Coast contains more river and flood river deltas than the two Highland regions (Figure 5.1D), which may allow the finest material to be easily transported there during floods and deposited (Johannesdottir, 2011). The South Coast receives more precipitation than the two Highland regions, so the surface is wetted more frequently (Rögnvaldsson et al., 2007). Possibly this results in less time during which fine material may be easily suspended and transported away.

Previous studies have shown a relationship between surface material sorting and material sizes, with greater sorting being associated with suspendable coarser material (Folk and Ward, 1957; Nickling, 1983; Pye, 1987). From field analysis the desert areas of Iceland (sandur) have moderately sorted surface material associated with coarser material capable of saltation as opposed to suspension (Table 5.2). The majority of the surface material (80-90%) for all of the sample areas was material greater than 63 μm. The saltation process may be the source of the finer grains that are suspended and measured by the OPC, but not found on the surface.

The OPC size distribution of the airborne material shows three peaks in particle size distribution for particle diameters ≤ 10 μm (within the size range capable of suspension). The Mastersizer 3000, analyzing surface samples and ash samples collected on the ground, compared with the in-situ measurements of airborne particles made by the OPC, did not replicate this size distribution pattern between 2.5-10 μm. This could be explained by the saltation process breaking up the material found on the surface (in source areas) into smaller pieces measured in the air (Folk and Ward, 1957; Nickling. 1983; Pye, 1987). Errors due to the assumed optical properties within the OPC calculations will also impact the particle size distribution but would not explain the difference between the two measurements (Shinozuka et al., 2004).

The fresh volcanic ash that was deposited away from the eruption vent (>30 km) location consists of a larger percentage of the finest particles compared to most of the surface samples taken in this study. The most probable reason for this is that the size of the volcanic ash is dictated by the rate of cooling of material in the volcanic plume, fragmentation processes, and where it was collected in reference to the eruption site. Whereas, the typical surface material in dust source areas is formed mostly through erosional processes, creating larger grains than the fresh volcanic ash (Arnalds, 2010). Through erosion grains can range from silt to pebble size depending on type, strength and duration of erosional events. The single peak in the size distribution measured for ash < 500 μm with an extending tail at the finest grains is consistent with what is observed during both the Eyjafjallajökull (2010) and Grímsvötn (2011) eruptions at various ash deposition sites (Gudmundsson et al., 2012; Jude-Eton et al., 2012; Thorsteinsson et al., 2012; Gudmundsson and Larsen, 2016).

When compared to other major dust sources in the world, particles in Iceland of ~20 μm and less (~10% of the surface material) appear to have similar blocky crystalline like structures (Pye 1987; Alastuey et al., 2005; Wang et al., 2011; Buck et al., 2013). The dimensional measurements also confirm the blocky crystalline like characteristics of the finest material in Iceland. At other major sources these structures are observed in all sizes. However, in Iceland particles > 20 μm (90%) have distinctive volcanic properties (see section 5.3.3).

The surface material and ash deposits in Iceland have similar densities. The density of non-Icelandic dust is 2.65 g/cm^3 (Frye, 1981; Pye, 1987; Haywood et al., 2003; Osborne et al., 2008) while the density of the average surface samples and ash samples collected in Iceland is 2.37 g/cm^3. From the calculations of sphericity, drag coefficient and settling velocity of particles ≤ 2.5 μm, the volcanic ash and surface material will behave similarly to dust particles of similar size from around the world. The lower density of the suspendable material in Iceland is not the main factor in how Icelandic dust is different

from other major sources; rather it is the shape of the material having greater significance. It is thought that for particles < 20 µm suspension, transport, and deposition will be similar to particles of comparable size from outside of Iceland. The lower density will play an important role with larger particles, as they may be more porous, or irregular in shape because of the volcanic morphology, and as a result, could be more easily suspended and transported for longer distances, than if they did not have these properties.

The melting experiments made on the Grímsvötn 2011 ash and the Markarfljótsaurar surface sample, the surface sample most compositionally different from the fresh ash, showed that both could have some melting within the range of temperatures airline engines operate (1200-1450°C), with the softening of glassy particles starting at 800-850°C (Alexander, D., 2013; Vasseur et al., 2013; Davison and Rutke, 2014; Kueppers et al., 2014; Song et al., 2016; Yang et al., 2018). The glassy material in both samples experienced the most melting in the tested temperature range, whereas the non-glassy grains experienced little to no sintering or melting. The volcanic ash had a much larger percentage of glass compared to the surface sample, with other samples' compositions laying between these two end-members. The more glass a dust particle contains, the more it may melt at engine operating temperatures, thereby increasing its threat to aircraft safety. There were varying amounts of glass found in all the samples.

5.5 Conclusions

The size distribution of the surface material in Iceland is moderately dependent on its source area conditions. The Western Highlands have coarser material (>500 µm) and the sediment is not as well sorted as in the Northern Highlands and the South Coast. The overall size distribution of the bulk surface material and fresh volcanic ash deposited away from the eruption vents of Eyjafjallajökull and Grímsvötn, are very similar and cannot be distinguished from one another by size alone. It is probable that distinguishing between fresh volcanic ash and dust source material is not possible by grain size alone for any future eruptions. In order to distinguish between volcanic ash and surface material, chemical composition and physical morphologies need to be examined.

The main difference between Icelandic dust and dust from other areas (e.g. Sahara and Gobi deserts) is the physical appearance. Particles from Iceland, that are greater than 20 µm have volcanic morphological properties such as bubble imprints, bubble wall shards, vesicles, and river line fractures. When any of these coarse-grained particles are suspended, they can be referred to as large grained Icelandic dust. Overall, despite its volcanic origin, the dust in Iceland that is 20 µm and less is remarkably similar to dust from other large source areas found globally, with crystalline block like structures. Very young volcanic ash that still has chemical coatings present from the eruption cloud should be considered to be more hazardous to health compared with other dusts, but this is assumed to be short-lived due to Iceland's wet conditions. Volcanic ash > 20 µm, that has been deposited on the surface, will fall into the large grained Icelandic dust category. Volcanic ash < 20 µm in size will be expected to behave similarly in the atmosphere to dust found in the large deserts of the world including Iceland, posing similar risks to human health and infrastructure. Volcanic ash typically has a higher percentage of glassy

grains than the bulk surface material in Iceland, but glass is still present in all the source areas of Iceland.

Finally, the risk to aviation flying through dust storms from Iceland due to grain melting is less than flying through eruption clouds rich in volcanic ash. Volcanic ash is more likely to melt within an engine than the bulk dust due to the greater number of glassy particles. The hazard may be greater immediately following an ash-producing eruption when volcanic ash may be suspended together with the bulk surface material in sufficient quantities to increase the amount of glassy particles present, but will diminish to the level of hazard of the bulk dust in Iceland as the ash is integrated into the other material. It is possible that there may be some harm from melting glass in the engines of planes that frequently fly in/out and through dusty areas of Iceland as glassy particles were present in all collected surface samples.

For future measurements of particulate matter in Iceland it is important to adjust the density, shape factor and optical properties for Icelandic dust, especially when the measurements are optical or fall velocity based. Specifically, for OPC measurements, it is recommended that adjustments be made to more closely resemble black carbon rather than typical dust outside of Iceland for the optical properties. The adjustment for these parameters would provide more accurate measurements, transport simulations, and understanding of the impact of Icelandic dust on the environment.

6 Conclusions

The amount of time fresh volcanic ash remains on the surface as a distinct component of the surface material available to be lofted as PM in Iceland is shorter than previously thought. The ash provided by explosive volcanic eruptions does not increase the number of PM events that are observed annually in Iceland above the 50-year average number of PM events. An increase in PM events only occurs locally and over a period of weeks to months rather than years. The local increase in PM events is very dependent on the size and timing of the eruption with the weather conditions following an eruption being the main factor in how many PM events dominated by fresh ash will occur. Regardless of when the last ash producing eruption was, it is important to note that the number of events that were observed is a minimum value. There may have been more events that were either short lived, small, or away from observers and as a result, did not get reported.

Only the minimum number of PM events is known because there are inherent weaknesses in relying only on manned weather observations for PM activity in Iceland. The first being that observations of PM when it is dark is extremely difficult if not impossible to make, especially for smaller events. Due to the long duration of darkness in winter the potential for observations being missed is much higher than in summer. Additionally, weather observers are not everywhere. Large source areas, such as the Highlands, do not have enough weather observers to adequately monitor PM events. Moreover, there has been a decrease in manned stations throughout Iceland over the past 50 years, with the greatest decrease occurring in the last decade. The reduction in coverage results in fewer PM events being observed.

The use of satellite data in Iceland is not a reliable way to monitor the number of PM events that occur, especially during wintertime. Due to the winter darkness, cloudy climate and the fact that Icelandic PM events do not typically rise above the boundary layer many PM events go unseen with visible imagery. Using specific spectral bands to detect aerosols is also difficult, even on clear days. The reason for the difficulty is that the particles are the same color as the surface and do not extend high enough into the atmosphere to have a large enough temperature difference to be detected. The use of satellite-based LIDAR is useful when detecting aerosols in the atmosphere, however, the data is dependent on when the satellite passes over an area. In addition, thick cloud layers also become troublesome as they block the LIDAR signal from reaching through the entire atmospheric column. Ground based LIDAR can also be used, however, it only gives information for a short radius of about 10 km. As a result, events can be missed entirely if they do not pass close enough to the LIDAR.

The synoptic scale weather pattern strongly influences the local scale conditions and based on surface in situ measurements, the weather conditions at the source and downwind of the PM determines the size and duration of an event. The drier and windier the conditions are, the larger the event. Events lasting a day or more typically occur when relative humidity is < 70 % and wind speeds are greater than 10 m/s. Smaller events lasting less than a day can occur during almost all weather conditions. However, the size distribution of particles during these shorter events can differ, depending on the weather, specifically wind speed and moisture content. During events whose duration is less than one day concentrations of particles > 5 µm in diameter do not exceed the background level of 10 particles/cm^3.

However, with a more robust data set for Iceland the PM event magnitude classifications may change. The conditions needed for PM suspension in Iceland are similar to the conditions from other dust sources in the world. However, compared with those areas, weather conditions in Iceland have a large variability. Due to Iceland being located in the North Atlantic storm track, weather conditions can change rapidly, and therefore also the conditions for PM suspension; from unfavorable to favorable and vice versa, especially when heavy precipitation is involved.

The sizes of PM events in Iceland are magnitudes smaller in terms of number concentration than events from other major dust sources, such as the Gobi and Saharan Deserts. Events of all magnitudes can last for days and over a wide area of Iceland. Additionally, PM events can occur at any time of year in Iceland; making the country a consistent source of PM that gets transported within and away from Iceland. Despite the smaller size, the events still greatly affect the local environment and communities.

The suspension of recently deposited fresh volcanic ash can change the size distribution of PM events. The size distribution of fresh volcanic ash can be different from that of older dust in the surface material, in that the distribution can be more uniform due to the better sorting of grains within the eruption cloud when the ash was first deposited. The typically finer nature of the grains in the ash increases risks to human health. Once resuspended, the difference in size distributions between dust dominated by fresh ash and older dust is no longer evident; this could be due to the breakup of the surface grains during saltation or the suspension of only smaller particles or that the resuspended fresh volcanic ash is generally accompanied by so much older dust that it´s unique size distribution is unseen in the mixture of airborne material. When the volcanic ash no longer has its volcanic salts, that were formed during the eruption, the health hazard is the same as bulk Icelandic dust. The volcanic ash and bulk Icelandic surface material are compositionally different in that the volcanic ash has a higher percentage of glass (>50% compared to 5-30%). This high glass content is an aviation hazard due to its lower melting temperature during eruptions and when resuspended in high concentrations. Little volcanic ash is identifiable within the surface material of the major dust source regions of Iceland within four years following an ash-producing eruption. This means that dust from Iceland has similar risks as dust from non-volcanic sources such as the Sahara, except that the lower number concentration of a typical Icelandic dust storm would make it less hazardous. The reason little volcanic ash is preserved on the surface is due to the frequent windy conditions. Ash deposits are quickly blown away or worked into the soils.

The high-resolution timing of the volcanic ash being blown away or integrated into the already existing surface material is not fully known at this time. Based on the long term study of the impacts of volcanic eruptions and the shorter term conditions needed for the resuspension of recently deposited volcanic ash, it is found to take between one month and two years. We suggest that the resuspension of volcanic ash be only considered for a maximum of two years after a large ash-producing eruption. A weather forecaster may choose to reduce the two-year time frame based on the timing of the eruption and weather conditions following the eruption.

7 Outlook

Volcanic ash has a relatively short “lifetime” on erodible surfaces in Iceland due to the windy and wet conditions. In order to precisely know the persistence of individual ash deposits, continuous monitoring would be needed. Preferably measurements of PM would be ongoing before an eruption and would be made in a location that is representative of an entire area. To have a full comprehensive picture of the environment multiple stations within one geographic region may be needed. Continuous monitoring would also give a better estimate of the number and strength of dust storms in Iceland. With the decreasing number of weather observers, the installation of automatic visibility sensors, or particulate sensors, as well as increasing the number of remote sensing instrumentation is recommended. Stations near active volcanoes known for producing large amounts of ash, that are also in persistent PM source areas should be the first places these sensors are installed. Followed by stations downwind of the large source areas. Additionally, following an explosive eruption it would be beneficial to take samples of suspended PM and analyze the chemistry in order to determine when the suspended material is no longer volcanic ash from that specific eruption.

During times when multiday PM events are forecasted it would be very beneficial to conduct measurements within the entire atmospheric column, not just at the surface. This could be done with either balloon launches, or with drones as well as through remote sensing using LIDARs and dual-polarization weather RADARs.

Additionally, surface material and/or collected suspended material should undergo analysis for its effectiveness as a CCN, as well as its albedo while suspended in the atmosphere. With these analyses completed it could be determined, how PM from Iceland effects meteorology and climate as compared to dust from other parts of the world. Once the physical, optical, and chemical properties of the PM in Iceland is known the parameters can be implemented in numerical models that forecast the impact or extent of dust events. This would allow for a more accurate representation of the atmosphere in and around Iceland.

Numerical modeling may also be a feasible way to narrow down the timeframe in which volcanic ash can be resuspended. The first step for this is to finish the work that has been started with WRF/Chem. Once all the land use parameters are set and correct for Iceland, model output could show when resuspension of volcanic ash from the 2010 Eyjafjallajökull eruption ended. If this work is successful, improving the usage of ash deposits in less computationally heavy models can be done, allowing for more accurate forecasts for PM events. These techniques could then potentially be used for future volcanic eruptions.

Furthermore, analysis of how the 2014-2015 Holuhraun lava field impacts the number of PM events originating in the Highlands would be a beneficial study. The new lava field covers approximately 85 km^2 of a known dust source region. It is hypothesized that the existence of the lava field will decrease the number of PM events over the long term. However, over a shorter time scale the lava field may amplify the number of PM events due to thermal circulations created by the heat of the lava.

It would also be beneficial to conduct a comparable study on the resuspension of volcanic ash in other high latitude areas with large ash deposits such as Katmai National Park, Alaska, USA. It would be interesting to find out if the overall meteorological conditions need to be the same for resuspension of volcanic ash to occur. These simulations could help ascertain if the resuspended ash concentrations are similar to those experienced during modern volcanic eruptions. If a similar study was done in Katmai, the main difference would be that there is little to no other sources of PM other than volcanic ash in the area. The Copper River Valley, across the Gulf of Alaska (~590 km) is the closest non-volcanic source area that produces large PM events on a regular basis.

Overall, there is still a lot of research that needs to be done in terms of high latitude dust, and high latitude volcanic eruptions, and how they impact the local and global environments. But what we do know is that "The answer, my friend, is blowin' in the wind, the answer is blowin' in the wind" – Bob Dylan

References

Alaska Volcano Observatory, (cited 2019). Novarupta Reported Activity [Available online at https://avo.alaska.edu/volcanoes/volcact.php?volcname=Novarupta].

Alastuey, A., Querol, X., Castillo, S., Escudero, M., Avila, A., Cuevas, E., Torres, C., Romero, P., Exposito, F., García, O., Diaz, J.P., van Dingenen, R., Putaud, J. P. (2005). Characterisation of TSP and PM2.5 at Izaña and Sta. Cruz de Tenerife (Canary Islands, Spain) during a Saharan dust episode (July 2002). *Atmospheric Environment*, *39*, 4715–4728. https://doi.org/10.1016/j.atmosenv.2005.04.018

Alexander, D. (2013). Volcanic ash in the atmosphere and risks for civil aviation: A study in European crisis management. *International Journal of Disaster Risk Science*, *4*(1), 9–19. https://doi.org/10.1007/s13753-013-0003-0

American Meteorological Society. Airborne particulates – AMS Glossary. (2012). Retrieved May 7, 2019, from http://glossary.ametsoc.org/wiki/Airborne_particulates

American Meteorological Society, (cited 2019). Glossary of Meteorology. [Available online at http://glossary.ametsoc.org/wiki/Main_Page].

Anderson, J. O., Thundiyil, J. G., & Stolbach, A. (2012). Clearing the Air: A Review of the Effects of Particulate Matter Air Pollution on Human Health. *Journal of Medical Toxicology*, *8*(2), 166–175. https://doi.org/10.1007/s13181-011-0203-1

Arason, Þ., Bjornsson, H., Nína Petersen, G., Björk Jónasdóttir, E., & Oddsson, B. (2015). Plume height during the 2014-2015 Holuhraun volcanic eruption. In *EGU General Assembly 2015, held 12-17 April, 2015 in Vienna, Austria. id.11498* (Vol. 17).

Arnalds, O., Gisladottir, F. O. and Sigurjonsson, H. (2001a). Sandy deserts of Iceland: an overview. *Journal of Arid Environments, 47*, 359–371.

Arnalds, O., Thorarinsdoittir, E. F., Metusalemsson, S., Jonsson, A., Gretarsson, E., & Arnason, A. (2001b). *Soil Erosion in Iceland*. Gutenberg. https://doi.org/ISBN 9979-60-641-X

Arnalds, Ó. (2005). Icelandic soils. *Developments in Quaternary Sciences*, *5*, 309–318. https://doi.org/10.1016/S1571-0866(05)80015-6

Arnalds, O. (2010). Dust sources and deposition of aeolian materials in Iceland, *23*, 3–21.

Arnalds, O., Gisladottir, F. O., & Orradottir, B. (2012). Determination of aeolian transport rates of volcanic soils in Iceland. *Geomorphology*, *167*, 4–12. https://doi.org/10.1016/j.geomorph.2011.10.039

Arnalds, O., Thorarinsdottir, E. F., Thorsson, J., Waldhauserova, P. D., & Agustsdottir, A. M. (2013). An extreme wind erosion event of the fresh Eyjafjallajökull 2010 volcanic ash. *Scientific Reports*, *3*(1), 1257. https://doi.org/10.1038/srep01257

Arnalds, O., Olafsson, H., & Dagsson-Waldhauserova, P. (2014). Quantification of iron-rich volcanogenic dust emissions and deposition over the ocean from Icelandic dust sources. *Biogeosciences*, *11*(23), 6623–6632. https://doi.org/10.5194/bg-11-6623-2014

Arnalds, O., Dagsson-Waldhauserova, P., & Olafsson, H. (2016). The Icelandic volcanic aeolian environment: Processes and impacts — A review. *Aeolian Research*, *20*, 176–195. https://doi.org/10.1016/j.aeolia.2016.01.004

Ashwell, I. Y. (1986). Meteorology and Duststorms in Central Iceland. *Arctic and Alpine Research*, *18*(2), 223–234. https://doi.org/10.1080/00040851.1986.12004081

Atkinson, J. D., Murray, B. J., Woodhouse, M. T., Whale, T. F., Baustian, K. J., Carslaw, K. S., Dobbie, S., O'Sullivan, D., Malkin, T. L. (2013). The importance of feldspar for ice nucleation by mineral dust in mixed-phase clouds. *Nature*, *498*(7454), 355–358. https://doi.org/10.1038/nature12278

Ágústsdóttir, A. M. (2015). Ecosystem approach for natural hazard mitigation of volcanic tephra in Iceland: building resilience and sustainability. *Natural Hazards*, *78*(3), 1669–1691. https://doi.org/10.1007/s11069-015-1795-6

Baddock, M. C., Strong C. L., Murray P. S., and McTainsh, G. H. (2013). Aeolian dust as a transport hazard. *Atmos. Environ.*, *71*, 7–14, doi:10.1016/J.ATMOSENV.2013.01.042.

Baddock, M. C., Mockford, T., Bullard, J. E., & Thorsteinsson, T. (2017). Pathways of high-latitude dust in the North Atlantic. *Earth and Planetary Science Letters*, *459*, 170–182. https://doi.org/10.1016/J.EPSL.2016.11.034

Bagheri, G. H., Bonadonna, C., Manzella, I., Vonlanthen, P. (2015). On the characterization of size and shape of irregular particles. *Powder Technology, 270*, 141-153.

Bagheri, G., Bonadonna, C. (2016). Aerodynamics of volcanic particles: characterization of size, shape, and settling velocity. In Elsevier, *Volcanic ash hazard observation* (pp. 39-52). Amsterdam, Netherlands.

Barnard, J. C., and J. D. Fast, G. Paredes-Miranda, W. P. Arnott, and A. Laskin, (2010). Technical note: Evaluation of WRF-Chem "aerosol chemical to aerosol optical properties" module using data from MILAGRO campaign. *Atmos. Chem. Phys.*, **10**, 7325-7340.

Beckett, F., Kylling, A., Sigurðardóttir, G., von Löwis, S., & Witham, C. (2017). Quantifying the mass loading of particles in an ash cloud remobilized from tephra deposits on Iceland. *Atmospheric Chemistry and Physics*, *17*(7), 4401–4418. https://doi.org/10.5194/acp-17-4401-2017

Beckett, W. S. (2000). Occupational Respiratory Diseases. *New England Journal of Medicine*, *342*(6), 406–413. https://doi.org/10.1056/NEJM200002103420607

Bergstrom, R. W., Russell, P. B., Hignett, P., Bergstrom, R. W., Russell, P. B., & Hignett, P. (2001). Wavelength Dependence of the Absorption of Black Carbon Particles: Predictions and Results from the TARFOX Experiment and Implications for the Aerosol Single Scattering Albedo. *Journal of the Atmospheric Sciences*, *59*(3), 567–577. https://doi.org/10.1175/1520-0469(2002)059<0567:WDOTAO>2.0.CO;2

Blott, S. J., & Pye, K. (2008). Particle shape: a review and new methods of characterization and classification. *Sedimentology*, *55(*1), 31-63 https://doi.org/10.1111/j.1365-3091.2007.00892.x

Boichu, M., Chiapello, I., Brogniez, C., Péré, J.-C., Thieuleux, F., Torres, B., Blarel, L., Mortier, A., Podvin, T., Goloub, P., Söhne, N., Clarisse, L., Bauduin, S., Hendrick, F., Theys, N., van Roozendael, M., & Tanré, D. (2016). Tracking far-range air pollution induced by the 2014-15 Bárdarbunga fissure eruption (Iceland). https://doi.org/10.5194/acp-2016-159

Boldo, E., Medina, S., Le Tertre, A., Hurley, F., Mücke, H.-G., Ballester, F., Aguilera, I., & Eilstein, D on behalf of the Apheis group (2006). Apheis: Health Impact Assessment of Long-term Exposure to PM2.5 in 23 European Cities. *European Journal of Epidemiology*, *21*(6), 449–458. https://doi.org/10.1007/s10654-006-9014-0

Brock, F. V. & Richardson, S. J. (2001). Meteorological Measurement Systems. Oxford University Press, New York, NY. ISBN 0-19-513451-6.

Buck, B. J., Goossens, D., Metcalf, R. V., McLaurin, B., Ren, M., & Freudenberger, F. (2013). Naturally Occurring Asbestos: Potential for Human Exposure, Southern Nevada, USA. *Soil Science Society of America Journal*, *77*(6), 2192. https://doi.org/10.2136/sssaj2013.05.0183

Bullard, J. E. (2013). Contemporary glacigenic inputs to the dust cycle. *Earth Surface Processes and Landforms*, *38*(1), 71–89. https://doi.org/10.1002/esp.3315

Bullard, J. E., Baddock, M., Bradwell, T., Crusius, J., Darlington, E., Gaiero, D., Gassó, S., Gisladottir, G., Hodgkins, R., McCulloch, R., McKenna-Neuman, C., Mockford, T., Stewart, H & Thorsteinsson, T. (2016). High-latitude dust in the Earth system. *Reviews of Geophysics*, *54*(2), 447–485. https://doi.org/10.1002/2016RG000518

Burritt, B.E., and Hyers, A., (1981). Evaluations of Arizona's highway dust warning system, in Pewe, T.L., ed. 1, *Desert dust: Origin, characteristics and effects on man*. Geological Society of America Special Paper 186, p. 281-292.

Butwin, M. K., von Löwis, S., Pfeffer, M. A., & Thorsteinsson, T. (2019a). The effects of volcanic eruptions on the frequency of particulate matter suspension events in Iceland. *Journal of Aerosol Science*, *128*. https://doi.org/10.1016/j.jaerosci.2018.12.004

Butwin, M. K., Pfeffer, M. A., von Löwis, S., Støren, E. W. N., Bali, E., Thorsteinsson, T. (2019b). Icelandic dust properties based on surface material and volcanic ash. *Submitted to Journal of Sedimentology*.

Büttner, R., P. Dellino, and B. Zimanowsky (1999). Identifying magma- water interaction from the surface features of ash particles, Nature, 401, 688–690, doi:10.1038/44364.

Büttner, R., P. Dellino, L. La Volpe, V. Lorenz, and B. Zimanowsky (2002), Thermohydraulic explosions in phreatomagmatic eruptions as evidenced by the comparison between pyroclasts and products from Molten Fuel Interaction experiments, J. Geophys. Res., 107(B11), 2277, doi:10.1029/2001JB000511.

Carter, J. (1979). *How dust fouled up the hostage problem in Iran.* Oval Office Tapes Service.

Casadevall, T. J., Delos Reyes, P. J., & Schneider, D. J. (1996). The 1991 Pinatubo eruptions and their effects on aircraft operations. *African Journal of Biotechnology*, *8*(14), 3382–3386.

Cashman, K., & Rust, A. (2016). Volcanic Ash: Generation and Spatial Variations. In S. Mackie, K. Cashman, H. Ricketts, A. Rust, & M. Watson (Eds.), *Volcanic Ash Hazard Observation* (1st ed., pp. 5–24). Amsterdam, Netherlands: Elsevier.

Chamberlain, A. C. (1975). *The movement of particles in plant communities*. In J. L. Monteith (ed.), *Vegetation and the Atmosphere*, vol. I. Academic Press, London, pp. 155-203.

Chen, Y., Cai, Q., & Tang, H. (2003). Dust Storm as an Environmental Problem in North China. *Environmental Management*, *32*(4), 413–417. https://doi.org/10.1007/s00267-003-0042-1

Chepil, W. S. (1951). Properties of soil which influence wind erosion: IV. State of dry aggregate structure. *Soil Science*, *72*(5), 387–402.

Chepil, W. S., and Woodruff, N. P., (1957). Sedimentary characteristics of dust storms; Part II, Visibility and dust concentration. *American Journal of Science*, *255*, 104–114, doi:10.2475/ajs.255.2.104.

Clarkson, R., Majewicz, E., and Mack, P. (2016). A re-evaluation of the 2010 quantitative understanding of the effects volcanic ash has on gas turbine engines. Proc IMechE Part G: J Aerospace Engineering, DOI: 10.1177/0954410015623372

Clements, T., Stone, R. O., Mann, J. F. and Eymann, J. L. (1963). A study of windborne sand and dust in desert areas. (Technology Report ES8). US Army Natick Laboratories, Earth Science Division.

Corey, A. T. (1949). Influence of shape and fall velocity of sand grains. (MSc Thesis, Colorado A&M College).

Coude-Gaussen, G., Rognon, P., Bergametti, G., Gomes, L., Strauss, B., Gros, J. M., & Le Coustumer, M. N. (1987). Saharan dust on Fuerteventura Island (Canaries): Chemical and mineralogical characteristics, air mass trajectories, and probable sources. *Journal of Geophysical Research*, *92*(D8), 9753. https://doi.org/10.1029/JD092iD08p09753

Crusius, J., Schroth, A. W., Gassó, S., Moy, C. M., Levy, R. C., & Gatica, M. (2011). Glacial flour dust storms in the Gulf of Alaska: Hydrologic and meteorological controls and their importance as a source of bioavailable iron. *Geophysical Research Letters*, *38*(6), n/a-n/a. https://doi.org/10.1029/2010GL046573

Csavina, J., Field, J., Félix, O., Corral-Avitia, A. Y., Sáez, A. E., & Betterton, E. A. (2014). Effect of wind speed and relative humidity on atmospheric dust concentrations in semi-arid climates. *Science of The Total Environment*, *487*, 82–90. https://doi.org/10.1016/J.SCITOTENV.2014.03.138

Dagsson-Waldhauserova, P., Arnalds, O., & Olafsson, H. (2013). Long-term frequency and characteristics of dust storm events in Northeast Iceland (1949–2011). *Atmospheric Environment*, *77*, 117–127. https://doi.org/10.1016/J.ATMOSENV.2013.04.075

Dagsson-Waldhauserova, P., Arnalds, O., Olafsson, H., Skrabalova, L., Sigurdardottir, G. M., Branis, M., Hladil, J., Skala, R., Navratil, T., Chadimova, L., von Lowis, S., Thorsteinsson, Th., Carlsen, H. K., and Jonsdottir, I. (2014a). Physical properties of suspended dust during moist and low wind conditions in Iceland. *Iceland Agricultural Sciences, 27*, 25–39, doi:10.1.1.970.4281

Dagsson-Waldhauserova, P., Arnalds, O., & Olafsson, H. (2014b). Long-term variability of dust events in Iceland (1949–2011). *Atmos. Chem. Phys*, *14*, 13411–13422. https://doi.org/10.5194/acp-14-13411-2014

Dagsson-Waldhauserova, P., Arnalds, O., Olafsson, H., Hladil, J., Skala, R., Navratil, T., Chadimova, L., & Meinander, O. (2015). Snow–Dust Storm: Unique case study from Iceland, March 6–7, 2013. *Aeolian Research*, *16*, 69–74. https://doi.org/10.1016/J.AEOLIA.2014.11.001

Damby, D. E., Horwell, C. J., Larsen, G., Thordarson, T., Tomatis, M., Fubini, B., & Donaldson, K. (2017). Assessment of the potential respiratory hazard of volcanic ash from future Icelandic eruptions: a study of archived basaltic to rhyolitic ash samples. *Environmental Health : A Global Access Science Source*, *16*(1), 98. https://doi.org/10.1186/s12940-017-0302-9

Damoah, R., Spichtinger, N., Forster, C., James, P., Mattis, I., Wandinger, U., Beirle, S., Wagner, T., & Stohl, A. (2004). Around the world in 17 days – hemispheric-scale transport of forest fire smoke from Russia in May 2003. *Atmos. Chem. Phys. Atmospheric Chemistry and Physics*, *4*, 1311–1321. Retrieved from www.atmos-chem-phys.org/acp/4/1311/

Davies, S. M., Larsen, G., Wastegård, S., Turney, C. S. M., Hall, V. A., Coyle, L., & Thordarson, T. (2010). Widespread dispersal of Icelandic tephra: how does the Eyjafjöll eruption of 2010 compare to past Icelandic events? *Journal of Quaternary Science*, *25*(5), 605–611. https://doi.org/10.1002/jqs.1421

Davison, C. R., & Rutke, T. A. (2014). Assessment and Characterization of Volcanic Ash Threat to Gas Turbine Engine Performance. *Journal of Engineering for Gas Turbines and Power*, *136*(8), 081201. https://doi.org/10.1115/1.4026810

Dellino, P., R. Isaia, L. La Volpe, and G. Orsi (2001). Statistical analysis of textural data from complex pyroclastic sequence: Implication for frag- mentation processes of the Agnano-Monte Spina eruption (4.1 ka), Phlegraean Fields, southern Italy, Bull. Volcanology., 63, 443–461, doi:10.1007/ s004450100163.

Dellino, P., Mele, D., Bonasia, R., Braia, G., La Volpe, L., & Sulpizio, R. (2005). The analysis of the influence of pumice shape on its terminal velocity. *Geophysical Research Letters*, *32*(21), L21306. https://doi.org/10.1029/2005GL023954

Dellino, P., Gudmundsson, M. T., Larsen, G., Mele, D., Stevenson, J. A., Thordarson, T., & Zimanowski, B. (2012). Ash from the Eyjafjallajökull eruption (Iceland): Fragmentation processes and aerodynamic behavior. *J. Geophys. Res*, *117*, 0–04. https://doi.org/10.1029/2011JB008726

Diehl, W. (1926). Report No . 218 Standard Atmosphere – Tables and Data.

Duce, R. A., Liss, P. S., Merrill, J. T., Atlas, E. L., Buat-Menard, P., Hicks, B. B., Miller, M. J., Prospero, J. M., Arimoto, R., Church, T. M., Ellis, W., Galloway, J. N., Hansen, L., Jickells, T. D., Knap, A. H., Reinhardt, K. H., Schneider, B., Soudine, A., Tokos, J.J., Tsungogai, S., Wollast, R., & Zhou, M. (1991). The atmospheric input of trace species to the world ocean. *Global Biogeochemical Cycles*, *5*(3), 193–259. https://doi.org/10.1029/91GB01778

Einarsson, M. A. (1984). Climate of Iceland. In *Climates of the Ocean* (pp. 673–697). Amsterdam, New York: Elsevier. Retrieved from https://rafhladan.is/bitstream/handle/10802/9550/Einarsson.pdf?sequence=1

Eliasson, J., Watson, I. M., & Weber, K. (2016). In situ observations of airborne ash from manned aircraft. In S. Mackie, K. Cashman, H. Ricketts, A. Rust, & M. Watson (Eds.), *Volcanic Ash Hazard Observation* (1st ed., pp. 89–98). Amsterdam, Netherlands: Elsevier.

Engelstaedter, S., Tegen, I., & Washington, R. (2006). North African dust emissions and transport. *Earth-Science Reviews*, *79*(1–2), 73–100. https://doi.org/10.1016/J.EARSCIREV.2006.06.004

European Environment Agency, Iceland country briefing – the European environment – state and outlook 2015 (2017). Retreived 30 October 2018, from https://www.eea.europa.eu/soer-2015/countries/iceland

European Environment Agency, Air quality standards (2019). Retrieved 10 May 2019, from https://www.eea.europa.eu/themes/air/air-quality-standards

Fedorovitch, G. (2019). Aerosol Particles in Lungs: Theoretical Modeling of Deposition and Mucociliary Clearance. In *Rhinosinusitis [Working Title]*. IntechOpen. https://doi.org/10.5772/intechopen.84254

Folk, R. L. and Ward, W. C. (1957). Brazos River Bar: a study in the significance of grain size parameters. *Journal of Sedimentology Petrology*, 27, 3-26.

Frye, K. (1981). *The Encyclopedia of Mineralology*. Hutchinson Ross, Stroudsberg, Pennsylvania, 794pp.

Fuller, K. A., Maim, W. C., & Kreidenweis, S. M. (1999). *Effects of mixing on extinction by carbonaceous particles*. *JOURNAL OF GEOPHYSICAL RESEARCH* (Vol. 104). https://doi.org/10.1029/1998JD100069

Geptner, A., Kristmannsdottir, H., Pikovskii, Y., & Richter, B. (2005). Abiogenic Hydrocarbon's Emission in the Modern Rift Zone, Iceland, 24–29. Retrieved from https://www.geothermal-energy.org/pdf/IGAstandard/WGC/2005/0860.pdf

Gillies, J. A., Nickling, W. G., & Mctainsh, G. H. (1996). Dust concentrations and particle-size characteristics of an intense dust haze event: Inland Delta Region, Mali, West Africa. *Atmospheric Environment*, *30*(7), 1081–1090. https://doi.org/10.1016/1352-2310(95)00432-7

Gíslason, S. R. (2008). Weathering in Iceland. *Jökull*, *58*, 387–408.

Gislason, S. R., Hassenkam, T., Nedel, S., Bovet, N., Eiriksdottir, E. S., Alfredsson, H. A., Hem, C. P., Balogh, Z. I., Dideriksen, K., Oskarsson, N., Sigfusson, B., Larsen, G., & Stipp, S. L. S. (2011). Characterization of Eyjafjallajokull volcanic ash particles and a protocol for rapid risk assessment. *Proceedings of the National Academy of Sciences of the United States of America*, *108*(18), 7307–12. https://doi.org/10.1073/pnas.1015053108

Global Volcanism Program (GVP), Smithsonian Institution. http://volcano.si.edu/.

Goudie, A. S. (2014). Desert dust and human health disorders. *Environment International*, *63*, 101–113. https://doi.org/10.1016/J.ENVINT.2013.10.011

Green, H. L. and Lane, W. R., (1964). Particulate Clouds: Dusts, Smokes, and Mists: Their physics and physical chemistry and industrial and environmental aspects. *Science, 147* (3660), 855-856.

Grell, G. A., Peckham, S. E., Schmitz, R., McKeen, S. A., Frost, G., Skamarock, W. C., and Eder, B. (2005) Fully coupled "online" chemistry within the WRF model. *Atmos. Environ.*, **39**, 6957-6975.

Groot Zwafftink, C. D., Arnalds, Ó., Dagsson-Waldhauserova, P., Eckhardt, S., Prospero, J. M., & Stohl, A. (2017). Temporal and spatial variability of Icelandic dust emissions and atmospheric transport. *Atmospheric Chemistry and Physics*, *17*(17), 10865–10878. https://doi.org/10.5194/acp-17-10865-2017

Gudmundsson, M. T., and H. Bjornsson, (1991). Eruptions in Grimsvotn, Vatnajokull, Iceland, 1934-1991. *Jokull*, *41*, 21–45.

Gudmundsson, M. T., F. Sigmundsson, and H. Björnsson, (1997). Ice–volcano interaction of the 1996 Gjálp subglacial eruption, Vatnajökull, Iceland. *Nature*, *389*, 954–957, doi:10.1038/40122.

Gudmundsson, M. T., Högnadóttir, T., Pálsson, F., and Björnsson, H. (2000). Grímsvötn: Eldgosið 1998 Og Breytingar Á Botni, Rúmmáli Og Jarðhita 1996-1999. *Raunvísindastofnun Háskólans*. (Text in Icelandic)

Gudmundsson, M. T., Höskuldsson, A., Larsen, G., Sigmarsson, O., Högnadottir, T., Oddsson, B., Magnússon, E., Óskarsson, N., Sigmundsson, F., Einarsson, P., Hreinsdóttir, I., Thordarson, T., Hayward, C., Hartley, M., Meara, R., Vogfjörd, K., Kjartansson, E., Jakobsdóttir, S. S., Björnsson, H., Karlsdóttir, S., & Zophoniasson, S. (2010). The April 2010 eruption of the ice-capped Eyjafjallajökull, South Iceland. Vienna, Austria: EGU.

Gudmundsson, G. (2011). Respiratory health effects of volcanic ash with special reference to Iceland. A review. *The Clinical Respiratory Journal*, *5*(1), 2–9. https://doi.org/10.1111/j.1752-699X.2010.00231.x

Gudmundsson, M. T., Thordarson, T., Höskuldsson, Á., Larsen, G., Björnsson, H., Prata, F. J., Oddsson, B., Magnússon, E., Högnadóttir, T., Petersen, G. N., Hayard, C. L., Stevenson, J. A., & Jónsdóttir, I. (2012). Ash generation and distribution from the April-May 2010 eruption of Eyjafjallajökull, Iceland. *Scientific Reports*, *2*(1), 572. https://doi.org/10.1038/srep00572

Gudmundsson, M.T., Höskuldsson, A. (2016). Grímsvötn. in: Ilyinskaya, Larsen and Gudmundsson (eds.): Catalogue of Icelandic Volcanoes. UI. http://icelandicvolcanos.is

Gudmundsson, M.T., Larsen, G. (2016). Eyjfjallajokull. in: Ilyinskaya, Larsen and Gudmundsson (eds.): Catalogue of Icelandic Volcanoes. UI. http://icelandicvolcanos.is

Gudnason, J., Thordarson, T., Houghton, B. F., & Larsen, G. (2017). The opening subplinian phase of the Hekla 1991 eruption: properties of the tephra fall deposit. *Bulletin of Volcanology*, *79*(5), 34. https://doi.org/10.1007/s00445-017-1118-8

Hadley, D., Hufford, G. L., Simpson, J. J., Hadley, D., Hufford, G. L., & Simpson, J. J. (2004). Resuspension of Relic Volcanic Ash and Dust from Katmai: Still an Aviation Hazard. *Weather and Forecasting*, *19*(5), 829–840. https://doi.org/10.1175/1520-0434(2004)019<0829:RORVAA>2.0.CO;2

Haider, A., & Levenspiel, O. (1989). Drag coefficient and terminal velocity of spherical and nonspherical particles. *Powder Technology*, *58*(1), 63–70. https://doi.org/10.1016/0032-5910(89)80008-7

Hanna, E., Jónsson, T., & Box, J. E. (2004). An analysis of Icelandic climate since the nineteenth century. *International Journal of Climatology*, *24*(10), 1193–1210. https://doi.org/10.1002/joc.1051

Hao, X., & Qu, J. J. (2007). Saharan dust storm detection using moderate resolution imaging spectroradiometer thermal infrared bands. *Journal of Applied Remote Sensing*, *1*(1), 013510. https://doi.org/10.1117/1.2740039

Hardardóttir, J., & Snorrason, Á. (2002). Sediment monitoring of glacial rivers in Iceland : new data on bed load transport. *Erosion and Sediment Transport Measurement in Rivers: Technological and Methodological Advances*, (January), 154–163.

Hardardóttir, J., S. B. Thorláksdóttir & Á. Snorrason (2005). New evaluation of suspended sediment load in Icelandic rivers. *EGU General Assembly 2005* Vienna, Austria.

Haywood, J., Francis, P., Osborne, S., Glew, M., Loeb, N., Highwood, E., Tanré, D., Myhre, G., Formenti, P., & Hirst, E. (2003). Radiative properties and direct radiative effect of Saharan dust measured by the C-130 aircraft during SHADE: 1. Solar spectrum. *Journal of Geophysical Research*, *108*(D18), 8577. https://doi.org/10.1029/2002JD002687

Heiken, G. (1972). Morphology and Petrography of Volcanic Ashes. *GSA Bulletin*, *83*(7), 1961–1988. https://doi.org/10.1130/0016-7606(1972)83[1961:mapova]2.0.co;2

Heiken, G., & Wohletz, K. (1985). *Volcanic ash. Volcanic ash*. London: University Presses of California, Chicago, Harvard & MIT. Retrieved from https://www.cabdirect.org/cabdirect/abstract/19851900752

Hitachi (2019). Tabletop Microscope TM3030Plus. Retrieved from https://www.hitachi-hightech.com/eu/product_detail/?pn=em-tm3030plus&version=

Hong, Y., Pan, X., Kim, S., Park, K., Park, E., Jin, X., Yi, S., Kim, Y., Park, C., Song, S., Kim, H. (2010). Asian Dust Storm and pulmonary function of school children in Seoul. *Science of The Total Environment*, *408*(4), 754–759. https://doi.org/10.1016/J.SCITOTENV.2009.11.015

Horwell, C. J., Fenoglio, I., Vala Ragnarsdottir, K., Sparks, R. S. J., & Fubini, B. (2003). Surface reactivity of volcanic ash from the eruption of Soufrière Hills volcano, Montserrat, West Indies with implications for health hazards. *Environmental Research*, *93*(2), 202–215. https://doi.org/10.1016/S0013-9351(03)00044-6

Horwell, C. J., & Baxter, P. J. (2006). The respiratory health hazards of volcanic ash: a review for volcanic risk mitigation. *Bull Volcanol*, *69*, 1–24. https://doi.org/10.1007/s00445-006-0052-y

Horwell, C. J. (2007). Grain-size analysis of volcanic ash for the rapid assessment of respiratory health hazard. https://doi.org/10.1039/b710583p

Horwell, C. J., Baxter, P. J., Hillman, S. E., Calkins, J. A., Damby, D. E., Delmelle, P., Donaldson, K., Dunster, C., Fubini, B., Kelly, F. J., Le Blond, J. S., Livi, K. J. T., Murphy, F., Nattrass, C., Sweeney, S., Tetley, T. D., Thordarson, T., Tomatis, M. (2013). Physicochemical and toxicological profiling of ash from the 2010 and 2011 eruptions of Eyjafjallajökull and Grímsvötn volcanoes, Iceland using a rapid respiratory hazard assessment protocol. *Environmental Research*, *127*, 63–73. https://doi.org/10.1016/J.ENVRES.2013.08.011

Houghton, B. F., Swanson, D. A., Rausch, J., Carey, R. J., Fagents, S. A., & Orr, T. R. (2013). Pushing the volcanic explosivity index to its limit and beyond: Constraints from exceptionally weak explosive eruptions at Kilauea in 2008. *Geology*, *41*(6), 627–630. https://doi.org/10.1130/G34146.1

Höskuldsson, Á., Janebo, M., Thordarson, T., Andrésdóttir, T. B., Jónsdóttir, I., Guðnason, J., Schmith, J., Moreland, W., & Magnúsdóttir, A. Ö. (2018). *Total Grain Size Distributi on in Selected Icelandic Erupti ons Work for the Internati onal Civil Aviati on Organizati on (ICAO) and the Icelandic Meteorological Offi ce*. Retrieved from https://earthice.hi.is/sites/earthice.hi.is/files/Pdf_skjol/total_grain-size_distribution_in_selected_icelandic_eruptions_01.pdf

Hu, Y., M., Vaughan, M., Liu, Z., Lin, B., Yang, P., Flittner, D., Hunt, B., Kuehn, R., Huang, J., Wu, D., Rodier, S., Powell, K., Trepte, C., & Winker, D. (2007). The depolarization - attenuated backscatter relation: CALIPSO lidar measurements vs. theory. *Opt. Express*, **15**, 5327–5332.

Huntingdon-Williams, A. G., Höskuldsson, Á., Janebo, M., Thordarson, T., & Bonadonna, C. (2018). Total grain size distribution of the Askja 1875 C tephra. *20th EGU General Assembly, EGU2018, Proceedings from the Conference Held 4-13 April, 2018 in Vienna, Austria, p.10193*, *20*, 10193. Retrieved from http://adsabs.harvard.edu/abs/2018EGUGA..2010193G

Icelandic Met Office. (2011). *The weather in Iceland 2010*. Reykjavík, Iceland. Retrieved from http://en.vedur.is/media/vedurstofan/utgafa/skylduskil/ved-eng-2010.pdf

Iwata, A., & Matsuki, A. (2018). Characterization of individual ice residual particles by the single droplet freezing method: a case study in the Asian dust outflow region. *Atmospheric Chemistry and Physics*, *18*(3), 1785–1804. https://doi.org/10.5194/acp-18-1785-2018

Jayaratne, E. R., Johnson, G. R., McGarry, P., Cheung, H. C., & Morawska, L. (2011). Characteristics of airborne ultrafine and coarse particles during the Australian dust storm of 23 September 2009. *Atmospheric Environment*, *45*(24), 3996–4001. https://doi.org/10.1016/J.ATMOSENV.2011.04.059

Johannesdottir, G. (2011). National Risk Assessment for Iceland Department of Civil Protection and Emergency Management the National Commissioner of the Icelandic Police. Retrieved from http://www.almannavarnir.is/wp-content/uploads/2016/10/NATIONAL-RISK-ASSESSMENT-FOR-ICELAND_.pdf

Jenkins, S., Wilson, T., Loughlin, S., Sparks, S., Brown, S., Jenkins, S., & Vye-brown, C. (2015). Volcanic ash fall hazard and risk. In J. F. Shroder & P. Papale (Eds. 1), *Global Volcanic Hazards and Risk* (pp. 173–222). Amsterdam, Netherlands: Elsevier. https://doi.org/10.1017/CBO9781316276273

Jude-Eton, T. C., Thordarson, T., Gudmundsson, M. T., & Oddsson, B. (2012). Dynamics, stratigraphy and proximal dispersal of supraglacial tephra during the ice-confined 2004 eruption at Grímsvötn Volcano, Iceland. *Bulletin of Volcanology*, *74*(5), 1057–1082. https://doi.org/10.1007/s00445-012-0583-3

Kahnert, M., & Nousiainen, T. (2005). Spherical and spheroidal model particles as an error source in aerosol climate forcing and radiance computations: A case study for feldspar aerosols. *J. Geophys. Res*, *110*, 18–31. https://doi.org/10.1029/2004JD005558

Kalashnikova, O. V., & Sokolik, I. N. (2004). Modeling the radiative properties of nonspherical soil-derived mineral aerosols. *Journal of Quantitative Spectroscopy and Radiative Transfer*, *87*(2), 137–166. https://doi.org/10.1016/J.JQSRT.2003.12.026

Kalashnikova, O. V., Kahn, R., Sokolik, I. N., & Li, W. (2005). Ability of multiangle remote sensing observations to identify and distinguish mineral dust types: Optical models and retrievals of optically thick plumes. *Journal of Geophysical Research*, *110*(D18), D18S14. https://doi.org/10.1029/2004JD004550

Kampa, M., & Castanas, E. (2008). Human health effects of air pollution. *Environmental Pollution*, *151*(2), 362–367. https://doi.org/10.1016/J.ENVPOL.2007.06.012

Kandler, K., Benker, N., Bundke, U., Cuevas, E., Ebert, M., Knippertz, P., Rodríguez, S., Schütz, L., Weinbruch, S. (2007). Chemical composition and complex refractive index of Saharan Mineral Dust at Izaña, Tenerife (Spain) derived by electron microscopy. *Atmospheric Environment*, *41*(37), 8058–8074. https://doi.org/10.1016/J.ATMOSENV.2007.06.047

Kaufman, Y. J., Koren, I., Remer, L. A., Tanré, D., Ginoux, P., & Fan, S. (2005). Dust transport and deposition observed from the Terra-Moderate Resolution Imaging Spectroradiometer (MODIS) spacecraft over the Atlantic Ocean. *Journal of Geophysical Research*, *110*(D10), D10S12. https://doi.org/10.1029/2003JD004436

Kim, K.-H., Jahan, S. A., Kabir, E., & Brown, R. J. C. (2013). A review of airborne polycyclic aromatic hydrocarbons (PAHs) and their human health effects. *Environment International*, *60*, 71–80. https://doi.org/10.1016/J.ENVINT.2013.07.019

Kinney, P. L. (2008). Climate Change, Air Quality, and Human Health. *American Journal of Preventive Medicine*, *35*(5), 459–467. https://doi.org/10.1016/j.amepre.2008.08.025

Kok, J. F., Parteli, E. J. R., Michaels, T. I., and Karam, D. B. (2012). The physics of wind-blown sand and dust. *Rep. Prog. Phys*, *75*, *72pp*. doi: 10.1088/0034-4885/75/10/106901

Koren, I., Kaufman, Y. J., Washington, R., Todd, M. C., Rudich, Y., Martins, J. V., & Rosenfeld, D. (2006). The Bodélé depression: a single spot in the Sahara that provides most of the mineral dust to the Amazon forest. *Environmental Research Letters*, *1*(1), 014005. https://doi.org/10.1088/1748-9326/1/1/014005

Kueppers, U., Cimarelli, C., Hess, K.-U., Taddeucci, J., Wadsworth, F. B., & Dingwell, D. B. (2014). The thermal stability of Eyjafjallajökull ash versus turbine ingestion test sands. *Journal of Applied Volcanology*, *3*(1), 4. https://doi.org/10.1186/2191-5040-3-4

Kuhn, N., (2015). Modeling Sedimentation. *Experiments in Reduced Gravity*, 39–51. https://doi.org/10.1016/B978-0-12-799965-4.00004-2

Kou, L., Scotla, N., & October, C. (1996). *BLACK CARBON: ATMOSPHERIC MEASUREMENTS AND RADIATIVE EFFECT BY*. Retrieved from https://www.collectionscanada.gc.ca/obj/s4/f2/dsk3/ftp04/nq24776.pdf

Laity, J., (2003). Aeolian Destabilization Along the Mojave River, Mojave Desert, California: Linkages Among Fluvial, Groundwater, and Aeolian Systems. *Physical Geography*, *24*, 196–221, doi:10.2747/0272-3646.24.3.196.

Langmann, B. (2013). Volcanic Ash versus Mineral Dust: Atmospheric Processing and Environmental and Climate Impacts. *ISRN Atmospheric Sciences*, *2013*(ii), 1–17. https://doi.org/10.1155/2013/245076

Larsen, G., Gudmundsson, M. T., (2016). Katla. in: Ilyinskaya, Larsen and Gudmundsson (eds.): Catalogue of Icelandic Volcanoes. UI. http://icelandicvolcanos.is

Larsen, G., Gudmundsson, M.T., Vogfjörð K., Ilyinskaya, E., Oddsson, B., Pagneux E. (2018). Catalogue of Icelandic Volcanoes. IMO, UI, CPD-NCIP. http://icelandicvolcanoes.is

Laurent, B., Marticorena, B., Bergametti, G., Léon, J. F., and Mahowald, N. M., (2008). Modeling mineral dust emissions from the Sahara desert using new surface properties and soil database. *Journal of Geophysical Research: Atmospheres*, *113*(D14). https://doi.org/doi:10.1029/2007JD009484

Lawrence, C. R., & Neff, J. C. (2009). The contemporary physical and chemical flux of aeolian dust: A synthesis of direct measurements of dust deposition. *Chemical Geology*, *267*(1–2), 46–63. https://doi.org/10.1016/J.CHEMGEO.2009.02.005

Leathers, C. R., (1981). Plant components of desert dust in Arizona and their significance for man. *Desert Dust: Origin, Characteristics and Effect on Man*, Péwé, T.L. (American A. for the Adv. of Sci.), 1 Ed., Boulder, CO, USA, 191–206.

Lei, H., & Wang, J. X. L. (2014). Observed characteristics of dust storm events over the western United States using meteorological, satellite, and air quality measurements. *Atmospheric Chemistry and Physics*, *14*(15), 7847–7857. https://doi.org/10.5194/acp-14-7847-2014

Leiva G, M. A., Santibañez, D. A., Ibarra E, S., Matus C, P., & Seguel, R. (2013). A five-year study of particulate matter (PM2.5) and cerebrovascular diseases. *Environmental Pollution*, *181*, 1–6. https://doi.org/10.1016/J.ENVPOL.2013.05.057

Lekas, T. I., Kallos, G., Kushta, J., Solomos, S., & Mavromatidis, E. (2011). Dust impact on aviation. Athens, Greece. Retrieved from http://forecast.uoa.gr/Dust-wshop-pdf/Lekas.pdf

Liang, T., Chamecki, M., & Yu, X. (2016). Sea salt aerosol deposition in the coastal zone: A large eddy simulation study. *Atmos. Res.*, *180*, 119–127, doi:10.1016/j.atmosres.2016.05.019.

Liu, Y., Liu, R., & Cheng, X. (2013). Dust detection over desert surfaces with thermal infrared bands using dynamic reference brightness temperature differences. *Journal of Geophysical Research: Atmospheres*, *118*(15), 8566–8584. https://doi.org/10.1002/jgrd.50647

Liu, E. J., Cashman, K. V., Beckett, F. M., Witham, C. S., Leadbetter, S. J., Hort, M. C., & Guðmundsson, S. (2014). Ash mists and brown snow: Remobilization of volcanic ash from recent Icelandic eruptions. *Journal of Geophysical Research: Atmospheres*, *119*(15), 9463–9480. https://doi.org/10.1002/2014JD021598

Liu, E. J., Cashman, K. V., & Rust, A. C. (2015a). Optimising shape analysis to quantify volcanic ash morphology. *GeoResJ*, *8*, 14–30. https://doi.org/10.1016/J.GRJ.2015.09.001

Liu, E. J., Cashman, K. V., Rust, A. C., & Gislason, S. R. (2015b). The role of bubbles in generating fine ash during hydromagmatic eruptions. *Geology*, *43*(3), 239–242. https://doi.org/10.1130/G36336.1

Malvern Panalytical (2019). Mastersizer 3000 laser particle size analyzer. Retrieved from https://www.malvernpanalytical.com/en/products/product-range/mastersizer-range/mastersizer-3000/?gclid=Cj0KCQiAkMDiBRDNARIsACKP1FHlGImncig4kVZGNaQmmiDAq-iRlSXNSX_hC-A2_H4UUMjRv2gBcbMaAj6LEALw_wcB

Mangold, N., Baratoux, D., Arnalds, O., Bardintzeff, J.-M., Platevoet, B., Grégoire, M., & Pinet, P. (2011). Segregation of olivine grains in volcanic sands in Iceland and implications for Mars. *Earth and Planetary Science Letters*, *310*(3–4), 233–243. https://doi.org/10.1016/J.EPSL.2011.07.025

Marren, P. M., Russell, A. J., & Rushmer, E. L. (2009). Sedimentology of a sandur formed by multiple jökulhlaups, Kverkfjöll, Iceland. *Sedimentary Geology*, *213*(3), 77–88. https://doi.org/10.1016/j.sedgeo.2008.11.006

Marzano, F. S., M. Lamantea, M. Montopoli, M. Herzog, H. Graf, and D. Cimini, (2013). Microwave remote sensing of the 2011 Plinian eruption of the Grímsvötn Icelandic volcano. *Remote Sens. Environ.*, **129**, 168–184, doi:10.1016/J.RSE.2012.11.005.

Mastersizer 3000 laser particle size analyzer. (2019). Retrieved from https://www.malvernpanalytical.com/en/products/product-range/mastersizer-range/mastersizer-3000/?gclid=Cj0KCQiAkMDiBRDNARIsACKP1FHlGImncig4kVZGNaQmmiDAq-iRlSXNSX_hC-A2_H4UUMjRv2gBcbMaAj6LEALw_wcB

Marticorena, B., & Bergametti, G. (1995). Modeling the atmospheric dust cycle: 1. Design of a soil derived dust emission scheme. *Journal of Geophysical Research: Atmospheres (1984–2012)*, *100*(D8), 16415–16430. https://doi.org/10.1029/95JD00690

McGimsey, R. G., Neal, C. A., & Girina, O. (2005). *2004 volcanic activity in Alaska and Kamchatka; summary of events and response of the Alaska Volcano Observatory*.

McGowan, H. A., Sturman, A. P., & Owens, I. F. (1996). Aeolian dust transport and deposition by foehn winds in an alpine environment, Lake Tekapo, New Zealand. *Geomorphology*, *15*(2), 135–146. https://doi.org/10.1016/0169-555X(95)00123-M

McTainsh, G. H., & Leys, J. F. (1993). Soil erosion by wind. *Land Degradation Processes in Australia*, 188-233.

McTainsh, G., Chan, Y., McGowan, H., Leys, J., & Tews, K. (2005). The 23rd October 2002 dust storm in eastern Australia: characteristics and meteorological conditions. *Atmospheric Environment*, *39*(7), 1227–1236. https://doi.org/10.1016/J.ATMOSENV.2004.10.016

McTainsh, G., & Strong, C. (2007). The role of aeolian dust in ecosystems. *Geomorphology*, *89*(1–2), 39–54. https://doi.org/10.1016/J.GEOMORPH.2006.07.028

Meinander, O. (2019). About Cryospheric Effects of High Latitude Dust versus Black Carbon in the Arctic. Reykjavík. Retrieved from https://icedustblog.files.wordpress.com/2018/10/preliminary-book-of-abstracts.pdf

Miller, S. D., Kuciauskas, A. P., Liu, M., Ji, Q., Reid, J. S., Breed, D. W, Walker, A. L., and Mandoos, A. A., (2008). Haboob dust storms of the southern Arabian Peninsula. *Journal of Geophysical Research*, *113*, D01202, doi:10.1029/2007JD008550.

Moreland, W. (2017). *Explosive activity in flood lava eruptions: a case study of the 10th century Eldgjá eruption, Iceland*. University of Iceland, School of Engineering and Natural Sciences, Faculty of Earth Sciences. Retrieved from https://opinvisindi.is/handle/20.500.11815/324

Moroni, B., Arnalds, O., Dagsson-Waldhauserová, P., Crocchianti, S., Vivani, R., & Cappelletti, D. (2018). Mineralogical and Chemical Records of Icelandic Dust Sources Upon Ny-Ålesund (Svalbard Islands). *Frontiers in Earth Science*, *6*, 187. https://doi.org/10.3389/feart.2018.00187

Moune, S., Faure, F., Gauthier, P.-J., & Sims, K. W. W. (2007). Pele's hairs and tears: Natural probe of volcanic plume. *Journal of Volcanology and Geothermal Research*, *164*(4), 244–253. https://doi.org/10.1016/J.JVOLGEORES.2007.05.007

Müller, D., Mattis, I., Wandinger, U., Ansmann, A., Althausen, D., & Stohl, A. (2005). Raman lidar observations of aged Siberian and Canadian forest fire smoke in the free troposphere over Germany in 2003: Microphysical particle characterization. *Journal of Geophysical Research*, *110*(D17), D17201. https://doi.org/10.1029/2004JD005756

National Aeronautics Space Administration (2019). MODIS. Retrieved from https://modis.gsfc.nasa.gov/about/

National Snow and Ice Data Center (2019). MODIS Data, Terra vs. Aqua. Retrieved from https://nsidc.org/data/modis/terra_aqua_differences

Natsagdorj, L., Jugder, D., & Chung, Y. . (2003). Analysis of dust storms observed in Mongolia during 1937–1999. *Atmospheric Environment*, *37*(9–10), 1401–1411. https://doi.org/10.1016/S1352-2310(02)01023-3

Neuberger, M., Schimek, M. G., Horak, F., Moshammer, H., Kundi, M., Frischer, T., Gomiscek, H., Puxbaum, H., Hauck, H., & AUPHEP-Team (2004). Acute effects of particulate matter on respiratory diseases, symptoms and functions: epidemiological results of the Austrian Project on Health Effects of Particulate Matter (AUPHEP). *Atmospheric Environment*, *38*(24), 3971–3981. https://doi.org/10.1016/j.atmosenv.2003.12.044

Newhall, C. G., & Self, S. (1982). The volcanic explosivity index (VEI) an estimate of explosive magnitude for historical volcanism. *Journal of Geophysical Research*, *87*(C2), 1231. https://doi.org/10.1029/JC087iC02p01231

Nickling, W. G. (1983): Grain-size characteristics of sediments transported during dust storms. *Journal of Sedimentology Petrology*, 53, 1011-1024.

Nicoll, K. A., Harrison, R. G., & Ulanowski, Z. (2011). Observations of Saharan dust layer electrification. *Environmental Research Letters*, *6*(1), 014001. https://doi.org/10.1088/1748-9326/6/1/014001

Nousiainen, T. (2009). Optical modeling of mineral dust particles: A review. *Journal of Quantitative Spectroscopy and Radiative Transfer*, *110*(14–16), 1261–1279. https://doi.org/10.1016/J.JQSRT.2009.03.002

Osborne, S. R., Johnson, B. T., Haywood, J. M., Baran, A. J., Harrison, M. A. J., & McConnell, C. L. (2008). Physical and optical properties of mineral dust aerosol during the Dust and Biomass-burning Experiment. *Journal of Geophysical Research*, *113*(D23), D00C03. https://doi.org/10.1029/2007JD009551

Peckham, S. E., Grell, G. A., McKeen, S. A., Barth, M., Pfister, G., Wiedinmyer, C., Fast, J. D., Gustafson, W. I., Ghan, S. J., Zaveri, R., Easter, R. C., Barnard, J., Chapman, E., Hewson, M., Schmitz, R., Salzmann, M., & Freitas, S. R. (2011). WRF/Chem Version 3.7 User's Guide.

Perepezko, J. H. (2009). The Hotter the Engine, the. *New Series*, *326*(5956), 1068–1069. https://doi.org/10.1126/science.ll79117

Petersen, G. N. (2010). A short meteorological overview of the Eyjafjallajökull eruption 14 April-23 May 2010. *Weather*, *65*(8), 203–207. https://doi.org/10.1002/wea.634

Pérez, C., S. Nickovic, J. M. Baldasano, M. Sicard, F. Rocadenbosch, and V. E. Cachorro, (2006). A long Saharan dust event over the western Mediterranean: Lidar, Sun photometer observations, and regional dust modeling. *J. Geophys. Res.*, *111*, D15214, doi:10.1029/2005JD006579.

Powell, C. R. (2018). *Modeling volcanic ash resuspension dynamics: the Eyjafjallajökull ash deposit case*. Univeristy of Iceland.

Prata, A. J., & Tupper, A. (2009). Aviation hazards from volcanoes: the state of the science. *Natural Hazards*, *51*(2), 239–244.

Prospero, J. M., Savoie, D. L., Arimoto, R., Olafsson, H., and Hjartarson, H. (1995). Sources of aerosol nitrate and non-sea-salt sulfate in the Iceland region. *Sci. Total Environ.*, *160–161*, 181–191, doi:10.1016/0048-9697(95)04355-5.

Prospero, J. M., Bullard, J. E., & Hodgkins, R. (2012). High-latitude dust over the North Atlantic: inputs from Icelandic proglacial dust storms. *Science (New York, N.Y.)*, *335*(6072), 1078–1082. https://doi.org/10.1126/science.1217447

Pye, K. (1987). *Aeolian dust and dust deposits*. Orlando, FL: Academic.

Rasband, W.S., ImageJ, U. S. National Institutes of Health, Bethesda, Maryland, USA, https://imagej.nih.gov/ij/, 1997-2018.

Renard, J.-B., Dulac, F., Durand, P., Bourgeois, Q., Denjean, C., Vignelles, D., Couté, B., Jeannot, M., Verdier, N., & Mallet, M. (2018). In situ measurements of desert dust particles above the western Mediterranean Sea with the balloon-borne Light Optical Aerosol Counter/sizer (LOAC) during the ChArMEx campaign of summer 2013. *Atmospheric Chemistry and Physics*, *18*(5), 3677–3699. https://doi.org/10.5194/acp-18-3677-2018

Reid, J. S., W. L. Westphal, J. Livingston, D. S. Savoie, H. B. Maring, P. Pilewskie, and D. Eleuterio, (2002). Dust vertical distribution in the Caribbean during the Puerto Rico Dust Experiment, Geo- phys. Res. Lett., 29(7), 1151, doi:10.1029/2001GL014092.

Riley, N. A. (1941). Projection sphericity. *Journal of Sedimentology Petrology*, 11, 94-97.

Rosenfeld, D., Rudich, Y., & Lahav, R. (2001). Desert dust suppressing precipitation: a possible desertification feedback loop. *Proceedings of the National Academy of Sciences of the United States of America*, *98*(11), 5975–5980. https://doi.org/10.1073/pnas.101122798

Rögnvaldsson, Ó., Jónsdóttir, J. F., & Ólafsson, H. (2007). Numerical simulations of precipitation in the complex terrain of Iceland - Comparison with glaciological and hydrological data. *Meteorologische Zeitschrift*, *16*(1), 71–85. https://doi.org/10.1127/0941-2948/2007/0174

Rögnvaldsson, O. (2018). Personal Communication.

Ryder, C. L., Marenco, F., Brooke, J. K., Estelles, V., Cotton, R., Formenti, P., McQuaid, J. B., Price, H. C., Liu, D., Ausset, P., Rosenberg, P. D., Taylor, J. W., Choularton, T., Bower, K., Coe, H., Gallagher, M., Crosier, J., Lloyd, G., Highwood, E. J., & Murray, B. J. (2018). Coarse-mode mineral dust size distributions, composition and optical properties from AER-D aircraft measurements over the tropical eastern Atlantic. *Atmospheric Chemistry and Physics*, *18*(23), 17225–17257. https://doi.org/10.5194/acp-18-17225-2018

Samadi, M., Darvishi Boloorani, A., Alavipanah, S. K., Mohamadi, H., & Najafi, M. S. (2014). Global dust Detection Index (GDDI); a new remotely sensed methodology for dust storms detection. *Journal of Environmental Health Science & Engineering*, *12*(1), 20. https://doi.org/10.1186/2052-336X-12-20

Sassen, K., & Khvorostyanov, V. I., (2008). Cloud effects from boreal forest fire smoke: Evidence for ice nucleation from polarization liar data and cloud model simulations. *Environ. Res. Lett.*, **3**, doi:10.1088/1748–9326/3/2/025006.

Savtchenko, A., Ouzounov, D., Ahmad, S., Acker, J., Leptoukh, G., Koziana, J., & Nickless, D. (2004). Terra and Aqua MODIS products available from NASA GES DAAC. *Advances in Space Research*, *34*(4), 710–714. https://doi.org/10.1016/J.ASR.2004.03.012

Saxby, J., Beckett, F., Cashman, K., Rust, A., & Tennant, E. (2018). The impact of particle shape on fall velocity: Implications for volcanic ash dispersion modelling. *Journal of Volcanology and Geothermal Research*, *362*, 32–48. https://doi.org/10.1016/J.JVOLGEORES.2018.08.006

Scheuvens, D., Schütz, L., Kandler, K., Ebert, M., & Weinbruch, S. (2013). Bulk composition of northern African dust and its source sediments — A compilation. *Earth-Science Reviews*, *116*, 170–194. https://doi.org/10.1016/J.EARSCIREV.2012.08.005

Schmidt, A., Leadbetter, S., Theys, N., Carboni, E., Witham, C. S., Stevenson, J. A., Birch, C. E., Thordarson, T., Turnock, S., Barsotti, S., Delaney, L., Feng, W., Grainger, R. G., Hort, M. C., Höskuldsson, A., Ialongo, I., Ilyinskaya. E., Jóhannsson, T., Kenny, P., Mather, T. A., Richards, N. A. D., & Shepherd, J. (2015). Satellite detection, long-range transport, and air quality impacts of volcanic sulfur dioxide from the 2014-2015 flood lava eruption at Bárðarbunga (Iceland). *Journal of Geophysical Research: Atmospheres*, *120*(18), 9739–9757. https://doi.org/10.1002/2015JD023638

Self, S., Sparks, R.S.J., Booth, B., Walker, G.P.L., (1974). The 1973 Heimaey Strombolian Scoria deposit, *Iceland. Geol. Mag*. *111*, 539. https://doi.org/10.1017/S0016756800041583.

Serreze, M. C., F. Carse, R. G. Barry, J. C. Rogers, M. C. Serreze, F. Carse, R. G. Barry, and J. C. Rogers, (1997). Icelandic Low Cyclone Activity: Climatological Features, Linkages with the NAO, and Relationships with Recent Changes in the Northern Hemisphere Circulation. *J. Clim.*, *10*, 453–464.

Shao, J., & Mao, J. (2016). Dust Particle Size Distributions during Spring in Yinchuan, China. *Advances in Meteorology*, *2016*, 1–8. https://doi.org/10.1155/2016/6940502

Shimozuru, D. (1994). Physical parameters governing the formation of Pele's hair and tears. *Bulletin of Volcanology*, *56*(3), 217–219. https://doi.org/10.1007/BF00279606

Sigmarsson, O., & Steinthórsson, S. (2007). Origin of Icelandic basalts: A review of their petrology and geochemistry. *Journal of Geodynamics*, *43*(1), 87–100. https://doi.org/10.1016/j.jog.2006.09.016

Simonella, L. E., Palomeque, M. E., Croot, P. L., Stein, A., Kupczewski, M., Rosales, A., Montes, M. L., Colombo, F., Garcia, M. G., Villarosa, G., & Gaiero, D. M. (2015), Soluble iron inputs to the Southern Ocean through recent andesitic to rhyolitic volcanic ash eruptions from the Patagonian Andes, Global Biogeochem. Cycles,29, 1125–1144, doi:10.1002/2015GB005177.

Skamarock, C. W., Klemp, J. B., Dudhia, J., Gill, D. O., Barker, D. M., Duda, M. G., Huang, X., Wang, W. & Powers, J. G. (2008). *A description of the advanced research WRF Version 3*. NCAR Tech. Note NCAR/TN–475+STR, 125 pp.

Smellie, J. L. (2000). Subglacial eruptions, in Encyclopedia of Volcanoes, edited by H. Sigurdsson et al., pp. 403–418, Academic, London.

Sneed, E. D. & Folk, R. L., (1958). Pebbles in the lower Colorado River, Texas: a study in particle morphogenesis. *Journal of Geology*, *66*, 114-150.

Sokolik, I. N., & Toon, O. B. (1999). Incorporation of mineralogical composition into models of the radiative properties of mineral aerosol from UV to IR wavelengths. *Journal of Geophysical Research Atmospheres*, *104*(D8), 9423–9444. https://doi.org/10.1029/1998JD200048

Song, W., Lavallée, Y., Hess, K.-U., Kueppers, U., Cimarelli, C., & Dingwell, D. B. (2016). Volcanic ash melting under conditions relevant to ash turbine interactions. *Nature Communications*, *7*(1), 10795. https://doi.org/10.1038/ncomms10795

Song, P., Fei, J., Li, C., & Huang, X. (2019). Simulation of an Asian Dust Storm Event in May 2017. *Atmosphere*, *10*(3), 135. https://doi.org/10.3390/atmos10030135

Stefanski, R., & Sivakumar, M. V. K. (2009). Impacts of sand and dust storms on agriculture and potential agricultural applications of a SDSWS. *IOP Conference Series: Earth and Environmental Science*, *7*, 012016. https://doi.org/10.1088/1755-1307/7/1/012016

Stevenson, J. A., Loughlin, S., Rae, C., Thordarson, T., Milodowski, A. E., Gilbert, J. S., Harangi, S., Lukács, R., Højfaard, B., Árting, U., Pyne-O'Donnell, S., MacLeod, A., Whitney, B., & Cassidy, M. (2012). Distal deposition of tephra from the Eyjafjallajökull 2010 summit eruption. *Journal of Geophysical Research: Solid Earth*, *117*(B9). https://doi.org/10.1029/2011JB008904

Stevenson, J. A., Loughlin, S. C., Font, A., Fuller, G. W., MacLeod, A., Oliver, I. W., Jackson, B., Horwell, C. J., Thordarson, T., & Dawson, I. (2013). UK monitoring and deposition of tephra from the May 2011 eruption of Grímsvötn, Iceland. *Journal of Applied Volcanology*, *2*(1), 3. https://doi.org/10.1186/2191-5040-2-3

Stuefer, M., Freitas, S. R., Grell, G., Webley, P., Peckham, S., & Mckeen, S. A. (2012). Inclusion of Ash and SO 2 emissions from volcanic eruptions in WRF-CHEM Geoscientific Model Development Discussions Inclusion of Ash and SO 2 emissions from volcanic eruptions in WRF-CHEM: development and some applications Inclusion of Ash and SO 2 emissions from volcanic eruptions in WRF-CHEM. *Geosci. Model Dev. Discuss*, *5*, 2571–2597. https://doi.org/10.5194/gmdd-5-2571-2012

Sturm, R., & Hofmann, W. (2009). A theoretical approach to the deposition and clearance of fibers with variable size in the human respiratory tract. *Journal of Hazardous Materials*, *170*(1), 210–218. https://doi.org/10.1016/J.JHAZMAT.2009.04.107

Tarr, R. S., & Martin, L. (1913). Glacial Deposits of the Continental Type in Alaska. *Journal of Geology*, *21*(4), 289–300. https://doi.org/https://doi.org/10.1086/622063

Thorarinsdottir, E. F., & Arnalds, O. (2012). Wind erosion of volcanic materials in the Hekla area, South Iceland. *Aeolian Research*, *4*(2012), 39–50. https://doi.org/10.1016/j.aeolia.2011.12.006

Thordarson, T., & Larsen, G. (2007). Volcanism in Iceland in historical time: Volcano types, eruption styles and eruptive history. *Journal of Geodynamics*, *43*(1), 118–152. https://doi.org/10.1016/J.JOG.2006.09.005

Thorsteinsson, T., Gísladóttir, G., Bullard, J., & McTainsh, G. (2011). Dust storm contributions to airborne particulate matter in Reykjavík, Iceland. *Atmospheric Environment*, *45*(32), 5924–5933. https://doi.org/10.1016/J.ATMOSENV.2011.05.023

Thorsteinsson, T., Jóhannsson, T., Stohl, A., & Kristiansen, N. I. (2012). High levels of particulate matter in Iceland due to direct ash emissions by the Eyjafjallajökull eruption and resuspension of deposited ash. *Journal of Geophysical Research: Solid Earth*, *117*(1), 0–5. https://doi.org/10.1029/2011JB008756

Tómasson, H. (1990). *Aurburður Í Íslenskum Ám. Vatnið og Landið*. Reykjavík, Orkustofnun, 169-174. (In Icelandic)

Torres, O., Bhartia, P. K., Herman, J. R., Ahmad, Z., & Gleason, J. (1998). *Derivation of aerosol properties from satellite measurements of backscattered ultraviolet radiation: Theoretical basis*. *JOURNAL OF GEOPHYSICAL RESEARCH* (Vol. 103). https://doi.org/10.1029/98JD00900

Tsoar, H. (1994). Bagnold, R.A. 1941: The physics of blown sand and desert dunes. London: Methuen. *Progress in Physical Geography: Earth and Environment*, *18*(1), 91–96. https://doi.org/10.1177/030913339401800105

United States Geological Society, (cited 2019). Volcano Hazards Program. [Available online at https://volcanoes.usgs.gov/vhp/tephra.html]

University Center for Atmospheric Research (2019). WPS V4 Geographical Static Data Downloads Page. Retreived from http://www2.mmm.ucar.edu/wrf/users/download/get_sources_wps_geog.html

Vainshtein, P., Shapiro, M., & Gutfinger, C. (2004). Mobility of permeable aggregates: effects of shape and porosity. *Journal of Aerosol Science*, *35*(3), 383–404. https://doi.org/10.1016/J.JAEROSCI.2003.09.004

van der Does, M., Korte, L. F., Munday, C. I., Brummer, G.-J. A., & Stuut, J.-B. W. (2016). Particle size traces modern Saharan dust transport and deposition across the equatorial North Atlantic. *Atmospheric Chemistry and Physics*, *16*(21), 13697–13710. https://doi.org/10.5194/acp-16-13697-2016

van der Does, M., Knippertz, P., Zschenderlein, P., Giles Harrison, R., & Stuut, J.-B. W. (2018). The mysterious long-range transport of giant mineral dust particles. *Science Advances*, *4*(12), eaau2768. https://doi.org/10.1126/sciadv.aau2768

Valavanidis, A., Fiotakis, K., & Vlachogianni, T. (2008). Airborne Particulate Matter and Human Health: Toxicological Assessment and Importance of Size and Composition of Particles for Oxidative Damage and Carcinogenic Mechanisms. *Journal of Environmental Science and Health, Part C*, *26*(4), 339–362. https://doi.org/10.1080/10590500802494538

Wang, Y. Q., Zhang, X. Y., Gong, S. L., Zhou, C. H., Hu, X. Q., Liu, H. L., Niu, T., & Yang, Y. Q. (2008). Surface observation of sand and dust storm in East Asia and its application in CUACE/Dust. *Atmos. Chem. Phys.*, **8**, 545–553, doi:10.5194/acp-8-545-2008.

Wang, X., Zhang, C., Wang, H., Qian, G., Luo, W., Lu, J., & Wang, L. (2011). The significance of Gobi desert surfaces for dust emissions in China: an experimental study. *Environmental Earth Sciences*, *64*(4), 1039–1050. https://doi.org/10.1007/s12665-011-0922-2

Washington, R., Todd, M., Middleton, & Goudie, A. S. (2003). Dust-Storm Source Areas Determined by the Total Ozone Monitoring Spectrometer and Surface Observations. *Ann. Assoc. Am. Geogr.*, **93**, 297–313, doi:10.1111/1467-8306.9302003.

Webley, P. W., Steensen, T., Stuefer, M., Grell, G., Freitas, S., & Pavolonis, M. (2012). Analyzing the Eyjafjallajökull 2010 eruption using satellite remote sensing, lidar and WRF-Chem dispersion and tracking model. *J. Geophys. Res*, *117*, 0–26. https://doi.org/10.1029/2011JD01681

Wheaton, E. E. (1990). Frequency and Severity of Drought and Dust Storms. *Canadian Journal of Agricultural Economics/Revue canadienne d'agroeconomie, 38, 695-700*. doi:10.1111/j.1744-7976.1990.tb03504.x

Williams, R.S., Moore, J.G., (1976). Man Against Volcano: The Eruption on Heimaey, Vestmannaeyjar, Iceland, 2nd ed. U.S. Geological Survey.

Wilshire, H. G., Nakata, J. K., and Hallet, B. (1981). Field observations of the December 1977 wind storm, San Joaquin Valley, California. *Geological Society of America Special Papers*, 186, 233-252.

Wittmann, M., Dorothea, C., Zwaaftink, G., Schmidt, L. S., & Guðmundsson, S. (2017). Impact of dust deposition on the albedo of Vatnajökull ice cap , Iceland, 741–754. https://doi.org/10.5194/tc-11-741-2017

World Health Organization (2013). Health effects of particulate matter. Copenhagen, Denmark. https://doi.org/ISBN 978 92 890 0001 7

World Meteorological Organziaiton, (2007). Aviation Hazards, Geneva, Switzerland. Retrieved from https://library.wmo.int/pmb_ged/wmo-td_1390_en.pdf

World Meteorological Organization. (2014). *Guide to Meteorological Instruments and Methods of Observation*. Retrieved from https://library.wmo.int/doc_num.php?explnum_id=4147

World Meteorological Organization, Manual on Codes. (2015). Geneva. Retrieved from http://www.wmo.int/pages/prog/www/WMOCodes/WMO306_vI1/Publications/2015update/306_vol_I1_2015_en.pdf

World Meteorological Organization, cited 2019. Meteoterm. [Available online at http://wmo.multitranstms.com/MultiTransWeb/Web.mvc]

Xing, Y.-F., Xu, Y.-H., Shi, M.-H., & Lian, Y.-X. (2016). The impact of PM2.5 on the human respiratory system. *Journal of Thoracic Disease*, *8*(1), E69-74. https://doi.org/10.3978/j.issn.2072-1439.2016.01.19Yang, S., Song, W., Lokachari, S., Dingwell, D. B., & Guo, H. (2018). Gradient damage spreading of molten volcanic ash on thermal barrier coatings. In B. Vaßen, R. Hazel, U. Schulz, M. J. Maloney, & R. Darolia (Eds.), *Thermal Barrier Coatings V*. Irsee, Germany: ECI Symposium Series. Retrieved from http://dc.engconfintl.org/tbcv/24

Zakšek, K., Hort, M., Zaletelj, J., & Langmann, B. (2013). Monitoring volcanic ash cloud top height through simultaneous retrieval of optical data from polar orbiting and geostationary satellites. *Atmospheric Chemistry and Physics*, *13*(5), 2589–2606. https://doi.org/10.5194/acp-13-2589-2013

Zhang, T., Gao, B., Zhou, Z., & Chang, Y. (2016). The movement and deposition of PM2.5 in the upper respiratory tract for the patients with heart failure: an elementary CFD study. *BioMedical Engineering OnLine*, *15*(S2), 138. https://doi.org/10.1186/s12938-016-0281-z

Appendix A

Table A.1 Weather observer station information, includes exact location as well as operation years.

Station	Station Name	Latitude	Longitude	Start Year	End Year
1	Reykjavík	64°07.648'	21°54.166'	1821	
108	Stafholtsey	64°38.516'	21°35.445'	1988	2017
130	Hamraendar í Stafholtstungum	64°40'	21°37'	1986	1988
155	Haukatunga	64°49'	22°16'	1943	1989
164	Neðri-Hóll	64°48'	23°02'	1994	1997
167	Bláfeldur	64°50.358'	23°18.021'	1997	
170	Gufuskálar	64°54'	23°56'	1970	1994
171	Hellissandur	64°55'	23°53'	1934	1970
178	Stykkishólmur	65°04.442'	22°44.033'	1845	
195	Ásgarður	65°13.782'	21°45.256'	1992	
206	Reykhólar	65°26.887'	22°11.985'	1948	2004
224	Kvígindisdalur	65°33.372'	24°00.704'	1927	2004
234	Hólar í Dýrafirði	65°52.073'	23°33.848'	1983	
250	Galtarviti	66°10'	23°34'	1953	1994
252	Bolungarvík	66°09.660'	23°15.192'	1994	
260	Æðey	66°05.993'	22°39.597'	1946	2012
285	Hornbjargsviti	66°25'	22°23'	1946	1995
295	Gjögur	65°59'	21°21'	1971	1995
309	Þóroddsstaðir	65°14'	21°05'	1966	1984
310	Tannstaðabakki	65°17'	21°06'	1984	1997
340	Hjaltabakki	65°38'	20°18'	1967	1981
341	Blönduós	65°39.485'	20°18.156'	1981	2003
366	Nautabú	65°27.542'	19°22.096'	1945	2004
400	Sauðanesviti	66°11.112'	18°57.204'	1990	
402	Siglunes	66°11'	18°50'	1968	1990
404	Grímsey	66°32'	18°01'	1874	2000
422	Akureyri	65°41.135'	18°06.014'	1881	
479	Mánárbakki	66°11.969'	17°06.191'	1956	2016
495	Grímsstaðir	65°38.539'	16°07.249'	1907	
505	Raufarhöfn	66°27.081'	15°56.917'	1920	2009
508	Sauðanes	66°14.846'	15°15.689'	1980	2004
510	Skoruvík	66°21'	14°46'	1944	1977
515	Miðfjarðarnes	66°03.957'	15°04.750'	1999	
521	Strandhöfn	65°54.367'	14°39.015'	1980	2005
527	Skjaldþingsstaðir	65°42.161'	14°49.267'	1994	
530	Hof í Vopnafirði	65°39'	15°01'	1946	1966
570	Egilsstaðir	65°18'	14°22'	1943	1998
598	Snæfellsskáli	64°48'	15°38'	1990	2002
620	Dalatangi	65°16.090'	13°34.556'	1938	

635	Kollaleira	65°02.180'	14°14.421'	1976	2007
660	Kambanes	64°48'	13°51'	1961	1991
670	Núpur	64°42'	14°06'	1992	2004
706	Hjarðarnes	64°17'	15°13'	1985	1992
707	Akurnes	64°18.605'	15°13.255'	1992	2006
745	Fagurhólsmýri	63°52.647'	16°38.830'	1903	2008
772	Kirkjubæjarklaustur	63°47.368'	18°03.256'	1926	2013
790	Mýrar í Álftaveri	63°30'	18°20'	1959	1986
791	Norðurhjáleiga	63°30.466'	18°22.300'	1986	2007
798	Vík í Mýrdal	63°25.211'	19°00.587'	1925	2014
802	Vatnsskarðshólar	63°25.416'	19°10.982'	1978	
815	Stórhöfði	63°23.985'	20°17.299'	1921	2013
830	Básar á Goðalandi	63°41'	19°29'	1991	2003
855	Hella	63°50.166'	20°23.584'	1957	2005
888	Versalir	64°27'	18°45'	1990	2000
892	Hveravellir	64°52.001'	19°33.723'	1964	2004
907	Hæll	64°03.904'	20°14.471'	1932	2012
923	Eyrarbakki	63°51.888'	21°09.022'	1923	2017
931	Hjarðarland	64°15.025'	20°19.855'	1990	
949	Heiðarbær	64°12'	21°14'	1965	1991
985	Reykjanes	63°49'	22°43'	1927	1998
990	Keflavíkurflugvöllur	63°58.481'	22°35.255'	1952	

Table A.2 Number of observations as well as number of days for each type of PM classification. Note that volcanic ash was observed even during times when there was no eruption.

Year	Total # Suspended Dust Observations for all of Iceland	# Unique Suspension Days	Total # Haze Observations for all of Iceland	# Unique Haze Days	Total # Ash Observations for all of Iceland	# Unique Ash Days
1966	50	29	671	124	21	13
1967	14	10	442	138	16	16
1968	228	76	676	115	43	18
1969	58	29	636	137	7	4
1970	106	33	726	139	2	2
1971	16	11	663	130	2	2
1972	21	18	911	172	7	5
1973	16	10	647	134	2	2
1974	50	32	1148	150	5	5
1975	28	18	850	145	2	2
1976	153	43	1184	145	26	9
1977	503	99	539	99	3	3
1978	637	121	179	55	2	2
1979	338	81	161	44	12	12
1980	197	74	907	142	28	14
1981	98	31	590	124	5	5
1982	2	2	443	103	0	0
1983	2	1	344	84	0	0
1984	44	11	482	80	81	31
1985	103	44	245	76	1	1
1986	102	30	251	74	1	1
1987	234	57	197	64	3	3
1988	123	34	413	70	1	1
1989	145	44	161	51	1	1
1990	116	39	314	62	0	0
1991	305	75	710	79	39	9
1992	285	63	691	86	3	3
1993	64	34	377	104	0	0
1994	125	26	354	69	8	1
1995	33	17	318	75	6	5
1996	89	42	265	76	1	1
1997	320	80	86	32	10	1
1998	194	69	20	11	45	17
1999	244	68	180	54	10	6
2000	249	59	206	62	21	9

2001	48	25	124	59	1	1
2002	38	20	405	112	1	1
2003	90	40	405	110	19	7
2004	85	31	474	90	23	9
2005	157	61	58	23	13	7
2006	162	50	162	51	28	11
2007	161	50	101	43	6	2
2008	108	52	133	59	1	1
2009	74	29	74	30	0	0
2010	384	82	226	85	3	3
2011	170	39	304	73	2	2
2012	224	56	271	57	0	0
2013	41	27	171	61	2	2
2014	66	29	484	100	26	15
2015	13	8	121	48	3	3
2016	10	8	72	48	4	2

Appendix B

Table B.1 MODIS spectral bands and their usage. From NASA (2019).

Primary Use	Band	Bandwidth[1]	Spectral Radiance[2]	Required SNR[3]
Land/Cloud/Aerosols Boundaries	1	620 - 670	21.8	128
	2	841 - 876	24.7	201
Land/Cloud/Aerosols Properties	3	459 - 479	35.3	243
	4	545 - 565	29.0	228
	5	1230 - 1250	5.4	74
	6	1628 - 1652	7.3	275
	7	2105 - 2155	1.0	110
Ocean Color/ Phytoplankton/ Biogeochemistry	8	405 - 420	44.9	880
	9	438 - 448	41.9	838
	10	483 - 493	32.1	802
	11	526 - 536	27.9	754
	12	546 - 556	21.0	750
	13	662 - 672	9.5	910
	14	673 - 683	8.7	1087
	15	743 - 753	10.2	586
	16	862 - 877	6.2	516
Atmospheric Water Vapor	17	890 - 920	10.0	167
	18	931 - 941	3.6	57
	19	915 - 965	15.0	250
Primary Use	**Band**	**Bandwidth[1]**	**Spectral Radiance[2]**	**Required NE[Δ]T(K)[4]**
Surface/Cloud Temperature	20	3.660 - 3.840	0.45(300K)	0.05
	21	3.929 - 3.989	2.38(335K)	2.00
	22	3.929 - 3.989	0.67(300K)	0.07
	23	4.020 - 4.080	0.79(300K)	0.07
Atmospheric	24	4.433 - 4.498	0.17(250K)	0.25

Temperature	25	4.482 - 4.549	0.59(275K)	0.25
Cirrus Clouds Water Vapor	26	1.360 - 1.390	6.00	150(SNR)
	27	6.535 - 6.895	1.16(240K)	0.25
	28	7.175 - 7.475	2.18(250K)	0.25
Cloud Properties	29	8.400 - 8.700	9.58(300K)	0.05
Ozone	30	9.580 - 9.880	3.69(250K)	0.25
Surface/Cloud Temperature	31	10.780 - 11.280	9.55(300K)	0.05
	32	11.770 - 12.270	8.94(300K)	0.05
Cloud Top Altitude	33	13.185 - 13.485	4.52(260K)	0.25
	34	13.485 - 13.785	3.76(250K)	0.25
	35	13.785 - 14.085	3.11(240K)	0.25
	36	14.085 - 14.385	2.08(220K)	0.35

[1] Bands 1 to 19 are in nm; Bands 20 to 36 are in µm
[2] Spectral Radiance values are (W/m^2 -µm-sr)
[3] SNR = Signal-to-noise ratio
[4] NE(Δ)T = Noise-equivalent temperature difference
Note: Performance goal is 30-40% better than required

Appendix C

Table C.1 Coordinates for surface samples and volcanic ash collection.

Location	Latitude	Longitude
1	64.07361	-19.7583
2	64.02639	-19.4283
3	64.03194	-19.0614
4	64.09222	-19.0625
5	64.14667	-19.1519
6	64.18361	-18.8011
7	64.24778	-18.5456
8	64.34417	-18.6375
9	64.36	-18.7542
10	64.37861	-18.8228
11	64.15972	-19.6114
12	65.09598	-16.1581
13	64.8993	-16.8224
14	64.90228	-16.7924
15	65.04743	-16.7259
16	64.8445	-16.4253
17	64.9278	-16.3891
18	64.935	-16.505
19	65.05913	-16.7396
20	65.06811	-16.3733
21	63.52982	-19.5139
22	63.58188	-20.0562
23	63.4782	-18.5656
24	63.53263	-20.1274
25	63.52929	-20.1099
26	63.4165	-19.0115
27	63.55243	-18.4462
28	63.50924	-19.6065